QUASICLASSICAL TRAJECTORY STUDY OF A PROTOTYPE ALKALI-HYDROGEN HALIDE EXCHANGE AND A MODEL SIX-CENTER EXCHANGE REACTION

A Thesis Submitted

In Partial Fulfilment of the Requirements

for the Degree of

DOCTOR OF PHILOSOPHY

by

I. NOORBATCHA

to the

DEPARTMENT OF CHEMISTRY

INDIAN INSTITUTE OF TECHNOLOGY, KANPUR

JULY, 1982

To Fatima

This thesis is dedicated to Fatima,
my dear wife, whose love, patience,
and understanding during my graduate
career were the chief source of all
that I may have accomplished, and
whose enthusiasm in seeing this work
completed in time cost her everything.

STATEMENT

I hereby declare that the matter embodied in this thesis is the result of investigations carried out by me in the Department of Chemistry, Indian Institute of Technology, Kanpur, India, under the supervision of Dr. N. Sathyamurthy.

In keeping with the general practice of reporting scientific observations, due acknowledgement has been made wherever the work described is based on the findings of other investigators.
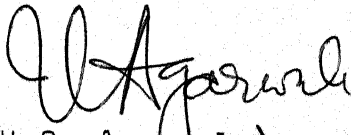
(I. NoorBatcha)
Candidate

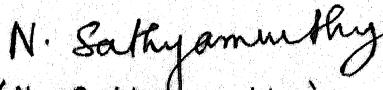DEPARTMENT OF CHEMISTRY
INDIAN INSTITUTE OF TECHNOLOGY KANPUR,INDIA

CERTIFICATE I

This is to certify that Mr. I. NoorBatcha has satis-
factorily completed all the courses required for the Ph.D.
degree programme. These courses include:

Chm 500	Basic Course in Mathematics I
Chm 521	Chemical Binding
Chm 524	Modern Physical Methods in Chemistry
Chm 541	Advanced Inorganic Chemistry I
Chm 600	Basic Course in Mathematics II
Chm 622	Chemical Kinetics
Chm 634	Symmetry and Molecular Structure
Phy 432	Quantum Mechanics I
Chm 800	General Seminar
Chm 801	Graduate Seminar
Chm 900	Research

Mr. I. NoorBatcha was admitted to the candidacy of the
Ph.D. degree in March 1980 after he successfully completed
the written and oral qualifying examinations.

(U.C. Agarwala)
Head,
Department of Chemistry,
I.I.T., KANPUR

(N. Sathyamurthy)
Convener,
Departmental Post-
Graduate Committee,
IIT-Kanpur

CERTIFICATE II

Certified that the work contained in this thesis entitled QUASICLASSICAL TRAJECTORY STUDY OF A PROTOTYPE ALKALI-HYDROGEN HALIDE EXCHANGE AND A MODEL SIX-CENTER EXCHANGE REACTION, has been carried out by Mr. I. NoorBatcha under my supervision and the same has not been submitted elsewhere for a degree.

N. Sathyamurthy

(N. Sathyamurthy)
Thesis Supervisor
Asst. Professor in Chemistry,
IIT-KANPUR

Kanpur,
July 28, 1982

ACKNOWLEDGEMENTS

I would like to express my sincere gratitude to Dr. N. Sathyamurthy for his invaluable guidance throughout the course of this study; his consideration and generosity during the critical period of my stay here have greatly helped me in reaching this point in my career. I treasure my association with him.

My special thanks go to Mr. R.D. Singh for his excellent typing job in the preparation of this thesis.

Finally, I wish to express my indeptedness to many people, whose names do not appear here and who have helped me in so many aspects. I thank them all.

I. NoorBatcha

CONTENTS

CHAPTER ONE

INTRODUCTION

In this era of state-to-state chemistry,[1] it is possible
to study elementary chemical reaction rates from reagents in
selected initial states to products in specific final states,
thanks to the molecular beam, laser excitation, laser-induced
fluorescence, chemiluminescence and related techniques. It is
also possible to select the relative orientation of the
reactants[2] and to monitor the product alignment.[3] Therefore,
it becomes necessary to use detailed dynamical theories to
predict the observables.[4] Although quantum mechanics is needed
to describe the molecular collision events, exact, (i.e., converg-
ed) quantal calculations are extremely difficult and time-
consuming and therefore have been reported only for two
reactions:[5,6]

$$H + H_2 \longrightarrow H_2 + H \qquad\qquad (R1)$$

$$\text{and} \quad F + H_2 \longrightarrow FH + H \qquad\qquad (R2)$$
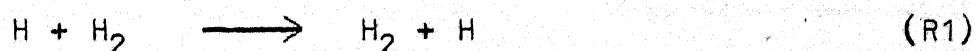
Quasiclassical trajectory (QCT) technique,[7,8] on the other hand

is easier and has been used extensively for studying the dynamics of a variety of model and real systems in the last two decades. By comparison with the available quantal and experimental results, it has been established[4] that, on the average the QCT method is a reliable tool provided purely quantal effects like tunneling, resonance etc. are not important. It has been particularly valuable in correlating the features of the potential-energy surface (PES) and the collisional outcome.[9] For example, it has been shown that for substantially endothermic reactions ($\Delta H^O \geqslant 10$ kcal mol^{-1}) of the type

$$A + BC \longrightarrow AB + C , \qquad (R3)$$

the saddle point is in the exit channel and that the reagent vibrational energy (V) is much more efficient than relative translational energy (T) in causing the reaction,[10] in qualitative agreement with the available experimental results.[11,12] Polanyi and Sathyamurthy[13] have refined this idea further. The effect of V on the reaction cross section (S_r) is much more on a sudden surface (where the change in the potential from the reactants to products is sudden) than on a gradual surface (on which the change is gradual).

In this thesis we report the results of our QCT investigation of the dynamics of the reaction,

$$Li + FH \longrightarrow LiF + H \qquad (R4)$$

which serves as a prototype for the family of alkali-hydrogen halide reactions and also a model six-center exchange reaction

$$(A_2)_2 + A_2' \longrightarrow 2 AA' + A_2 \qquad\qquad (R5)$$
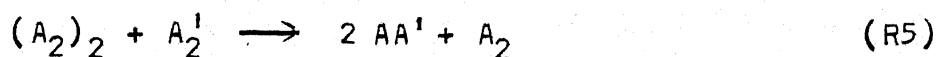
Since the first successful molecular beam investigation[14] of the reaction

$$K + BrH \longrightarrow KBr + H \qquad\qquad (R6)$$

the alkali-hydrogen halide reactions have received considerable attention from several research groups. Brooks and coworkers[15] showed that for the reaction

$$K + ClH \longrightarrow KCl + H \qquad\qquad (R7)$$
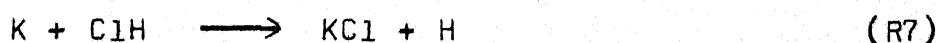
HCl ($v = 1$) is nearly 100 times more effective than HCl ($v = 0$) and that V is much more efficient than T in causing the reaction. Heismann and Loesch[16] have reported recently that for the reaction

$$K + XH \longrightarrow KX + H \ (X = Cl, \ F) \qquad\qquad (R8)$$
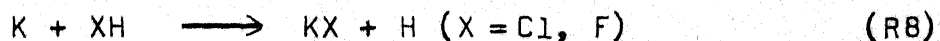
V is more efficient in promoting the more endothermic reaction ($X = F$) and that the efficiency decreases at higher collision energies. The chemiluminescence depletion study of the sodium analog

$$Na + XH \longrightarrow NaX + H \ (X = Cl, \ F) \qquad\qquad (R9)$$
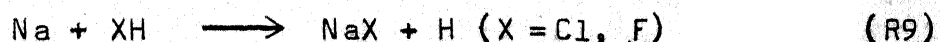
has shown[17] that with over 90% of the total energy (E) present as vibration, the collision efficiency is approximately unity. Similar vibrational enhancement has been observed for the alkaline-earth analogues of these reactions[18] also. On the basis of these results, these reactions are expected to have a <u>sudden</u> type PES.

When compared to the effect of T and V, the role of rotational energy (R) on reaction dynamics is not well understood. The effect of R on various reaction attributes has been reviewed recently.[19] There are some experimental results available on the effect of R on S_r for a few alkali-hydrogen halide reactions. From a chemiluminescent depletion study of the reaction (R9), Blackwell et al.[20] found that there was an initial decrease followed by an increase in the reaction rate coefficient (k) with increase in R, with a minimum occurring at a rotational quantum number, $J \simeq 7 - 10$. An initial decline in $S_r(J)$ has been reported[16,21] for the potassium analog and there are some indications of a subsequent increase in $S_r(J)$.

Lee and coworkers[22] have recently studied the reaction (R4) using the crossed molecular beam technique. From the near forward-backward symmetry of the product angular distribution (PAD) at $T = 3.0$ kcal mol^{-1}, they concluded that this reaction proceeded via complex formation, with coplanar geometries being preferred. However, at $T = 8.7$ kcal mol^{-1} the PAD became more forward peaked for LiF indicating the diminished importance of the complex formation at higher collision energies. Because of the possibili

of tunnelling, they were not able to ascertain the classical barrier height (E_b) for the reaction. The effect of R and V on S_r remain to be investigated for this reaction.

Despite the number of experimental studies for a variety of alkali-hydrogen halide reactions the results have been interpreted mainly in terms of the simple "harpoon mechanism".[23] Even though this has been successful in explaining the large magnitude of S_r and its change with change in the metal and the halogen atom involved, it cannot explain certain aspects of the dynamics like specific energy disposal. Also, vibrational enhancement of S_r cannot be accounted for satisfactorily. Polanyi and coworkers[24] had proposed a simple DIPR (Direct Interaction with Product Repulsion) model, which provides a qualitative explanation for the product energy and angular distribution, for reactions forming an ionic bond. However, this model is applicable for direct reactions only.

QCT studies of the dynamics of the alkali-hydrogen halide exchange reactions have not been reported until recently as there were no accurate PES available. The only system amenable to elaborate ab initio investigation is the reaction (R4). The nonreactive part of the PES for this system was published by Lester and Krauss[25] which showed the presence of an attractive well. This has been confirmed subsequently by Trenary and Schaefer.[26] Balint-Kurti and Yardley[27] (BKY) published an ab initio PES including a semiempirical correction for the reaction in the collinear LiFH configuration. They also found

an attractive well in the entrance channel and calculated E_b to be 21.6 kcal mol^{-1}. In addition, they found E_b to decrease as the LiFH angle decreased from 180°. Zeiri and Shapiro (ZS) reported[28] a semi-empirical PES for a series of alkali-hydrogen halide reactions including (R4). They predicted the lowest value of E_b to be 12.4 kcal mol^{-1} at $\theta(LiFH) = 105^O$. An extensive ab initio PES for (R4) was published recently by Chen and Schaefer.[29] Their PES for the collinear geometry was found to be similar to that of BKY in many respects. The classical endoergicity was calculated to be 2.9 kcal mol^{-1}, but with zero-point corrections, the reaction was found to be exothermic by 1.7 kcal mol^{-1}. Their surface also contained a well in the entrance channel with a well depth of 4.5 kcal mol^{-1} corresponding to the bent complex with $\theta(LiFH)=114^O$. The saddle point was located in the exit channel, 10 kcal mol^{-1} above the reactants with $\theta(LiFH)=74^O$. This surface has been fitted to an analytic function by Carter and Murrell,[30] after appropriate scaling as suggested by Chen and Schaefer. The standard deviation of this fitted surface (CSCM surface) from that of the scaled ab initio points was 1.9 kcal mol^{-1} with a maximum error of 6.7 kcal mol^{-1}.

After this thesis work was begun, some quantum mechanical (QM) as well as QCT results on ZS surface were reported in the literature. In their QM study of the collinear reaction on the ZS surface, Walker et al.[31] found a large number of resonance peaks in the reaction probability (P^R) vs E curves suggesting

the formation of long-lived complexes. For $T > 11.5$ kcal mol^{-1} the HF molecule from its ground vibrational state (V) was found to react with significant P^R. However, the collinear QM calculation[32] on the CSCM surface resulted in a negligible value of P^R ($\simeq 0.05$) for HF (v = 0) at T = 21 kcal mol^{-1}. On the other hand, when V was higher than E_b, P^R was nearly unity at very low values of T. Zeiri et al.[33] have reported the results of their QCT calculations on their (ZS) semi-empirical PES. Their calculated S_r of 2.46 $\overset{o}{A}{}^2$ and the pronounced backward scattering of the product molecule were not in agreement with the experimental result meaning that this surface is not accurate enough for describing the LiFH dynamics. Therefore it becomes necessary to investigate the dynamics of this prototype alkali-hydrogen halide exchange reaction on an accurate surface. Fortunately, a reliable ab initio PES (CSCM) is available for the collinear as well as noncollinear geometries and we have carried out detailed QCT studies for this reaction on this surface. We compare our results with the available experimental results and assess the accuracy of the ab initio PES. A detailed investigation of the effect of V and R (in comparison to that of T) on S_r for this reaction would shed light on the dynamical factors operative in this as well as other members of this family of reactions.

We report in Chapter 2 the results of collinear QCT studies for this reaction. Details of the three dimensional(3D) dynamical studies and results are given in Chapter 3, with

special attention being given to the effect of R and the relative orientation,on various reaction attributes for this reaction.

In this thesis, we also report on the development of a software package to study the detailed dynamics of a six-centre (6-C) exchange reaction using the QCT technique and present the preliminary results obtained for a model system.

Historically, the reaction

$$H_2 + I_2 \longrightarrow 2 \; HI \qquad\qquad (R10)$$

had been considered, to proceed in one step through a four-centered (4-C) transition state. In the sixties, it was shown to proceed via a chain mechanism involving atomic iodine.[34,35] Raff et al.[36] had subsequently examined the dynamics of this reaction on a semiempirical PES[37] by the QCT technique and concluded that the direct reaction of H_2 with I_2 was prohibited by dynamical effects and that the reaction occurred primarily via the formation of an H_2I complex. Their conclusions were corroborated by the combined phase-space/trajectory calculations of Jaffe et al.[38] By a molecular beam investigation using a supersonic nozzle, Jaffe and Anderson[39] had earlier found the reverse reaction

$$HI + DI \longrightarrow HD + I_2 \; , \qquad\qquad (R11)$$

not to occur even with a relative translational energy of

upto 110 kcal mol^{-1}. They suspected that vibration or rotational excitation of the colliding partners was required for the reaction to proceed through the molecular mechanism. Recent experiments by Horiguchi and Tsuchiya[40] show the vibrational excitation of the HI molecules to enhance the rate of this reaction. The other potential 4-C reactions which have been studied by the QCT technique are[41,42]

$$H_2 + F_2 \longrightarrow 2\ HF \qquad\qquad (R12)$$

$$HBr + Cl_2 \longrightarrow HCl + BrCl \qquad\qquad (R13)$$

$$HBr + BrCl \longrightarrow HCl + Br_2 \qquad\qquad (R14)$$
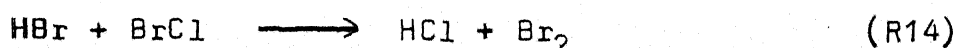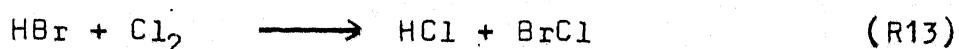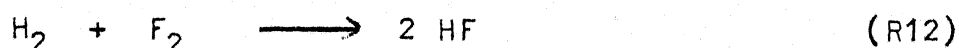
and the results indicate that these reactions also must be proceeding mainly via chain mechanism.

The hydrogen-deuterium exchange reaction

$$H_2 + D_2 \longrightarrow 2\ HD \qquad\qquad (R15)$$

has been in the forefront because of the severe conflict between the theoretical and experimental results.[43] Shock-tube studies of Bauer and Ossa[44] and others[45,46] yielded an activation energy (E_a) of 42 kcal mol^{-1}. The results were explained by postulating a vibrational excitation mechanism _via_ a 4-C transition state. Initial doubts on the reliability of the shock-tube results were removed by the stimulated Raman experiments of Bauer and coworkers.[47] Yet several investigators[48,49] maintain that only the atomic mechanism can sufficiently explain all

the observations. Also, a recent laser-beam investigation[50] of the reaction

$$HD + HD \longrightarrow H_2 + D_2 \qquad\qquad (R16)$$
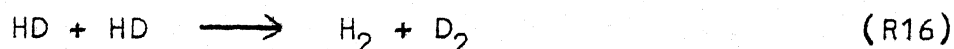
showed that this bimolecular reaction did not occur even when one of the HD molecules was excited upto $v = 5$ level.

These intriguing experimental results had led to a series of theoretical investigations of the reaction (R15). An extensive ab initio search of Silver and Stevens[51] failed to produce a 4-C transition state with an E_b lower than the dissociation energy of the hydrogen molecule. The collinear symmetrical transition state, which lies below the dissociation limit for H_2, cannot serve as the transition state for a 4-C exchange reaction since the end atoms must depart from the collinear array to recombine. A detailed QCT study of H_2/D_2 collisions was carried out by Brown and Silver[52] on a London-type PES which showed that only $\sim 7\%$ of the total number of trajectories led to the products when both the molecules were in the ground vibrational state $(v = 0)$. However, when both the molecules were excited to $v=3$ level no reaction was observed. Another study[53] on a semi-empirical repulsive type PES, however, resulted in $\sim 3\%$ reaction when both the molecules were excited to $v = 3$.

The failure to realise a 4-C transition state has been explained on the basis of Woodward-Hoffmann rules.[54] Since

the (electronically) ground state reactants are not correlated
with the ground state of the products because of the conserva-
tion of orbital symmetry, a large barrier for the reaction
(R15) results. This led Wright[55] to suggest a 6-C transition
state as an alternative. His LCAO-MO-SCF calculations[56] yielded
an E_b of 90 kcal mol^{-1}, which is well below the dissociation
energy of H_2, for the formation of H_6 from 3 H_2. Using London-
Eyring-Polanyi formalism, Thompson and Suzukawa[57] predicted a
value of E_b = 88 kcal mol^{-1} whereas a large basis set ab initio
calculation of Dixon et al.[58] yielded an E_b of 69 kcal mol^{-1}.
The arguments in favour of the 6-C transition state gained
further support, through the crossed molecular beam experiments
of Herschbach and coworkers.[59,60] They found that the reaction
between Cl_2 and Br_2 or HI did not occur at collision energies
as high as 25 kcal mol^{-1}. However, at high pressures and
low temperatures in the supersonic nozzle expansion where there
was a high concentration of $(Cl_2)_2$ they found the reaction to
proceed at collision energies as low as ∼3 kcal mol^{-1}. This
they ascribed to the 6-C reactions:

$$(Cl_2)_2 + Br_2 \longrightarrow 2\ BrCl + Cl_2 \qquad (R17)$$

$$(Cl_2)_2 + HI \longrightarrow HCl + ICl + Cl_2 \qquad (R18)$$
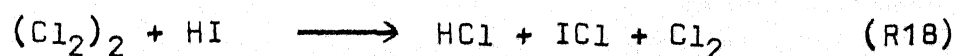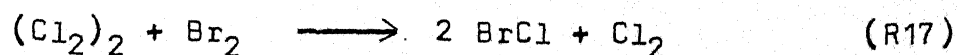
A similar 6-C reaction

$$(HI)_2 + F_2 \longrightarrow HF + HI + IF \qquad (R19)$$
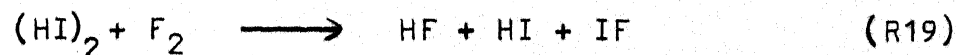
has been observed by Durana and McDonald.[61]

Therefore, it would be worth investigating the detailed dynamics of a 6-C exchange reaction by the QCT method on a realistic PES. Such a study would also enhance our understanding of other interesting processes like collision-induced dissociation of a van der Waals molecule, and vibrotational energy transfer of a diatom by a van der Waals species. The details of the development of a software package (for the first time) to study a model 6-C exchange reaction along with some preliminary results are presented in Chapter 4. Summary and conclusions of the thesis are given in Chapter 5.

CHAPTER TWO

DYNAMICS OF THE COLLINEAR Li + FH $\longrightarrow$ LiF + H REACTION

2.1 Computational Procedure

Balint-Kurti and Yardley[27] have reported the ab initio

potential energy (PE) values over a rectangular grid of $R_1 =$

R_{LiF} = 2.0, 2.5, 3.0, 3.2, 3.5, 3.8, 4.0, 4.5, 5.0 and 6.0 au

(1 au = 0.529167 Å) and $R_2 = R_{HF}$ = 1.00, 1.25, 1.50, 1.76, 2.00,

2.25, 2.50, 2.75, 3.00, 3.50, 4.00, 4.50 and 5.00 au. However,

for QCT calculations, PE values are needed at larger R_i , i = 1,2

values. We have assumed the interaction potential to become

zero at R_i = 10.0 au. The LiFH potential at this distance would,

therefore, be the ab initio value [62] for the isolated LiF and

HF molecules. The PE values at R_1 = 7,8 and 9 au and R_2 = 6,

7, 8 and 9 au were calculated using an R^{-n} interpolant. The PE

and its first derivatives with respect to R_1 and R_2 at an

arbitrary geometry were calculated by the two-dimensional spline

interpolation procedure.[63,64] The resulting PES is displayed

in the form of a contour plot on scaled and skewed coordinates[65]

in Fig. 1. The ab initio (CSCM) surface of Chen and Shaefer[29]

as fitted by Carter and Murrell[30] is plotted in Fig. 2. The

functional form and the parameters used are given in Chapter 3.
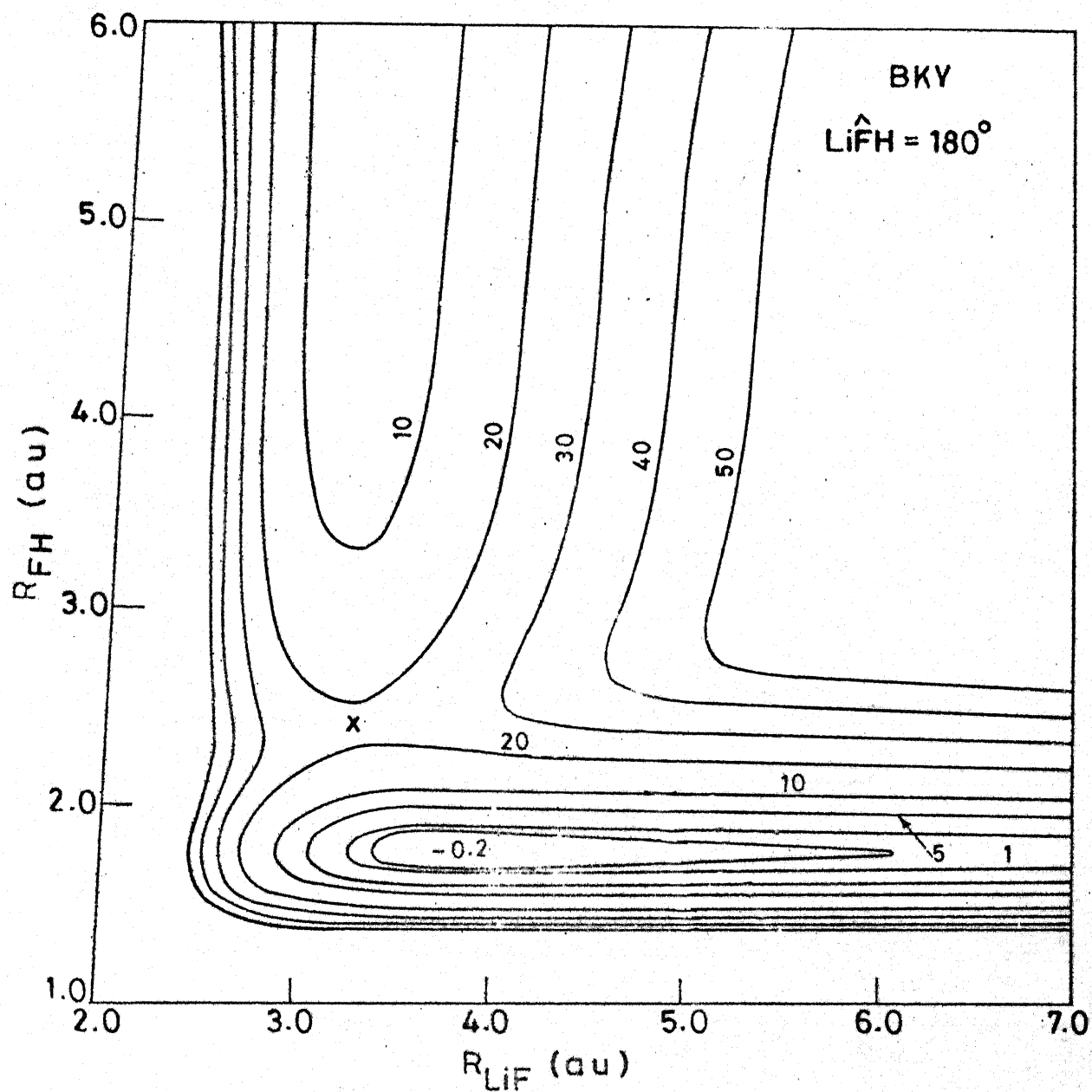
Fig.1 PE contours for the BKY surface in kcal mol^{-1}, relative to the reactants in scaled and skewed coordinates.
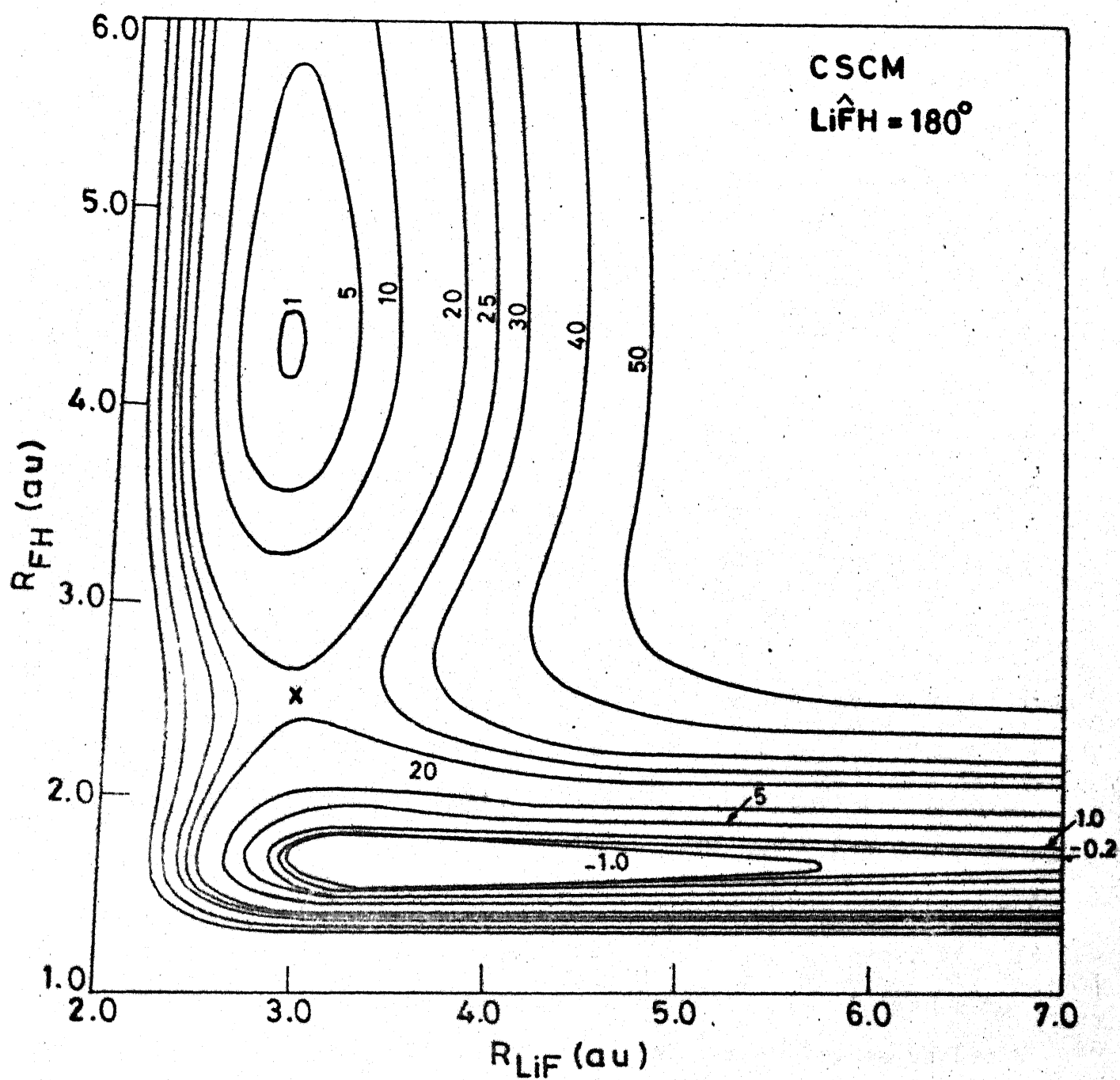
Fig. 2   Same as fig. 1 for the CSCM surface.

We have constructed a semi-empirical London-Eyring-Polanyi-Sato (LEPS) surface with E_b equal to that of the BKY surface and it is shown in Fig. 3. The functional form and the parameters for this surface are given in Appendix I. We have carried out collinear QCT calculations on all the three (BKY, CSCM and LEPS) surfaces. The details of the calculations can be found elsewhere.[7] For a fixed initial V and T, 50 trajectories were run, varying the vibrational phase systematically between 0 and 2π, with all the trajectories starting at 12 au on the BKY and LEPS surfaces. On the CSCM surface, we had to start the trajectories at $R_1 = 22$ au as the potential was not negligible at shorter distances.

2.2 Results and Discussion

The p^R values, calculated using the BKY and CSCM surfaces are plotted as a function of V at different values of $E = T + V = 1.5$, 2.0, 2.5, and 3.0 eV, in Fig. 4. Both surfaces lead to nearly the same result. Even at the highest $E = 3.0$ eV, p^R is zero for V corresponding to vibrational quantum numbers $v = 0$ and 1, although T is at least two times E_b. However, if v is changed to 2, p^R rises to unity even at low T. In order to assess quantitatively the vibrational threshold, we varied V in small intervals near $V = 1.0$ eV, at $E = 1.5$ eV. It is found that unless all the energy required to cross the barrier is in the form of reagent vibration, the reaction does not take place. There is very little effect of T on p^R on both surfaces as

17
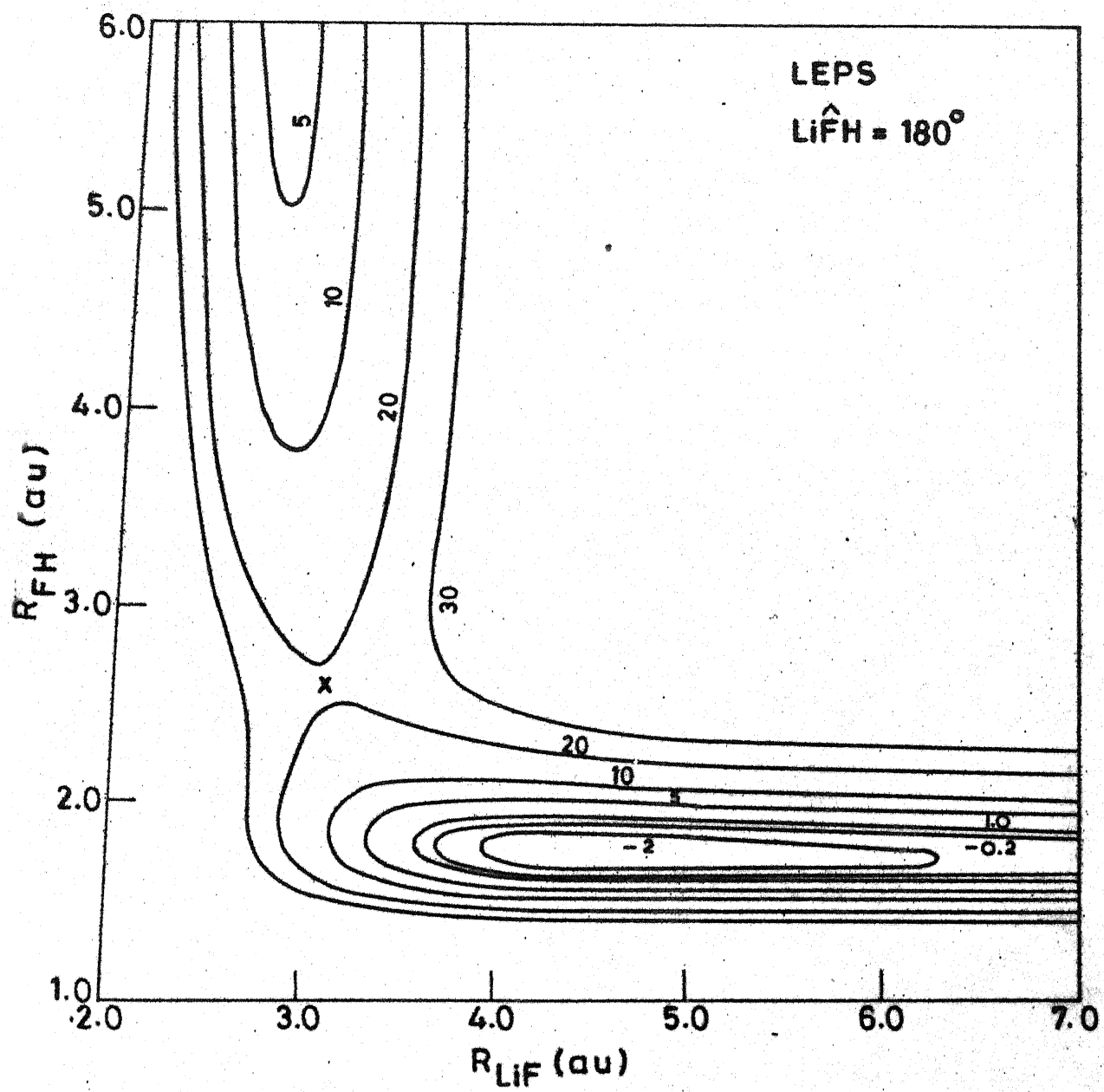
Fig. 3 Same as fig.1 for the LEPS surface.
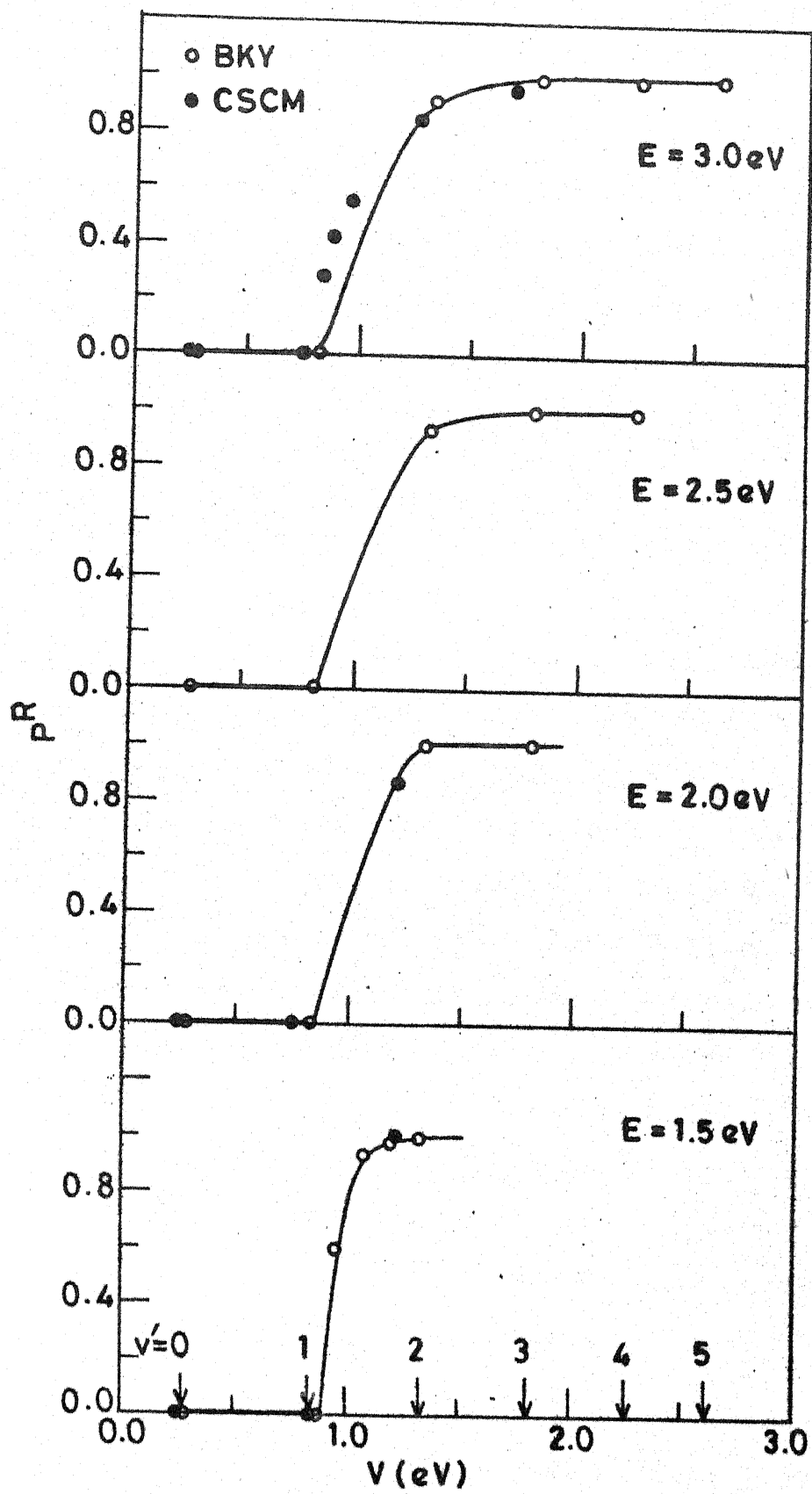
Fig.4 V dependence of P^R at different E.

shown in Fig. 5 for $v = 2$. This is confirmed by the QM results of Alvarino et al.[32] on the CSCM surface. The QM results also show a marked vibrational enhancement noticed in the QCT results except for the nonzero p^R due to tunnelling in the former. Except for the oscillations, there is a good agreement between the two results as shown in Fig. 5. Similar agreement has been obtained for other systems.[68]

We have investigated the product vibrational energy distribution on the two surfaces for $v = 2$ at different T. The QCT state-to-state transition probabilities displayed in Fig.6 for the CSCM surface show a bimodal (double-peaked) distribution in v' at low T. With increase in T the distribution shifts to higher v' and loses the bimodal character. These results are in qualitative agreement with the QM results. Unfortunately, we could not make a quantitative comparison as the two results are not available at identical energies. Product vibrational energy distribution on the BKY surface does not show any significant bimodality (Fig. 7) but shifts to higher v' with increase in T . The T dependence of the average fraction of the product vibrational energy ($\langle f_v \rangle$) is identical on both surfaces at low T as shown in Fig. 8. At higher T, however, CSCM surface leads to a larger $\langle f_{v'} \rangle$.

The vibrational threshold equal to E_b noticed for the reaction (R4) should be attributed to the sudden nature of the PES[13] arising possibly from a change in the bonding character-
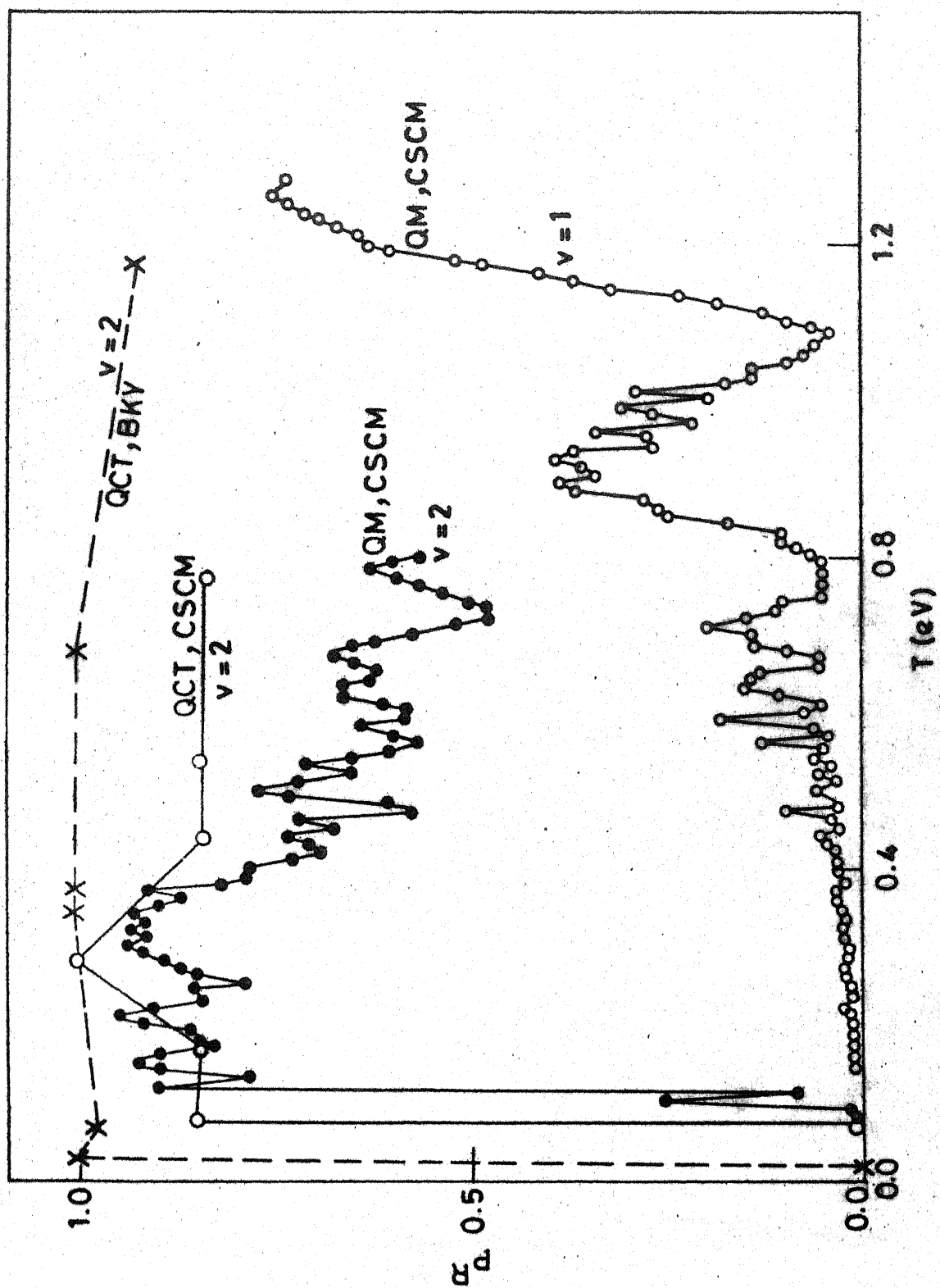
Fig. 5 Comparison of QM and QCT results on the CSCM surface.
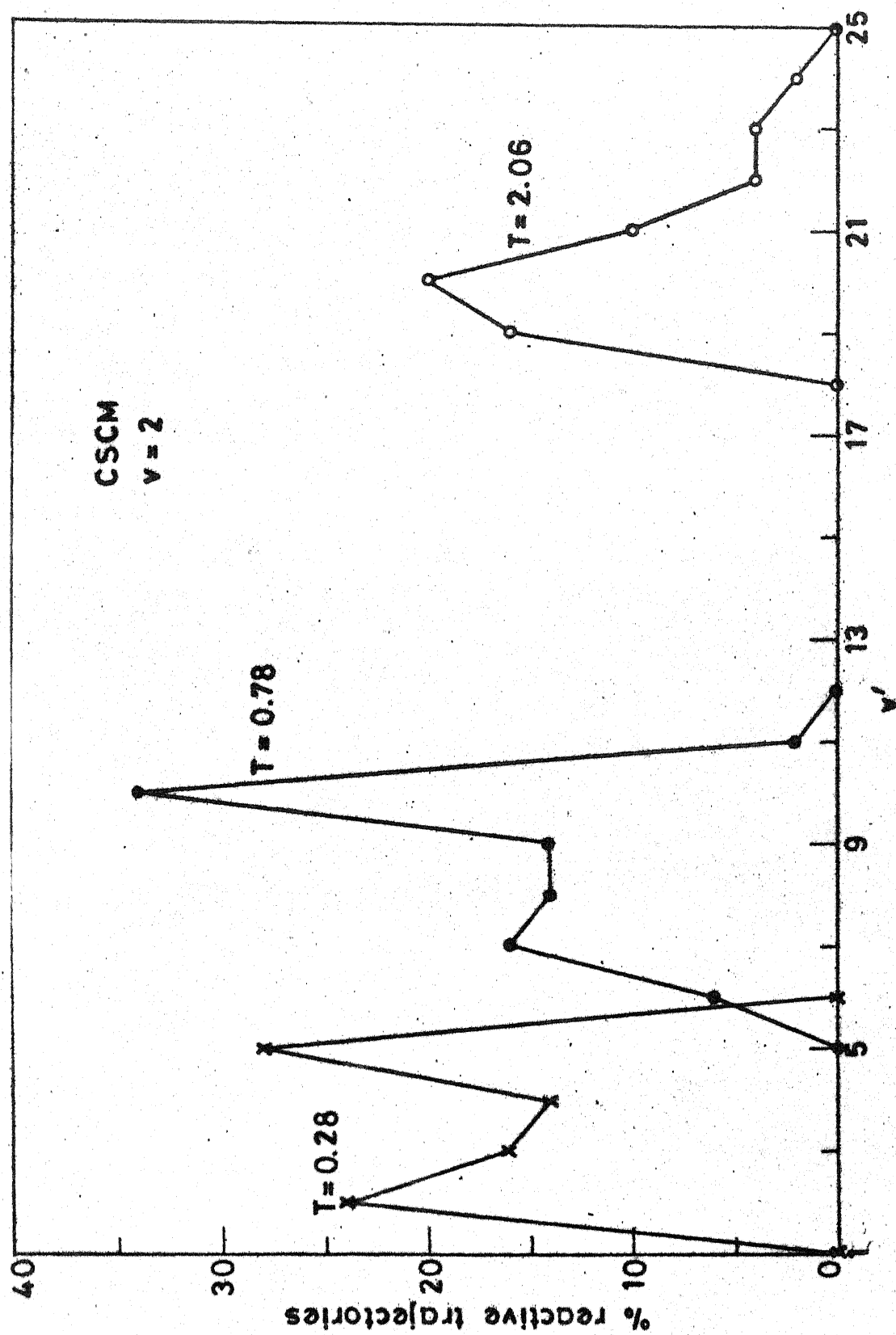
Fig. 6   Product vibrational state distribution on the CSCM surface. T is in eV.

21
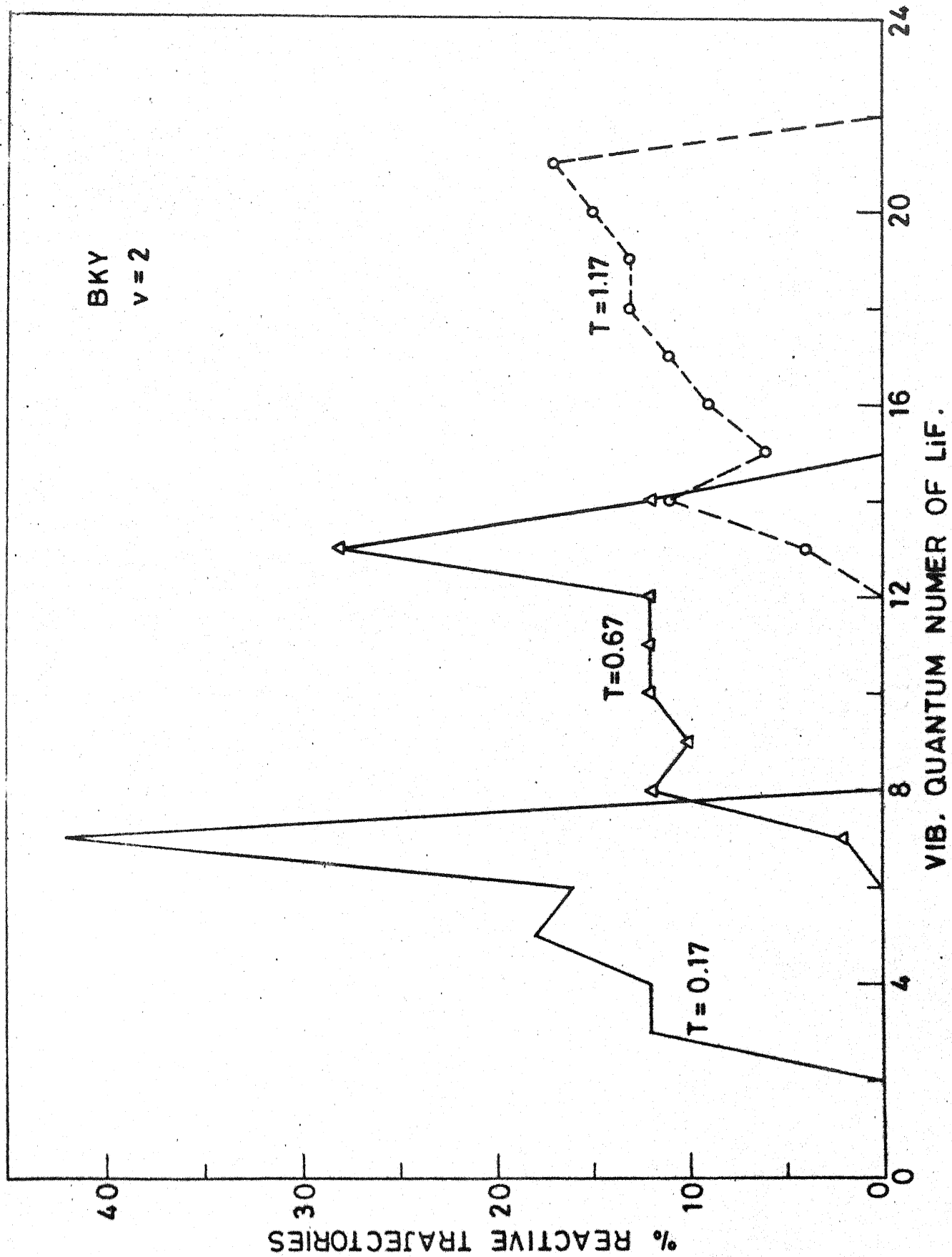
Fig. 7 Same as fig.6 for the BKY surface.
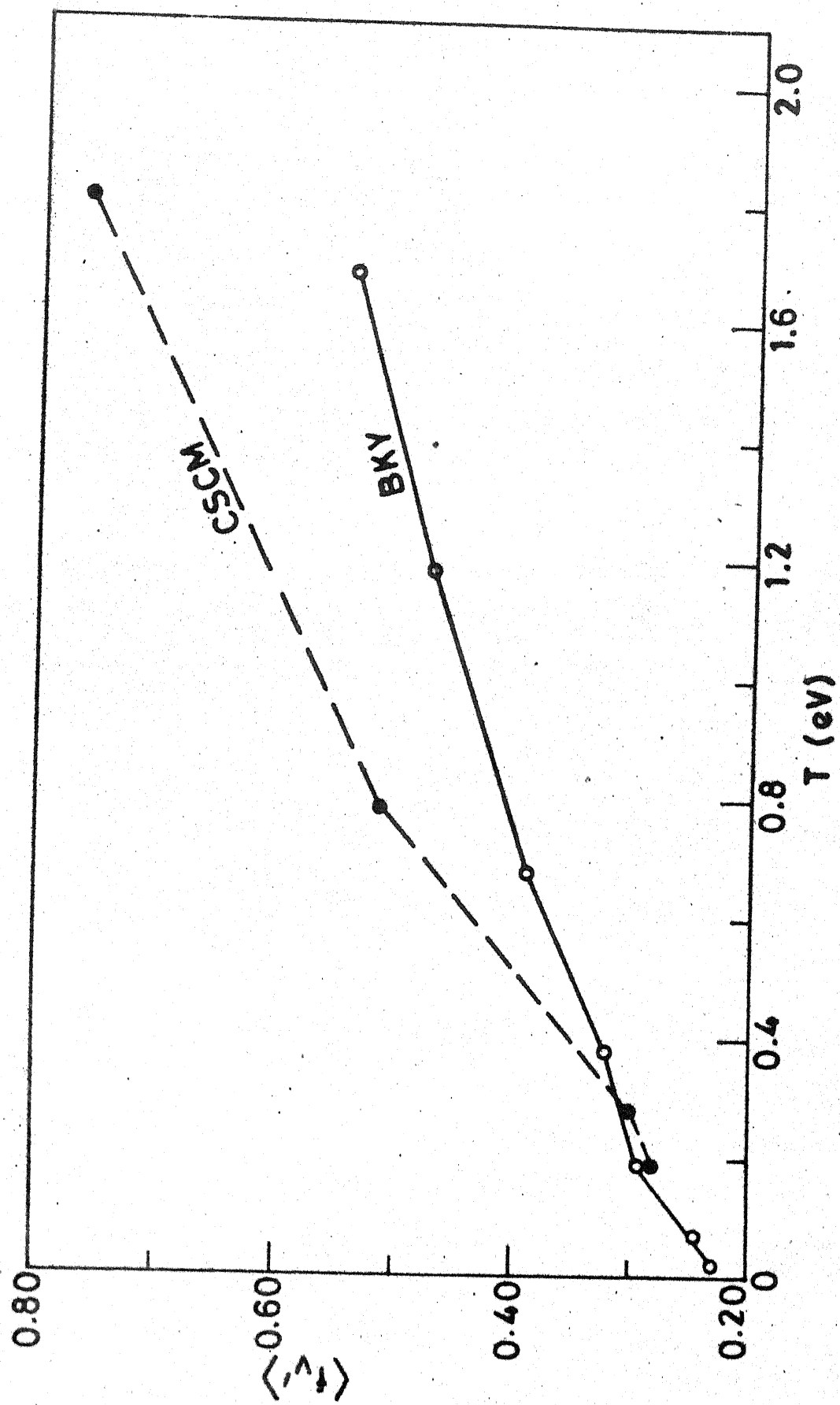
Fig. 8 Comparison of $\langle t_{v'} \rangle$ on the two surfaces.

covalent in the reactant (HF) to ionic in the product (LiF).

As the reagents approach each other, there is very little
increase in the PE along the approach coordinate and then there
is a sudden increase in the PE towards the barrier crest. Since
most of the barrier is located in the product channel, there
is a need for almost all of the energy required to cross the
barrier to be in the form of V. The presence of a negligible
fraction of the barrier in the entry channel accounts for the
near-nonexistence of a translational threshold. This is
perhaps the first time that such a threshold has been predicted.
It would be interesting to find out whether such a threshold
persists in 3D collisions. The chemiluminescence depletion
experiments of Bartoszek et al.[17] showed that the sodium analog
of the reaction (R4) does not occur unless V is greater than E_b
and under these conditions the collision efficiency is near
unity, even if T is as low as 4% of the total energy. Therefore,
we infer that the reaction (R9) has a sudden type PES.

So far our discussion has been restricted to the dynamics
on an ab initio PES. For most of the systems, ab initio
surfaces are not available and are not likely to be available
for some time to come because of the complexity of the electro-
nic structure calculations for many-electron systems. Therefore,
the tendency has been to use semiempirical or even empirical
surfaces with spectroscopic parameters for the reactants and
products as the only input. LEPS surfaces have been used in

the past for a variety of systems if only to identify the major

qualitative features of the PES by predicting product energy

distribution and comparing the results with the IR chemilumi-

nescence data.[69]   There are several limitations to this func-

tional form.   Schor et al.[70] have shown that the LEPS function

could not reproduce the sudden nature of the PES for the reac-

tion

$$Be + FH \longrightarrow BeF + H \qquad\qquad (R20)$$

This is not surprising as the LEPS formalism was developed

originally for $H + H_2$ type systems.   By searching a three

dimensional grid of sato parameters in the range $-1 \leqslant 0 \leqslant 1$, we

formulated an LEPS surface that met various criteria: (i) saddle

point in the exit channel, (2) E_b same as that of the BKY surface,

(3) not too unrealistic potential well or barrier in the

entrance/exit channel and (4) the overall nature of the surface

is sudden. In order to test its utility, we have computed the

trajectories on this surface and the results are shown in Fig. 9.

The reaction takes place for all v and there is no vibrational

threshold.   There is, however, a translational threshold for

v = 0 and 1 as shown in Fig. 10.   This arises from the fact

that the LEPS surface is not as _sudden_ as the other two surfaces.

We could not get an LEPS surface which had more _sudden_ character

without simultaneously introducing an unrealistically deep
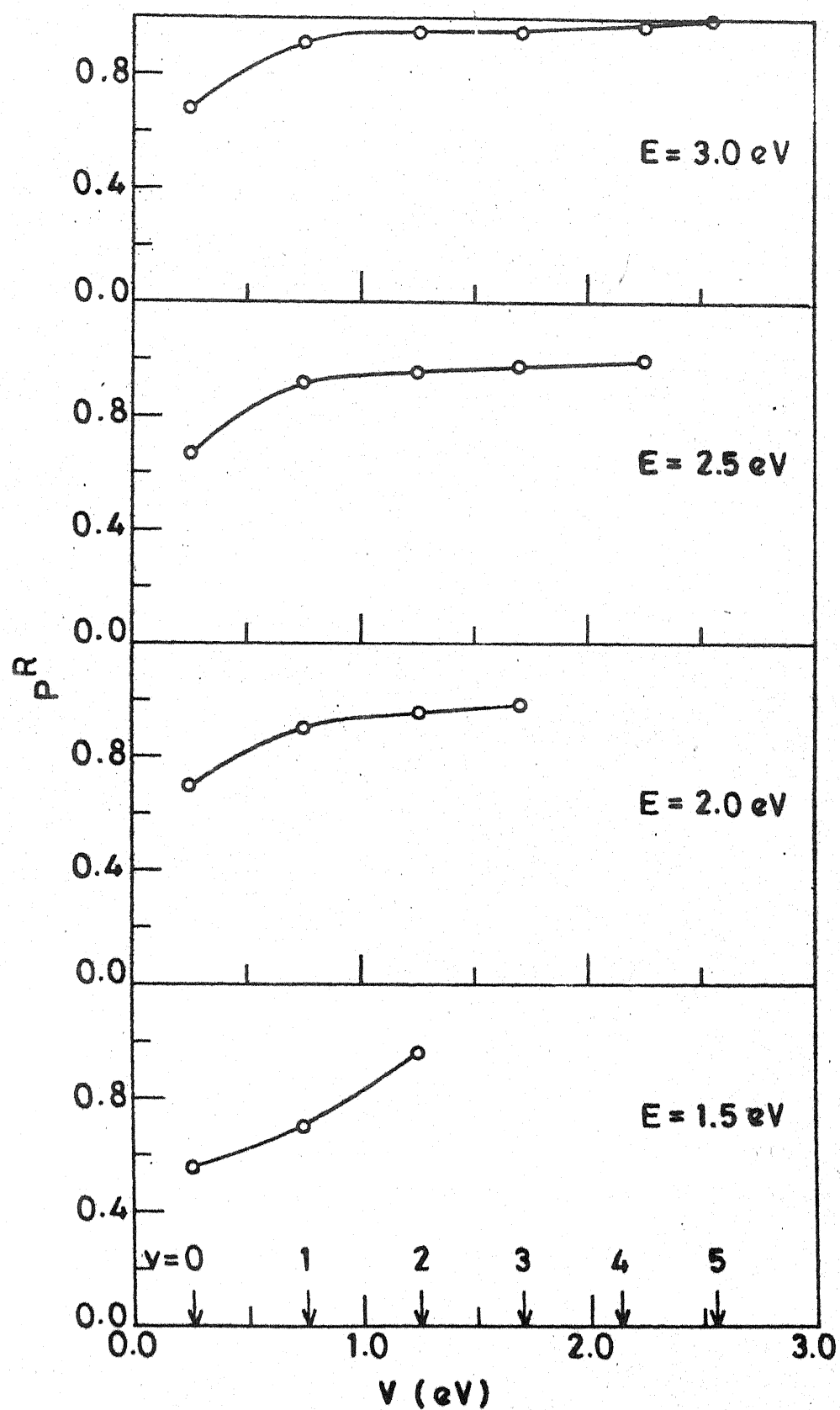
Fig.9 Same as fig.4 for the LEPS surface.
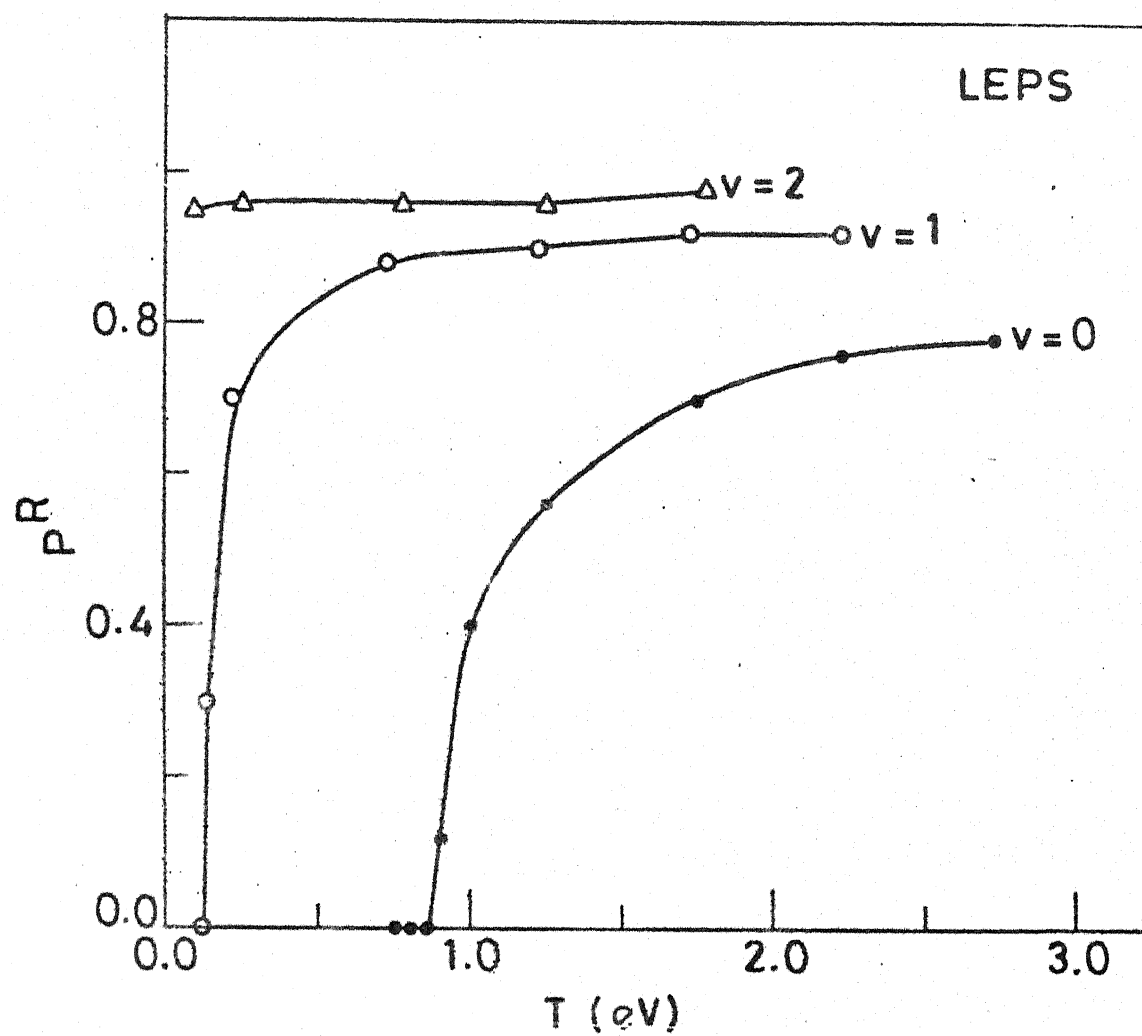
Fig.10   T dependence of P^R for different v on the LEPS surface.

potential well ($\geqslant 10$ kcal mol^{-1}) in the entry channel. Therefore, we had to abandon the idea of developing a model LEPS surface that would be suitable for a detailed dynamical investigation of the reaction (R4) and its analogs.

CHAPTER THREE

LiFH DYNAMICS IN THREE DIMENSIONS

3.1 Potential-Energy Surface

We had used three different (BKY, CSCM and LEPS) surfaces
for studying the collinear collisions of the reaction (R4) but
only one of them, the CSCM surface has been used for studying
the 3D collisions. The BKY surface was restricted to collinear
geometries. Although Balint-Kurti and Yardley[27] published PE
values for a few noncollinear geometries and investigated the
dependence of E_b on the LiFH angle, there was not enough infor-
mation for a numerical interpolation of the surface nor could
any reasonable analytic function be fitted to the data to yield
a PES for the noncollinear geometries. The LEPS surface has
provision for the noncollinear geometries but does not lead to
results similar to that of the two ab initio surfaces available
for this system. Therefore, it is not expected to be realistic
for the noncollinear geometries. Also, the LEPS formalism leads

generally to the collinear conformation as the most preferred pathway whereas the _ab initio_ calculations clearly favour sideways approach. As a result, we have not used the LEPS surface in our 3D dynamical investigation of the reaction (R4).

The CSCM surface[30] is defined by the analytical function:

$$V(r_1, r_2, r_3) = V_1(r_1) + V_2(r_2) + V_3(r_3) + V_{LiFH}(r_1, r_2, r_3)$$

where the subscripts 1, 2 and 3 stand for the molecules LiF, HF and LiH respectively. The diatomic potential V_i, is given by

$$V_i(r) = -D_e(1 + a_1 \rho + a_2 \rho^2 + a_3 \rho^3) \exp(-a_1 \rho)$$

where $\rho = r - r_e$. The triatomic potential V_{LiFH} is given by

$$V_{LiFH}(r_1, r_2, r_3) = \prod_{i=1}^{3} [1 - \tanh(\gamma_i \rho_i / 2)]$$

$$\times V_I^0 (1 + \sum_i C_i \rho_i + \sum_{i \leqslant j} C_{ij} \rho_i \rho_j + \ldots)$$

The values of the parameters are listed in Table 1. We describe here the different aspects of the CSCM surface and point out its shortcomings also. Although we had displayed the PE contours for the collinear configuration in scaled and skewed coordinates in Fig. 2, we reproduce the same in the (r_1, r_2) coordinates

Table 1. Parameters for the CSCM surface

DIATOMIC PARAMETERS

	$r_e/Å$	D_e/eV	$a_1/Å^{-1}$	$a_2/Å^{-2}$	$a_3/Å^{-3}$
HF	0.9168	6.1173	4.0604	3.3165	3.0396
LiF	1.5639	5.9457	2.0221	0.7432	0.9094
LiH	1.5953	2.5161	2.1822	1.1094	0.4576

TRIATOMIC PARAMETERS

$C_1/Å^{-1}$	-1.8971	$C_{111}/Å^{-3}$	-9.7549	$C_{1111}/Å^{-4}$	3.6954	$C_{1123}/Å^{-4}$	0.2290
C_2	0.3390	C_{222}	0.2230	C_{2222}	-0.0917	C_{1223}	0.1840
C_3	0.0774	C_{333}	0.0822	C_{3333}	-0.1050	C_{1233}	-0.3421
$C_{11}/Å^{-2}$	10.0494	C_{112}	1.5351	C_{1112}	-0.0472	V_I^o/eV	12.1649
C_{22}	0.0972	C_{122}	0.2157	C_{1122}	0.3544	$\gamma_1/Å^{-1}$	2.5058
C_{33}	-0.0658	C_{113}	3.2750	C_{1222}	-0.0769	$\gamma_2/Å^{-1}$	1.1114
C_{12}	-0.4097	C_{133}	0.1000	C_{1113}	-2.0080		
		C_{223}	-0.4650	C_{1133}	-0.3388		

...contd.

Table 1 (contd.)

C_{23}	-1.6688	C_{233}	0.2617	C_{1333}	0.3155	$\gamma_3/\text{Å}^{-1}$	0.1406
C_{23}	-0.1330	C_{123}	-0.5099	C_{2223}	0.1368		
				C_{2233}	-0.0582	$\rho_1 = R_{HF} - 0.4687$ Å	
				C_{2333}	0.0962	$\rho_2 = R_{FLi} - 1.6211$ Å	
						$\rho_3 = R_{LiH} - 1.7020$ Å	

in Fig. 11 for comparison with the PE contours for the $\widehat{LiFH} = 114^O$ & 74° in Fig. 12 & 13 respectively. The value of E_b decreases from 20.5 kcal mol^{-1} to 7.8 kcal mol^{-1} as the $\widehat{LiFH}$ is changed from 180° to 74° and then it increases sharply as the angle is decreased further. The saddle point is located in the exit channel for all the three different configurations but the sudden nature of the surface decreases as the LiFH angle is decreased from 180° suggesting that the vibrational threshold noted for the collinear geometry (Chap. 2) is not likely to persist in the bent collisions. There are also other changes in the PES as the $\widehat{LiFH}$ changes. The depth of the well in the entry channel changes as can be seen from Table 2. During a detailed investigation of the features of the PES, we have discovered that there are 'unexpected' additional hills and valleys in the potential-energy terrain as illustrated in Fig. 14. The heights and depths of these additional barriers and wells respectively are listed in Table 2. Fortunately, the dynamical investigations reported in this thesis are at such high energies that these additional features are not likely to have much influence on the dynamics. Also, the shape of the inner repulsive wall is known to be more important than the additional wells. Nevertheless, their existence reveals two important factors:

(1) It is not enough to examine the PE contours in the interaction region; it is essential to ensure the smooth
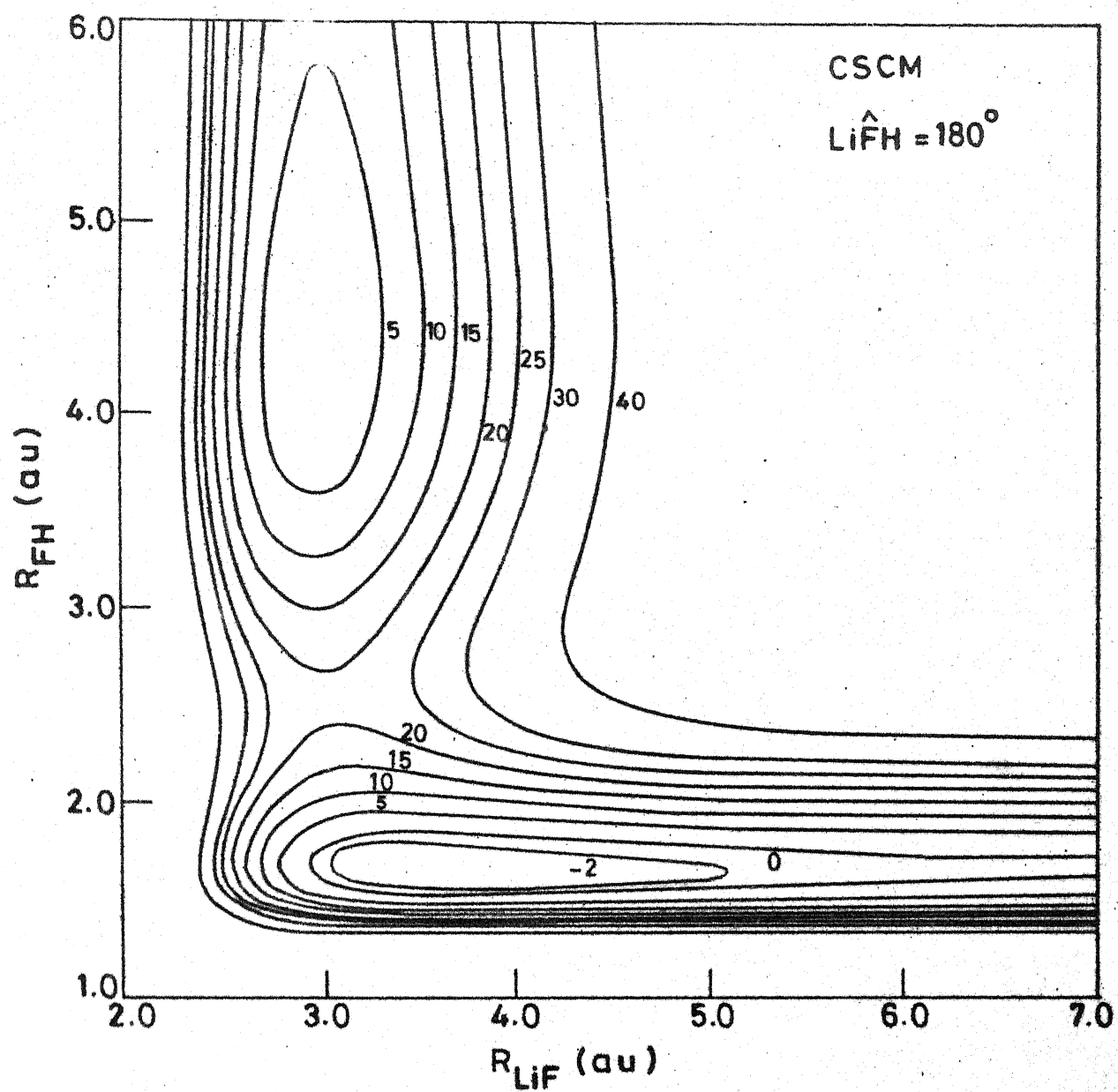
Fig. 11 Same as fig. 2 on unscaled and unskewed coordinates.
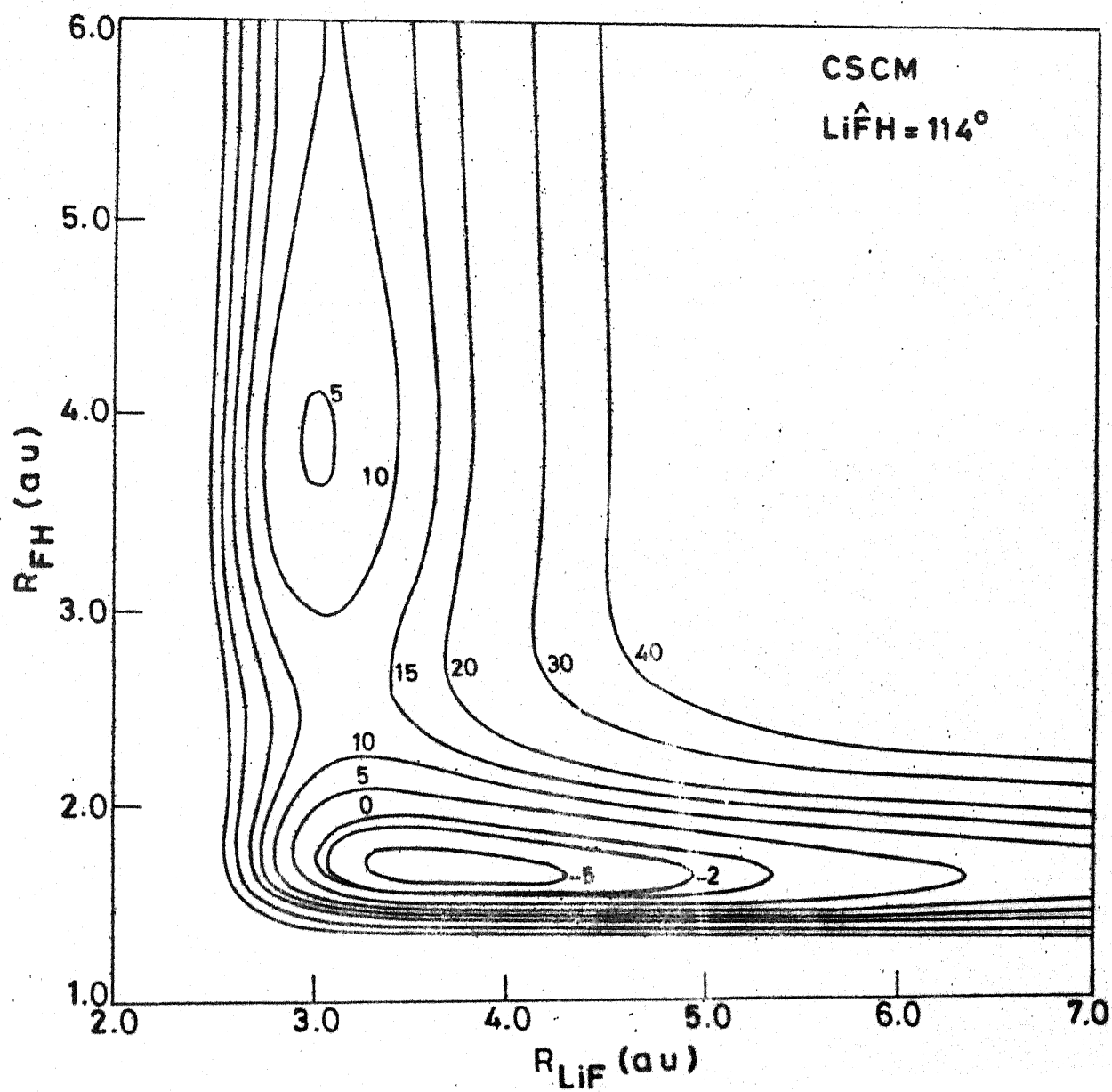
Fig. 12   Same as fig. 11 for LiF̂H = 114°.
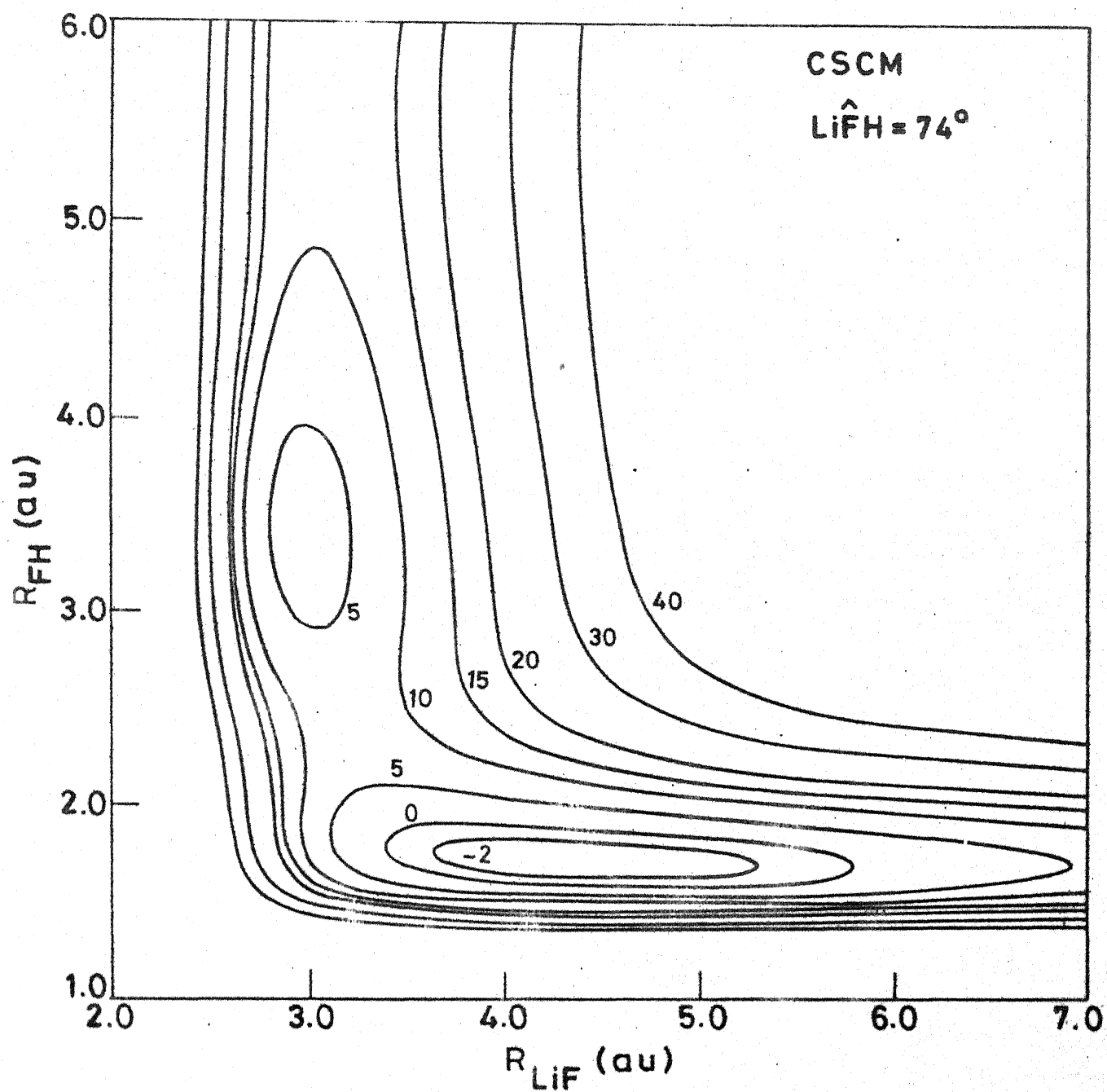
Fig. 13   Same as fig. 11 for LiF̂H = 74°.

Table 2. Barrier heights and well depths for different LiFH geometries[a]

$\widehat{\text{LiFH}}$	Saddle point barrier height (E_b)	Well depth near the saddle point region (small R_{LiF})	Barrier in the entry channel	Barrier in the exit channel	Well in the entry channel at large R_{LiF}
180°	20.5	4.0	0.8	6.2	4.5
114°	13.0	6.0	7.9	9.8	-
74°	7.8	3.3	7.8	11.2	-

a, Energies are relative to the separated reactants in kcal mol^{-1}.
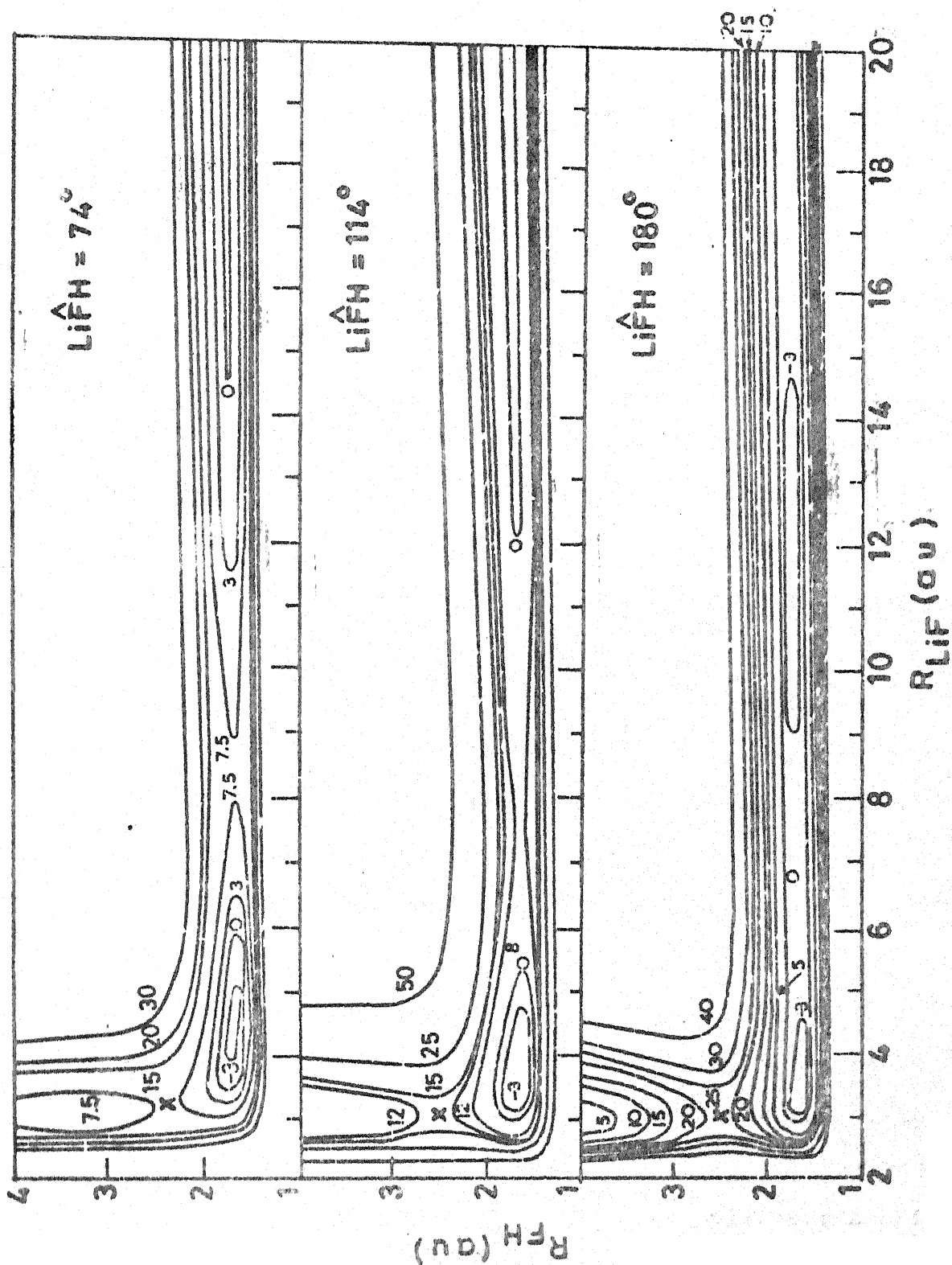
Fig. 14. Same as Fig. 2 for three different LiF̂H for a longer range of R_{LiF}

behaviour of the PES at large R_i, i = 1, 2, 3 values also as the trajectories are invariably started at large distances.

(2) It is necessary to ensure that the fitting of an analytic function to the PE values does not introduce any spurious bumps and troughs that were not present in the original data. In this particular case, for example, the original *ab initio* values were not reported in the region where the new hills and valleys have been discovered. This is an instance where a constrained optimization[72] may be more useful than a simple nonlinear least squares fit of the parameters of the chosen analytic function to the data. Clearly, a better analytic fit is required for the LiFH system and to obtain the same is not a simple matter. The problem of fitting *ab initio* surfaces continues to be a 'bottle neck' in going from electronic structure calculations to dynamical studies and poses a challenge to the practicing molecular dynamicist.[73] In this particular case, the *sudden* nature of the PES poses a special problem. We have already indicated in Chapter 2, our failure to make the LEPS function reproduce the major features of the surface. This experience is shared by others — for example, Schor et al.[70] in their attempts to fit the collinear BeFH surface. Efforts[74] in this laboratory to use a Rotated-Morse-Curve-Spline and its variations to fit the LiFH surface for the collinear configurations have not been successful and we attribute it to the *sudden* nature of the PES.

Since we are investigating the dynamics in collinear as well as noncollinear geometries it is essential to examine the angular variation of the LiFH potential in detail. A traditional way to do this is to make fixed-bond-distance polar plot in R, θ space where R is the center-of-mass separation between Li and FH and θ is the angle between $\vec{R}$ and $\vec{r}_{HF}$. Such a plot is shown in Fig. 15 for HF fixed at its equilibrium bond distance and θ is varied. Since we are reporting the effect of reagent vibration on reaction dynamics, we are including the polar plots of the PES when HF is fixed at its inner and outer turning points of v = 0, 1, and 2 states, in Fig. 16. The existence of the spurious bumps and troughs is shown by these plots also. It must be pointed out that the PES for the rigid rotor HF-Li shown in Fig. 15 differs significantly from the potential reported earlier by Lester and Krauss,[25] reproduced in Fig. 17.

All plots shown in Fig. 11 - 16 are displays of different cross-sections of the CSCM surface and are deficient[75] in that, constraints in the form of fixed $\widehat{LiFH}$ and fixed r_{HF} have been introduced. Plots of the PE contours in hyperspherical coordinates[76] may be more revealing but they remain to be plotted for this system. Until such a plot is available, we have to synthesize in our mind the composite four dimensional PES in the (R_1, R_2, R_3) space.
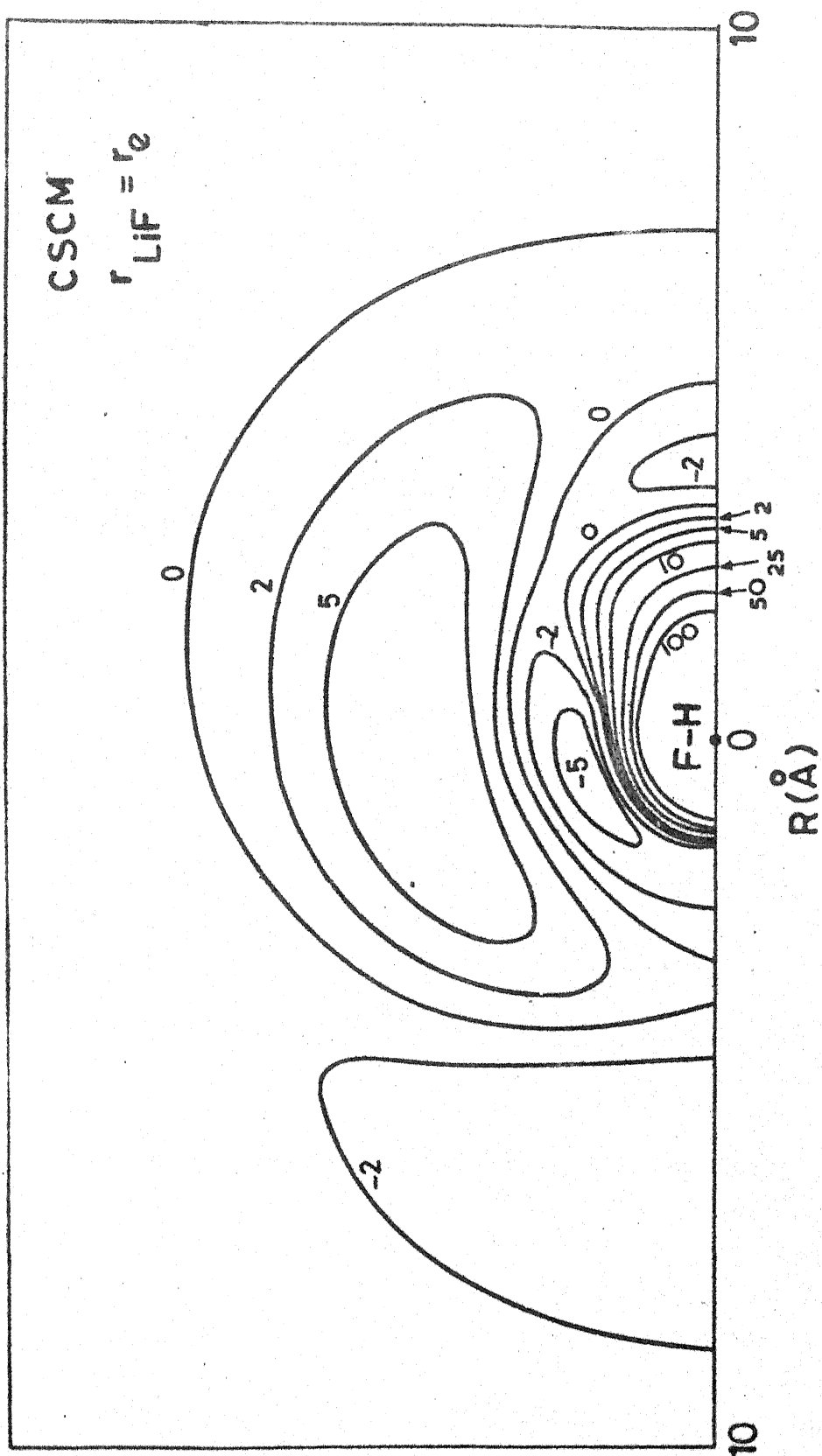
Fig. 15 P E contours for the CSCM surface in polar coordinates for $r_{LiF} = r_e$.
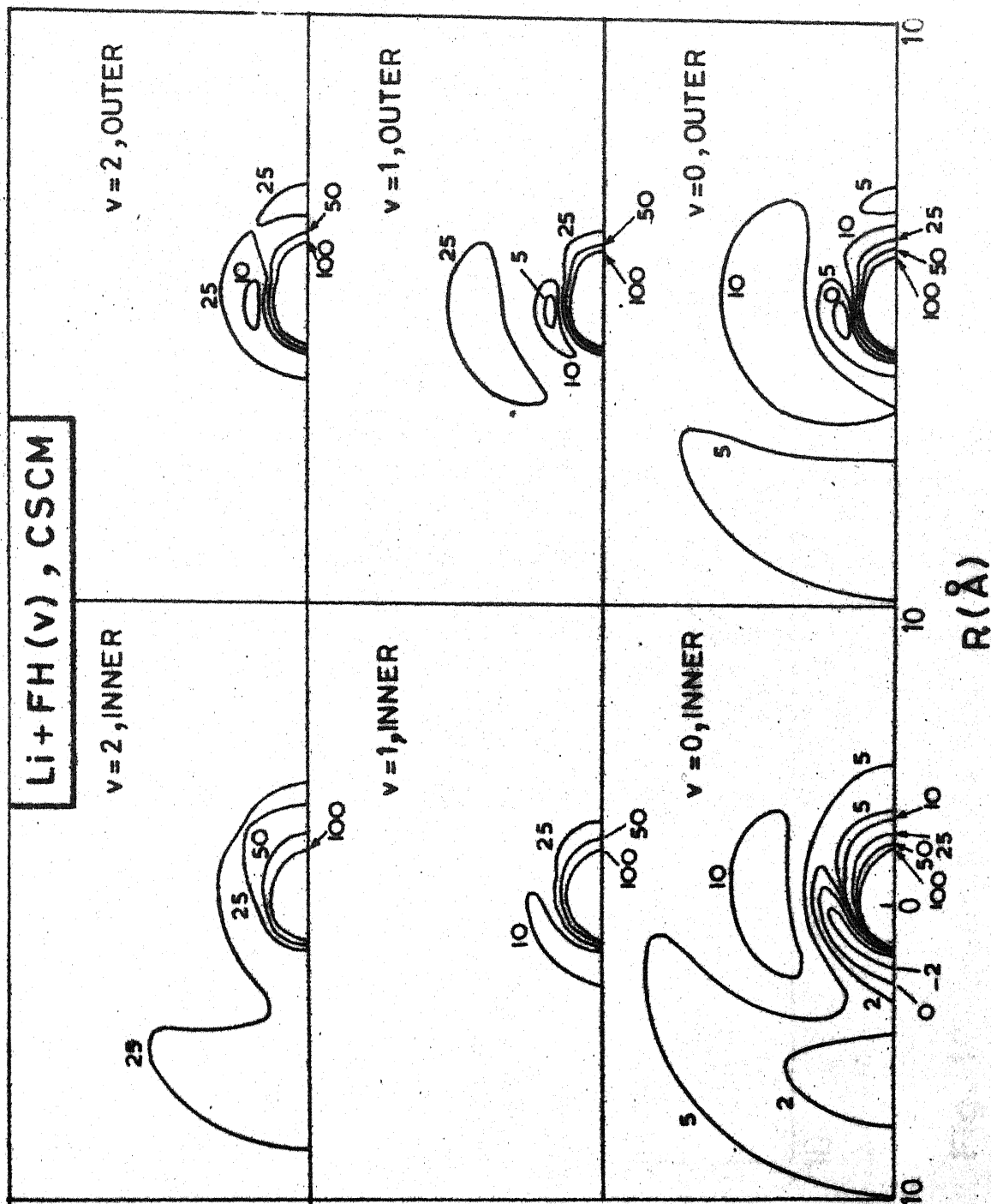
Fig. 16 Same as fig. 15 for different r_{LiF}.
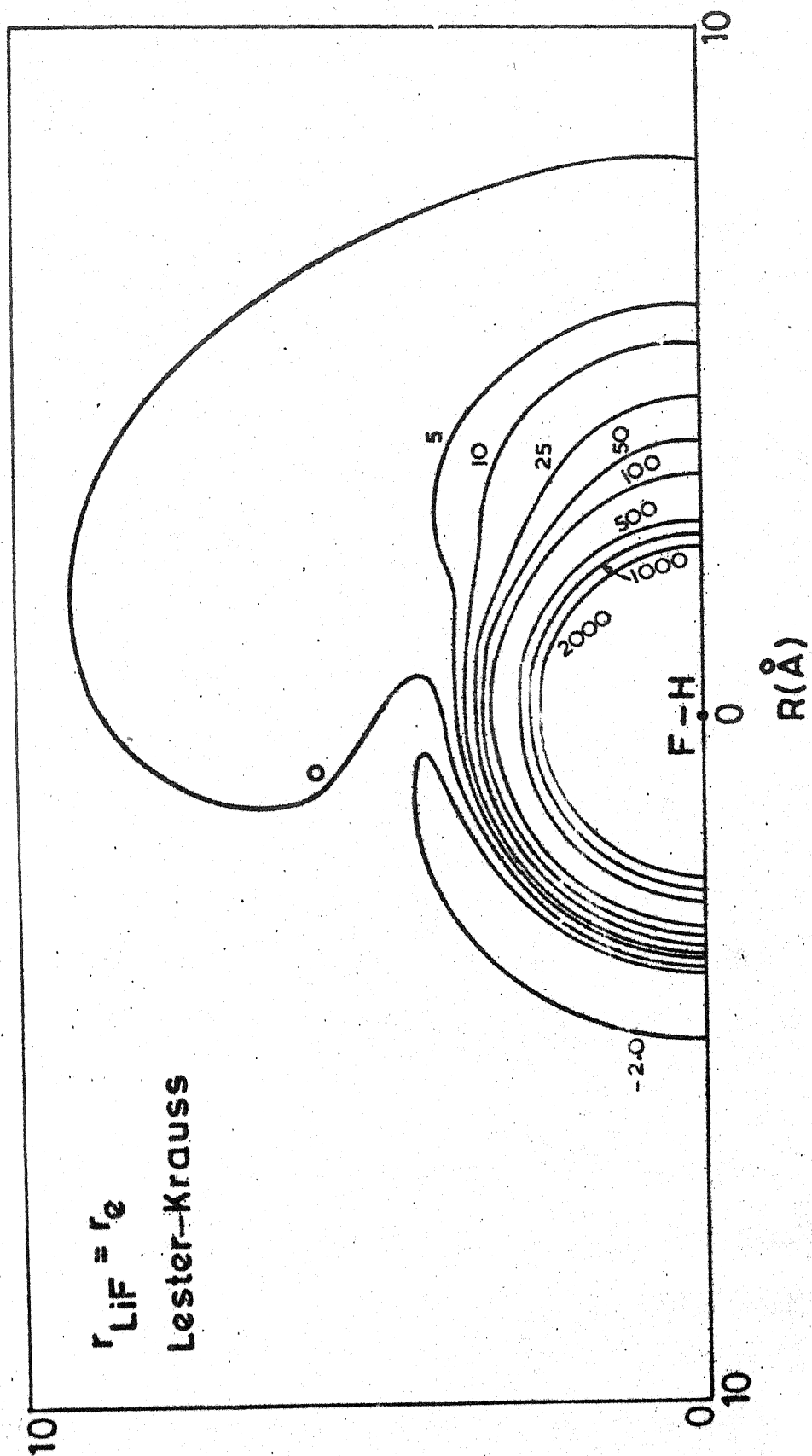
Fig. 17   Same as fig. 15 for Lester-Krauss surface.

3.2 Computational Procedure

The QCT technique has been described elsewhere.[7,8,77] The coordinate system and the procedure for initial state selection and final state analysis are the same as in ref. 77. We have used the REACTS program of J.L. Schreiber[78] with appropriate modifications. The IMSL subroutine[79] GGUB has been utilised for the generation of pseudo-random numbers for selecting the initial variables. It has been shown to have no nonrandom behaviour.[80] Stratified sampling technique[81] was used for selecting the impact parameters (b) at 0.5 $\overset{\circ}{A}$ intervals and on the whole 300-700 trajectories were run for each set of fixed values of V, R and T. The trajectories were started with the reagents set apart at 12 $\overset{\circ}{A}$. All other variables were selected randomly by the standard procedure.[7,8] Hamilton's equations were solved numerically by the 5th order Adams-Bashford predictor and 6th order Adams-Moulton corrector.[82] The accuracy of the integration was checked by energy and angular momentum conservation and step-size reduction criteria.

3.3 Reactive Collisions: Results and Discussion

3.3.1 Effect of V, T and R on reaction cross section

Since we are investigating the LiFH dynamics as a prototype alkali-hydrogen halide exchange reaction and no experimental result other than that of product scattering for the ground

vibrational state of the reagents at selected T are available for this reaction, we have chosen to investigate the effect of V, T and R on S_r for this reaction in a systematic manner and unravel the major features of the dynamics rather than to report rate constants etc.

We have computed the 3D trajectories at T = 8.7 and 20.46 kcal mol^{-1} for v = 0, J = 0. For fixed T = 8.7 kcal mol^{-1} and J = 0, we have increased v to 1 and 2. At the same T, we have investigated the variation of S_r with J for v = 0 and 2. The results are displayed in Fig. 18 along with the Monte Carlo error estimates of 2 σ (95% confidence) value.

Under the conditions of our study there is <u>no vibrational threshold for the 3D collisions</u>. Nevertheless, there is a <u>large vibrational enhancement</u> of the reaction. At fixed J= 0, as V increases from 5.87 kcal mol^{-1} to 17.24 and 28.11 kcal mol^{-1}, S_r increases from 0.75 $\pm$ 0.24 $Å^2$ to 8.67 $\pm$ 0.94 and 12.41 $\pm$ 1.04 $Å^2$ respectively. In comparison, for v = 0, J = 0 increase in T from 8.7 to 20.46 kcal mol^{-1} results in an increase in S_r from 0.75 $\pm$ 0.24 to 1.76 $\pm$ 0.40 $Å^2$ only. In particular, repartitioning of energy from T to V by $\sim$ 12 kcal mol^{-1} increases S_r by a factor of eight. These results can be attributed[13] to: (1) the saddle point lying in the exit channel and (2) the <u>sudden</u> nature of the PES as has been discussed in Chapter 2. The lack of a substantial enhancement of S_r by T can be explained by the incoming trajectories reaching the inner repulsive wall as if in a 'cul de sac'-

45
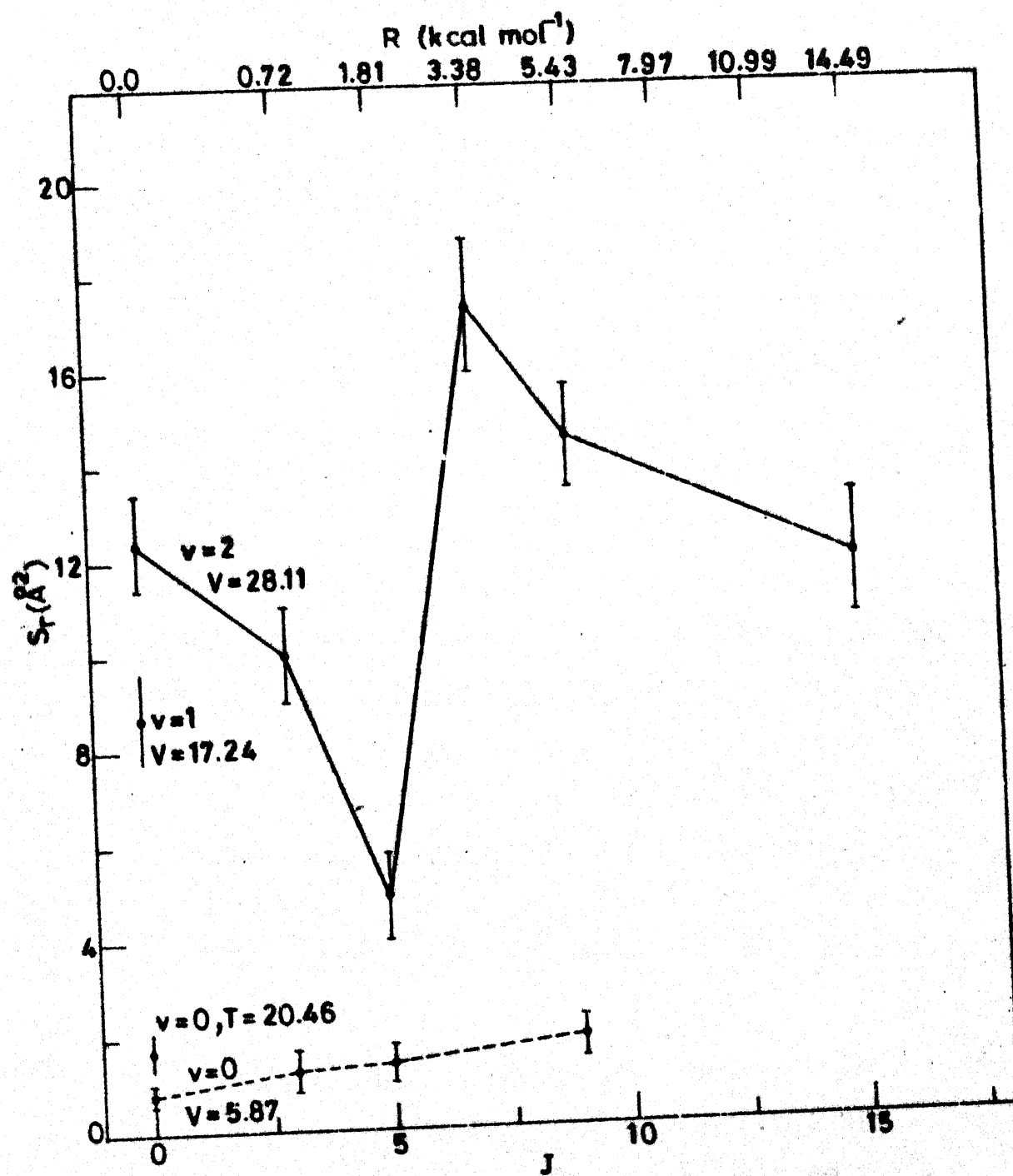
Fig. 18. Reaction cross-section as a function of V, J and T

similar to the light scattering from a mirror kept at $\sim 90^\circ$ incident angle. Increasing V means increasing the momentum along the retreat coordinate and therefore, helps in crossing the barrier located in the exit channel. Also, the trajectory is able to 'cut the corner' and reach the product channel readily.

The fact that the origin of the vibrational enhancement is different from that of trnslation is evident from the plots of the reaction probability (P^R) and partial cross section as a function of b in Fig. 19 and 20. Increase in S_r with increase in T arises from increase in P^R at the moderate impact parameter strata, whereas the increase in S_r with increase in V arises from two factors: (1) increase in P^R in each impact parameter stratum and (2) increase in the b_{max} upto which the reaction occurs. The latter would have its implications on the reaction attributes which depend on the orbital angular momentum ($|\vec{L}| = \mu v_{rel} b$).

The effect of R on S_r deserves special attention. First of all, very limited amount of data is available on this topic both experimentally and theoretically.[19] For the ground vibrational state of HF, increasing R increases S_r slightly. Even then R leads to an enhancement slight larger than T: $\Delta S_r / \Delta R = 0.2 \, \mathring{A}^2 /$ (kcal mol^{-1}) when compared to $\Delta S_r / \Delta T = 0.086 \, \mathring{A}^2 /$ (kcal mol^{-1}). For v = 2, the dependence of S_r on J is entirely different. Initially there is a sharp decline in $S_r(J)$; then there is a dramatic increase followed by a possible levelling off of S_r
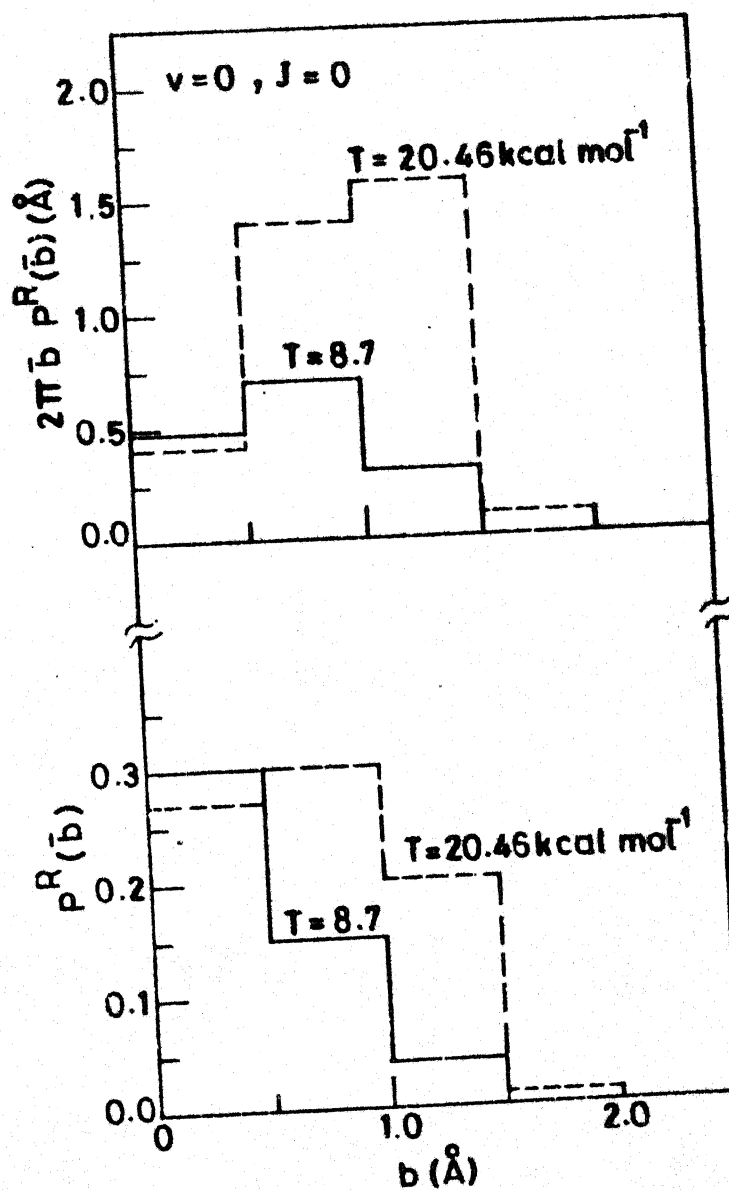
Fig. 19. Reaction probability and partial cross section as a function of impact parameter for v = 0, J = 0 at two different T.
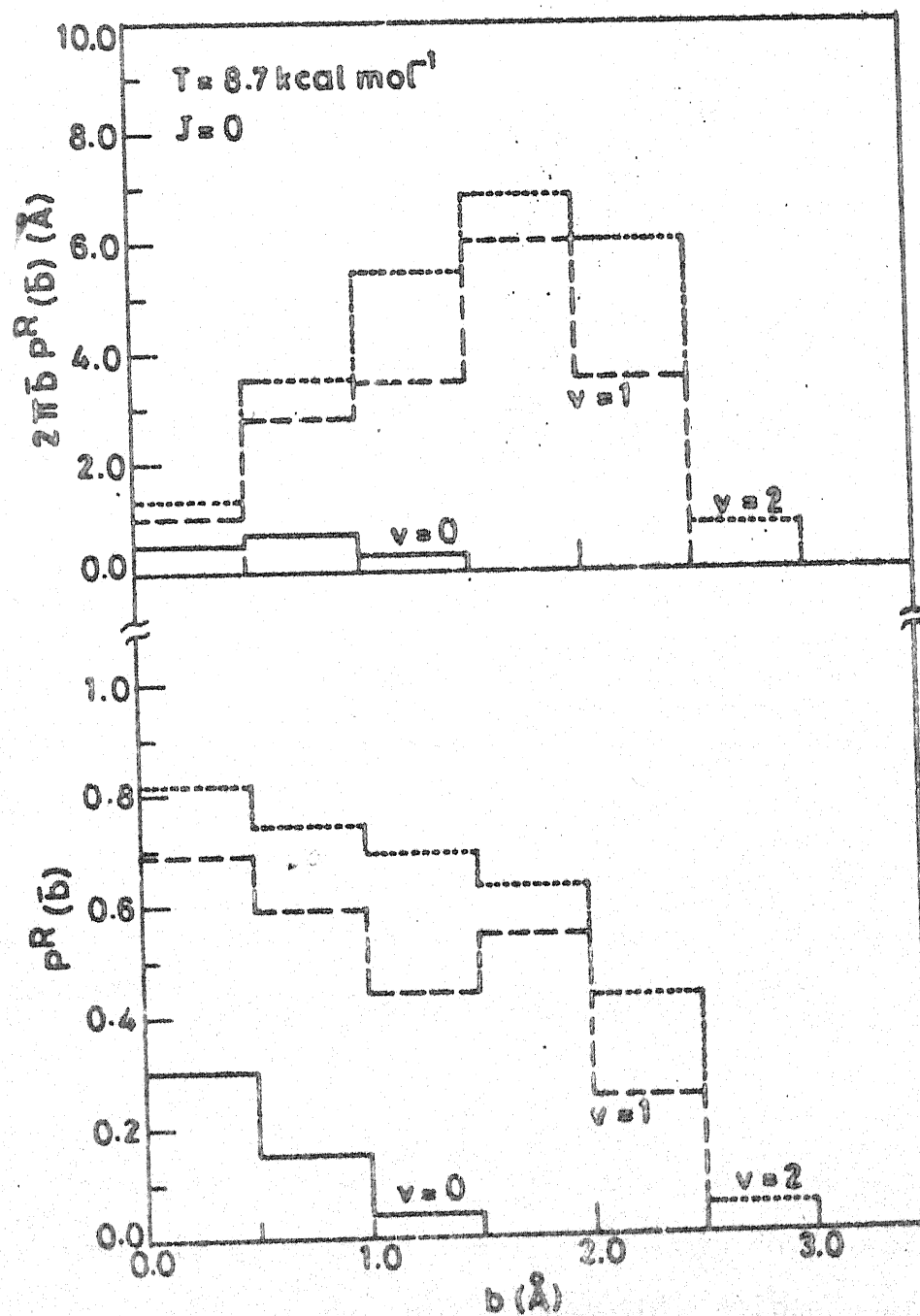
Fig. 20. Same as Fig. 19 for different v(= 0, 1, 2) at
$T = 8.7$ kcal mol^{-1}

with increase in J upto 15 with a minimum occurring around J = 5. In the J range 5-9, <u>reagent rotation is nearly four times more efficient than vibration in causing the reaction.</u>

The plot of P^R and $2\pi \bar{b}.P^R$ <u>vs</u> b in Fig. 21 illustrates how the decline in $S_r(J)$ arises from a decline in $P^R(J)$ at all the impact parameter strata. Although we have the results at other J values also, we have displayed the results only for J = 0, 5 and 7 for the sake of clarity. The increase in S_r for J = 7, over and above that of J = 0 arises <u>mainly</u> from the <u>large b</u> collisions and this would be worth investigating further.

In a preliminary communication of our results[83] (Appendix-II) we had attributed the initial decline in S_r to the disruption of the preferred orientation as this reaction has the lowest E_b when Li approaches FH at an $\widehat{LiFH}$ = 74°. The increase in $S_r(J)$ was considered to arise from vibration-rotation coupling resulting in the HF bond stretch and the molecule behaving as if it has been vibrationally excited. Such an explanation was proposed first by Polanyi and coworkers.[20] We reiterated the same explanation on the basis of the fact that for v = 0 there is only a slight increase in S_r with increase in J; but for v = 2, the change is substantial. We realise that this evidence is not strong enough to justify this explanation. Nevertheless it remains a fact that there is a <u>cooperative effect</u>[19] of v and J on S_r.
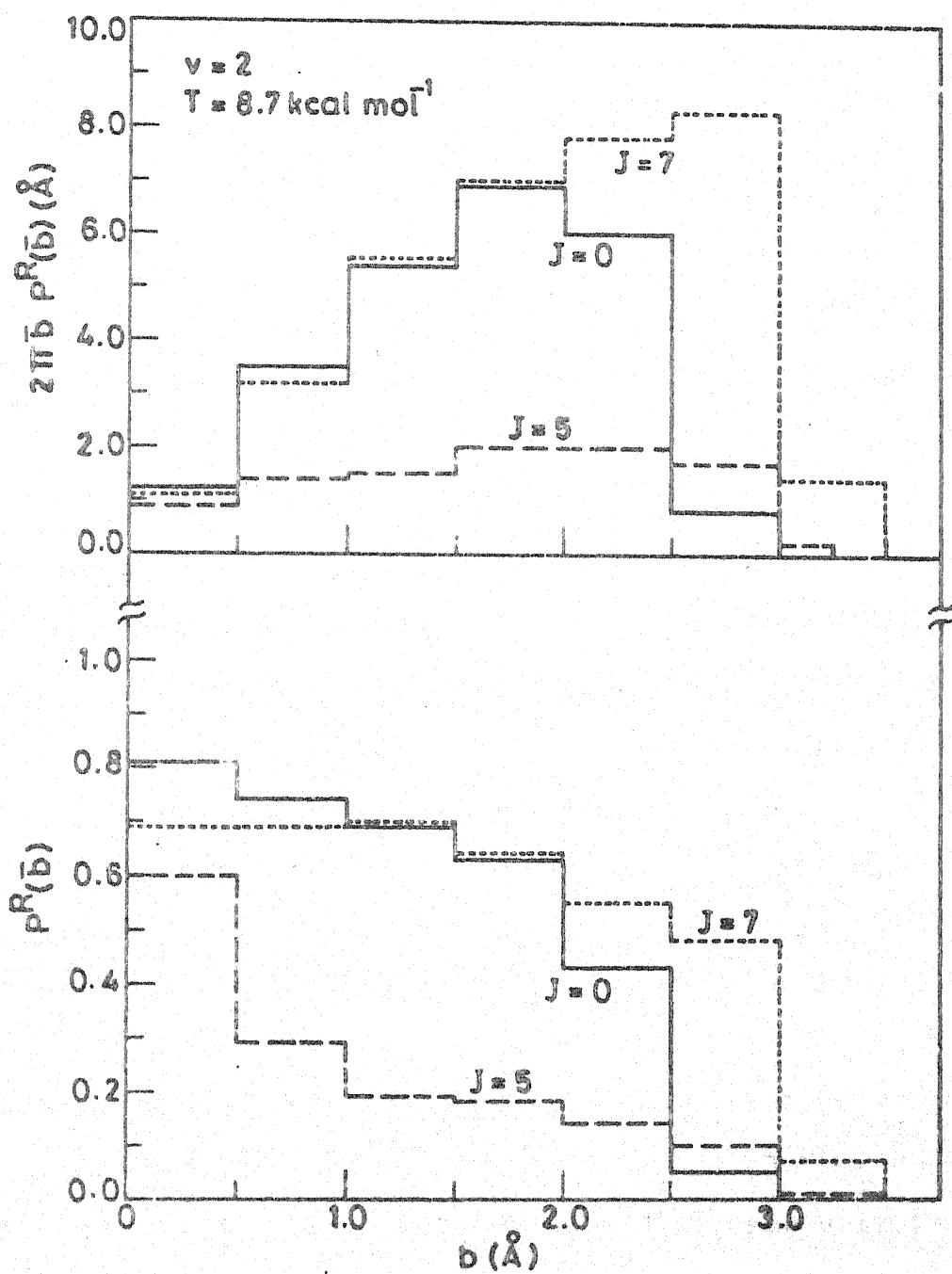
Fig. 21. Same as fig. 19 for different J(= 0, 5, 7) for V = 2 at T = 8.7 kcal mol^{-1}

Just as the molecule rotates away from the preferred

orientation for small J, it should also return to the preferred

orientation for a reasonably larger J and this is perhaps what

is responsible for the increase in S_r at the higher J values.

Rotational velocity greater than a particular value has no

influence on the orientation alignment and the molecule would

appear as a blur. This would explain the possible levelling off

of S_r at J = 15.

The orientation alignment is best illustrated through

'daisy' plots which give the position of the three particles in

the center-of-mass coordinates for coplanar trajectories. There

are reasons to believe (see later in the chapter) that the LiFH

dynamics is dominated by planar collisions. Therefore planar

trajectories would serve as a diagnostic tool in understanding

the effect of J on S_r for this reaction. A representative

trajectory that is reactive for J = 0, becomes nonreactive for

J = 5 and becomes reactive again for J = 9 at b = 1.5 $\overset{o}{A}$, is

shown in Figs. 22-24. At J = 0, as Li approaches FH, the

anisotropy of the potential steers it towards the most preferred

orientation and the reaction occurs as shown in Fig. 22. We

should add that in these plots we have displayed only the inter-

action part of the trajectory and omitted the uninteresting part

of the approach and the departure. At J = 5, rotation of the

molecule leads to an unfavourable orientation and hence the

trajectory becomes nonreactive. At J=9, by the time the
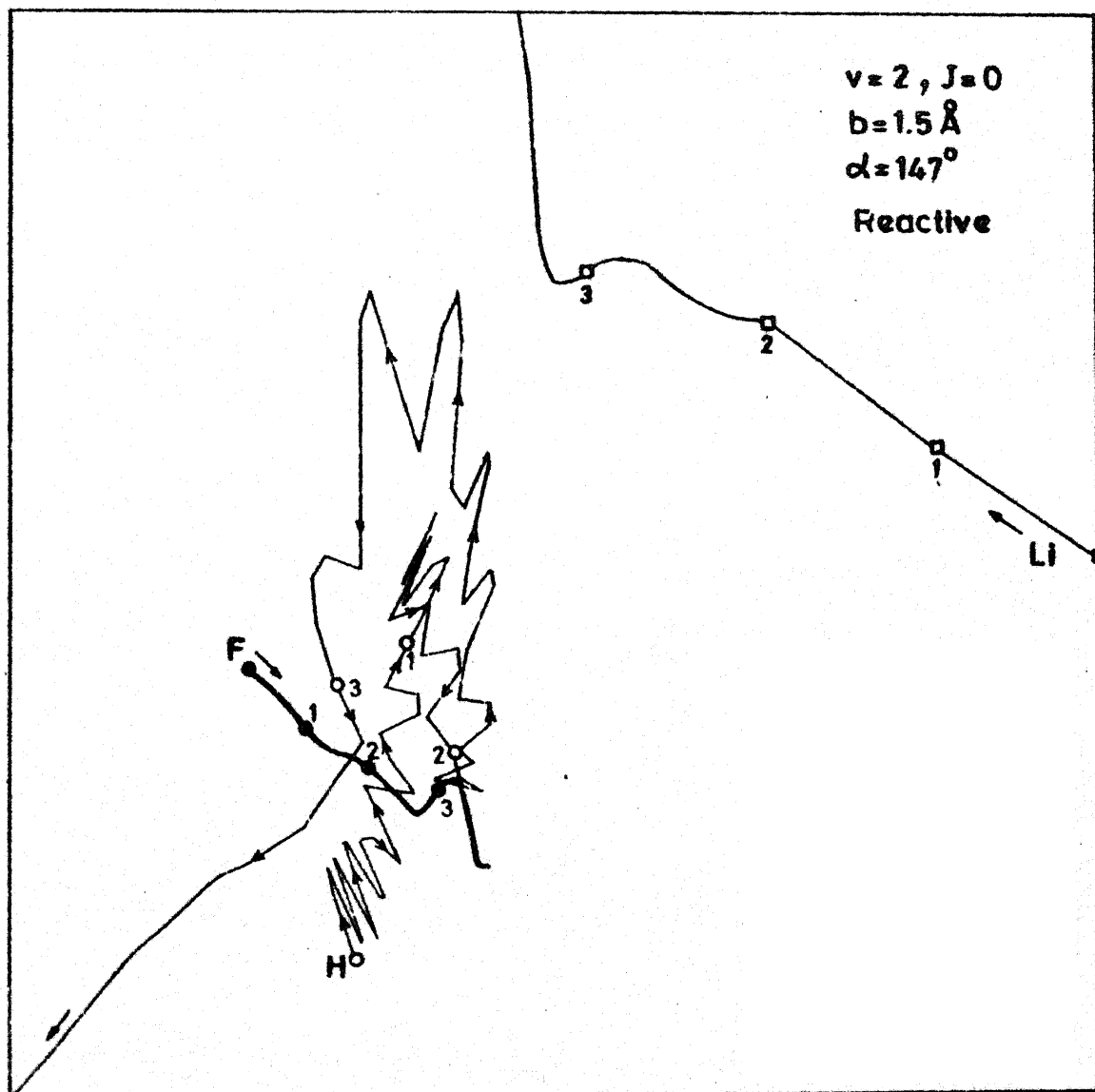
Fig. 22. A Sample 'daisy' plot for J=0. Numbers 1, 2, 3 etc. indicate multiples of 1.25×10^{-14} s.

v = 2 , J = 5
b = 1.5 Å
α = 147°
Non reactive
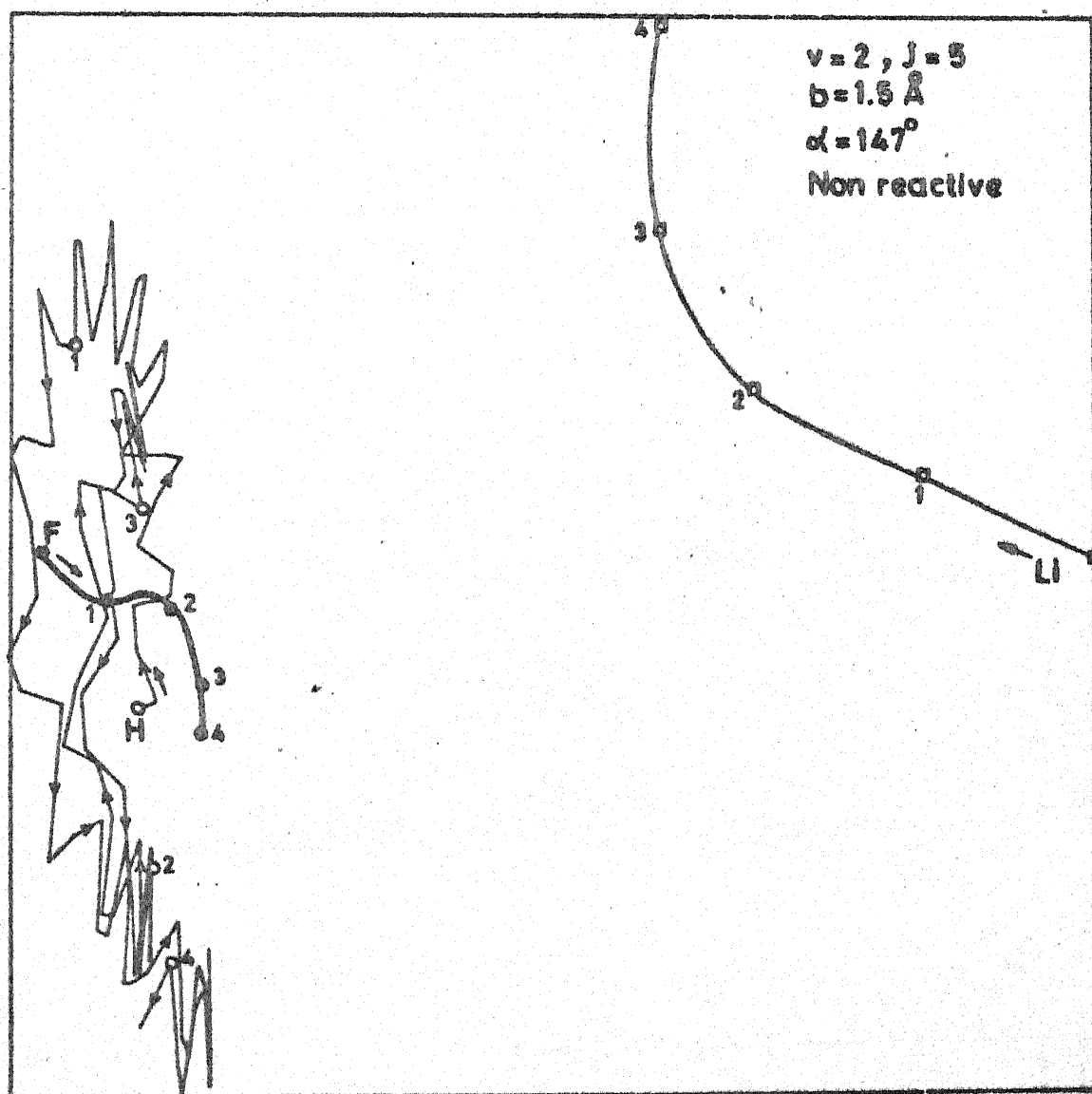
Fig. 23.   Same as Fig. 22 for J = 5

$v = 2$, $J = 9$
$b = 1.5 Å$
$\alpha = 147°$
Reactive
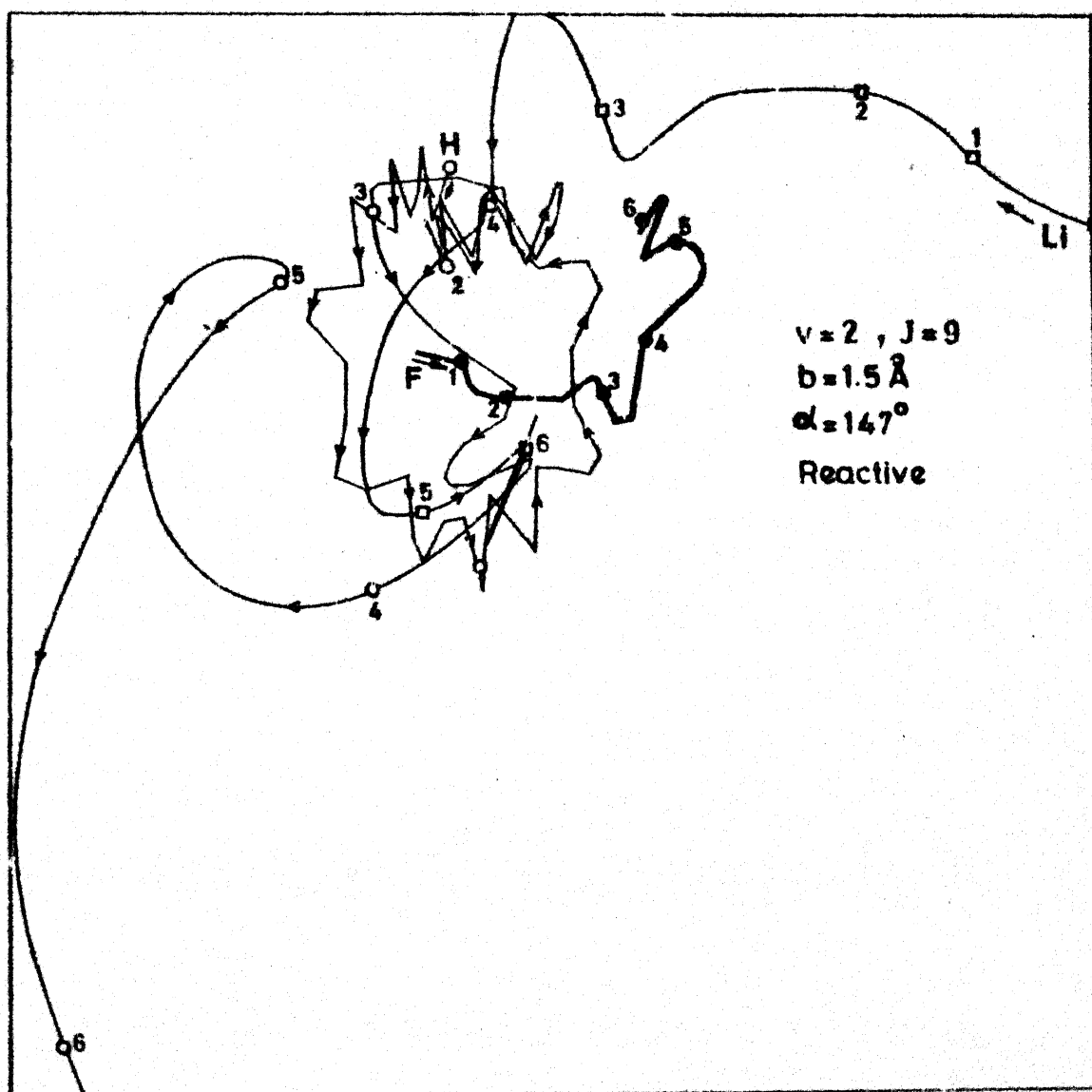
Fig. 24. Same as Fig. 22 for $J = 9$

reactants approach each other the molecule has rotated more than once and there is a favourable encounter leading to reaction. We have made an explicit study of the effect of the initial orientation on this reaction and the results are reported and discussed later in the chapter.

The effect of J on S_r for $v = 0$ is different from that of $v = 2$. One possibility is that the magnitude of S_r is so small for $v = 0$ that the variation in $S_r(J)$, except for the overall increase in S_r from $J = 0$ to 9, becomes unnoticeable. Another possibility is that there is a steady increase in S_r due to the fact that there is an increase in the number of product channels becoming available due to increase in E. That is the rotational enhancement is 'statistical' in origin. If this is the case, the QCT results would agree with the phase space theoretic (PST) predictions[84] and also the trajectories would be long-lived. As a matter of fact, molecular beam results[22] suggest the complex formation. We also find some of the trajectories to be long-lived and to show multiple collisions. A particular trajectory is illustrated in Fig. 25. The declining r_{LiF} shows that the incoming Li atom approaches the F end of the HF molecule and normally this would have resulted in the formation of LiF and r_{HF} would have increased suddenly. But in this particular trajectory. After reaching a minimum, r_{LiF} increases again, reaches a maximum and then decreases before it sets into oscillate indicating the LiF formation. This is clearly a case of a secondary encounter.
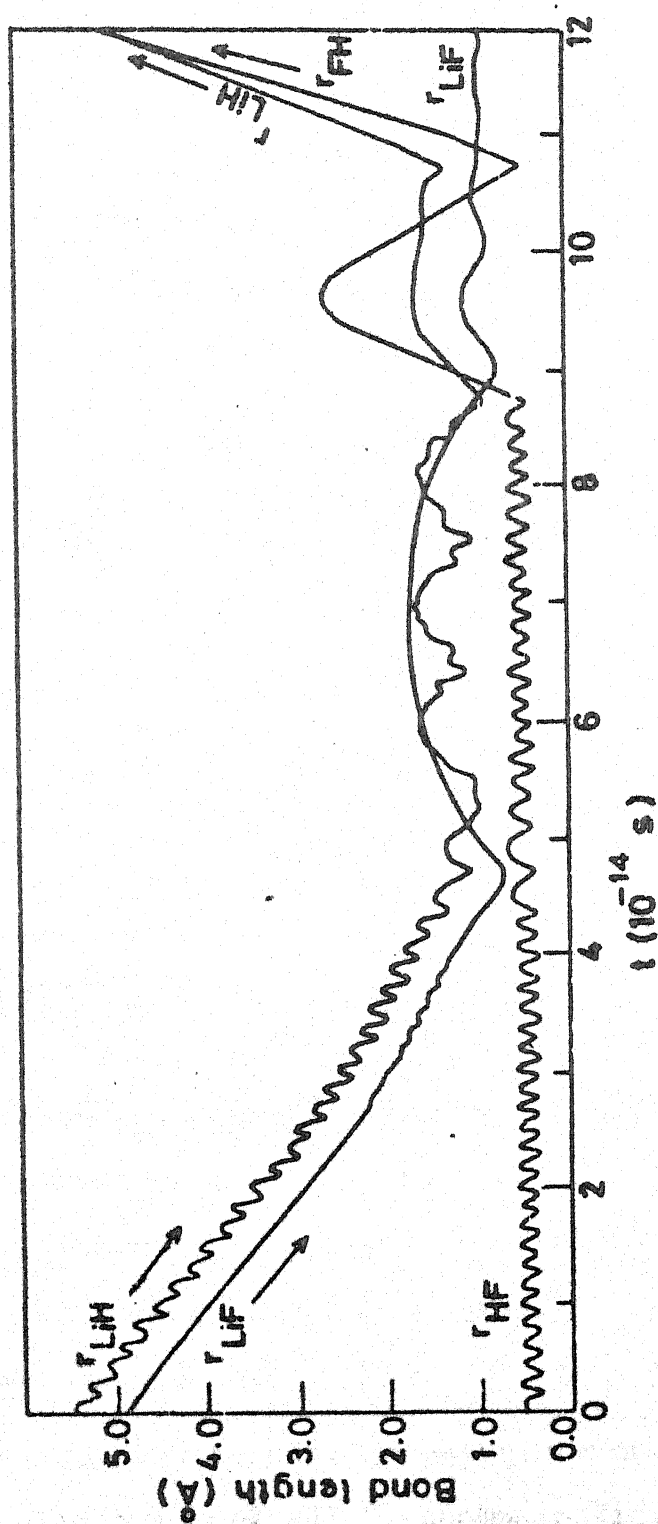
Fig. 25. Illustration of multiple collisions in a long-lived trajectory

The statistical behaviour is relfected in the product energy and angular distribution also as will be shown later in the text. It must be stressed that <u>not all</u> trajectories are long-lived. There is only a <u>qualitative</u> agreement between the QCT and PST results[85] for this reaction. Therefore we could only say that the dynamics for the HF (v = 0) shows more statistical behaviour than the HF (v = 2) and that the decline in $S_r(J)$ observed for v = 2 is distinctly <u>dynamical</u> in origin. We should also add that studies of the J - dependence of S_r for other systems[19] show that orbital angular momentum also plays an important role and that any attempt to predict the J-dependence of S_r should take into account the angular momentum factors also.

3.3.2 <u>Product energy distribution</u>

While a study of the effect of V, R and T on S_r reveals the nature of the PES in the entry channel, a study of the product energy distribution provides clues to the nature of energy release as the products separate. Its dependence on V, R and T provides additional clues on the details of the dynamics.

Product vibrational energy distribution (PVD) for v = 0, J = 0 at T = 8.7 kcal mol^{-1}, shown in Fig. 26 is nearly statistical and it remains so, for other values of J (=3, 5, 9) reiterating our earlier observation that the LiFH dynamics exhibits certain amount of statistical behaviour for HF in its
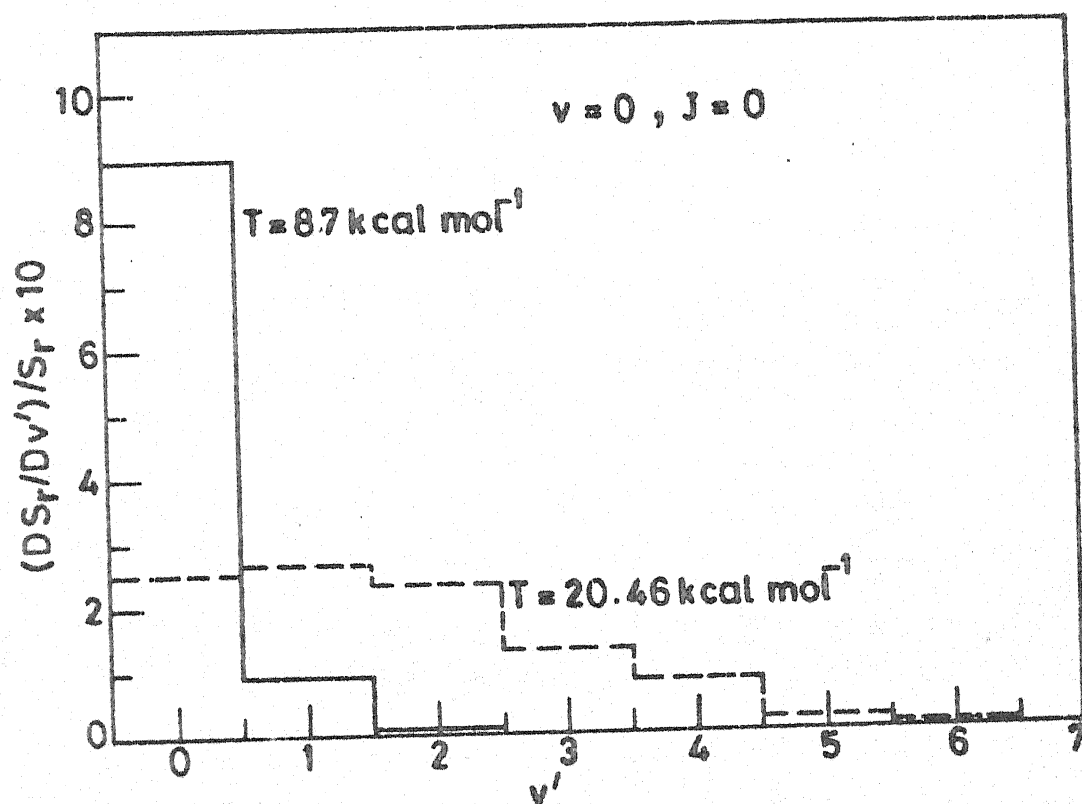
Fig. 26   Product vibrational state distribution for v = 0,
          J = 0 at two different T.

ground vibrational state. Increase in T to 20.46 kcal mol^{-1} broadens the PVD and populates LiF upto v' = 6 (in contrast to v' = 2 for v = 0). Increase in v from 0 to 1 under identical conditions (J = 0, T = 8.7 kcal mol^{-1}) also broadens the PVD and v = 2 leads to a definitely nonequilibrium distribution as shown in Fig. 27. Increase in J for v = 2 further broadens the PVD resulting in a distinct <u>bimodal</u> distribution for J = 9 and broadens still further for J = 15. It must be added that the decline in $S_r(J)$ is associated with an increasing population at higher v' and the increase in $S_r(J)$ with an increase in the population at the lower v'.

Product rotational energy distribution (PRD) also spreads out with increase in v (from 0 through 2) and T as shown in Fig. 28. The characteristic feature of this plot is that with increase in V, the maximum value of $J'(J'_{max})$ that is populated also increases. An increase in T shifts the peak of the distribution from $J' \sim 20$ to $J' \sim 30$ in addition to shifting J'_{max} from 49 to 69. This must have its origin in the increased E as well as $|\vec{L}|$. For example, the maximum b at which reaction occurs increases from 1.28 Å to 1.58 Å as T increases from 8.7 to 20.46 kcal mol^{-1}. Since the PRD is more spread out than the PVD, it becomes difficult to comment on the effect of J on PRD.

The simplest way to characterise a distribution is to report the first moment of the dependent variable. For v = 0, J = 0 at T = 8.7 kcal mole^{-1}, $\langle v' \rangle = 1.09 \pm 0.34$, $\langle R' \rangle = 2.56 \pm 0.76$,
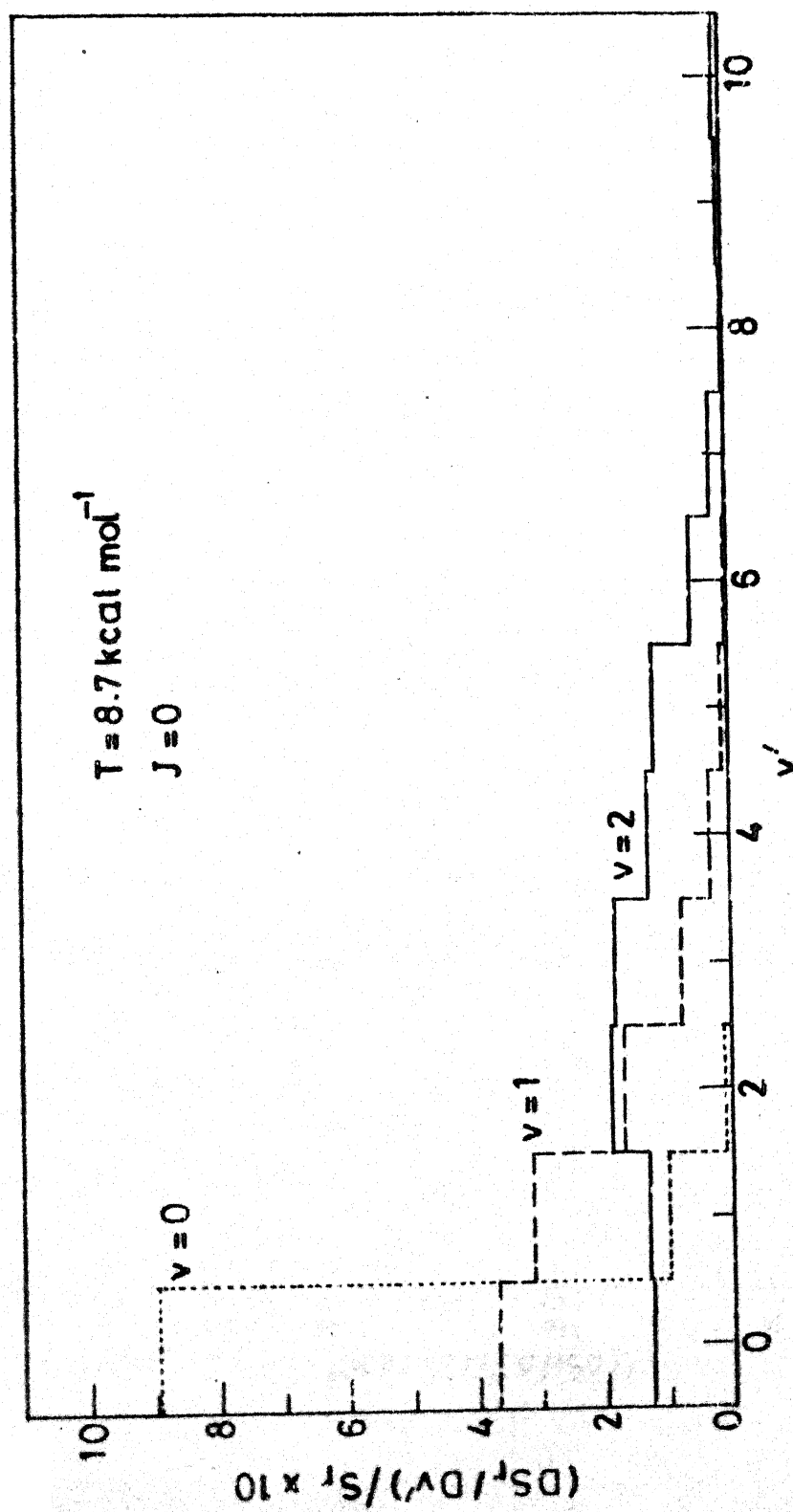
Fig. 27. Same as Fig. 26 for different v at T = 8.7 kcal mol⁻¹
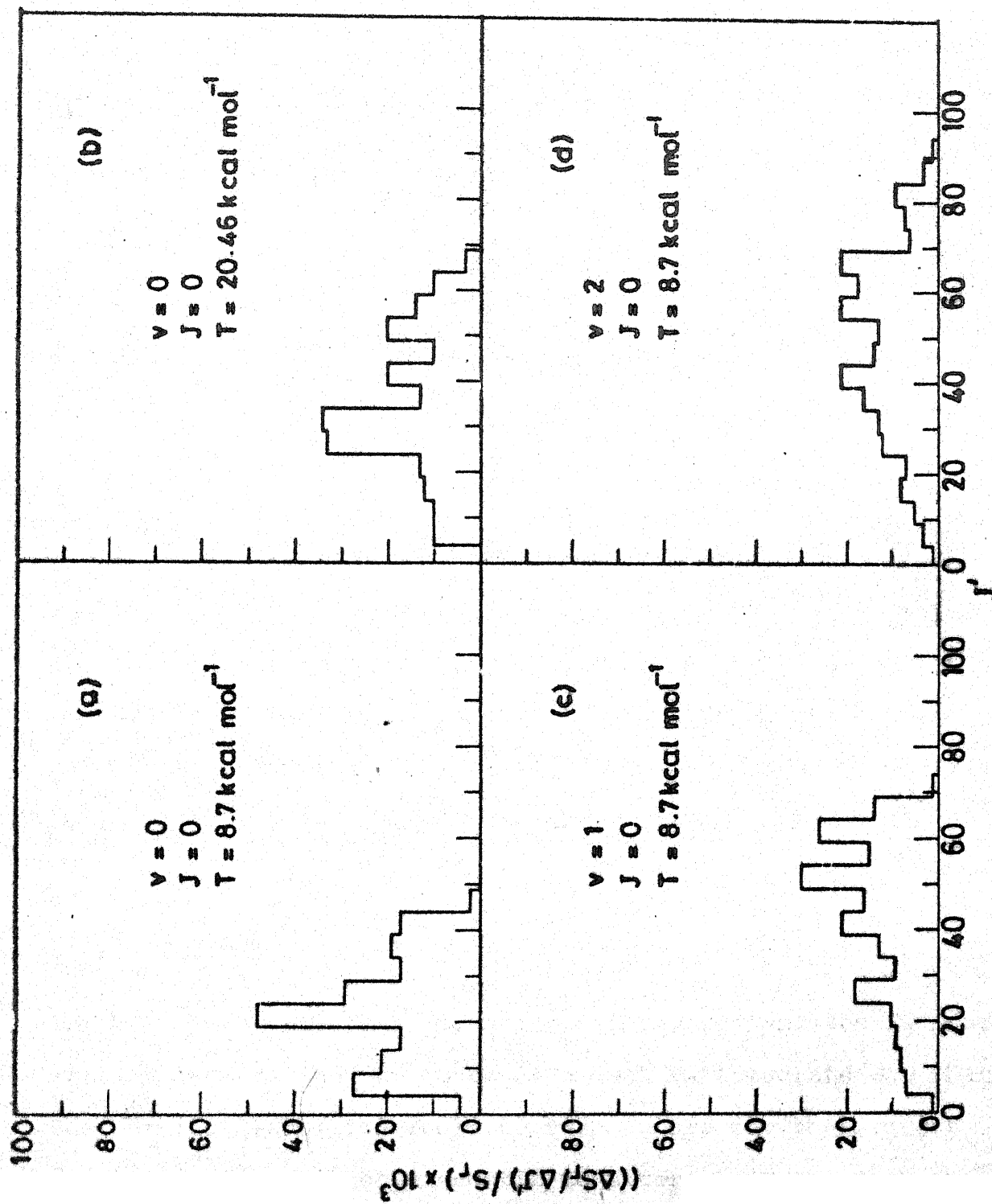
Fig. 28. Product rotational state distribution for J = 0, for different v and T

$\underline{L}$ = light) category and have been predicted[87] to show the $\vec{L} \rightarrow \vec{J}'$ conversion as the initial reduced mass of the reactants is very much larger than that of the products. When $\vec{L}'$ is small (as it would be when the product reduced mass is small) at $\vec{J} \sim 0$ the angular momentum conservation $\vec{L} + \vec{J} = \vec{L}' + \vec{J}'$ requires that $\vec{L} \simeq \vec{J}'$. In the case of the reaction (R4), Li is not heavy enough to lead to a 100% conversion. Particularly for v = 0, the reaction takes place at small b and therefore, there is very little correlation between $\vec{L}$ and $\vec{J}'$ as shown in Fig. 29. For v = 1 and 2, however, the reaction is dominated by collisions at larger b and hence $\vec{L} - \vec{J}'$ correlation becomes substantial as illustrated for v = 2 in Fig. 30. An implication of this correlation is that $\theta_{\vec{J}.\vec{L}} = 0^{\circ}$ or 180° and this has been found to be the case. This condition also implies coplanarity of the collision (see later). With very little change in reactive b, increasing J from 0 through 15 would mean a lesser correlation between $\vec{L}$ and $\vec{J}'$ and this is reflected in the correlation coefficient changing from 0.57 to 0.48.

The fate of additional reagent energy in a reaction has been the subject of a series of investigations and conversion rules like $\Delta V \rightarrow \Delta V'$ and $\Delta T \rightarrow \Delta T' + \Delta R'$ have emerged in recent years[88] for several bimolecular exchange reactions. We report in Fig. 31 the variation of $\langle V' \rangle$, $\langle R' \rangle$ and $\langle T' \rangle$ with V at T = 8.7 kcal mol^{-1} for J = 0. At low V, ΔV ends up predominantly as $\Delta R'$. But at a higher V, $\Delta V \rightarrow \Delta V'$ conversion is more important. Detailed studies[88] on model systems have shown the
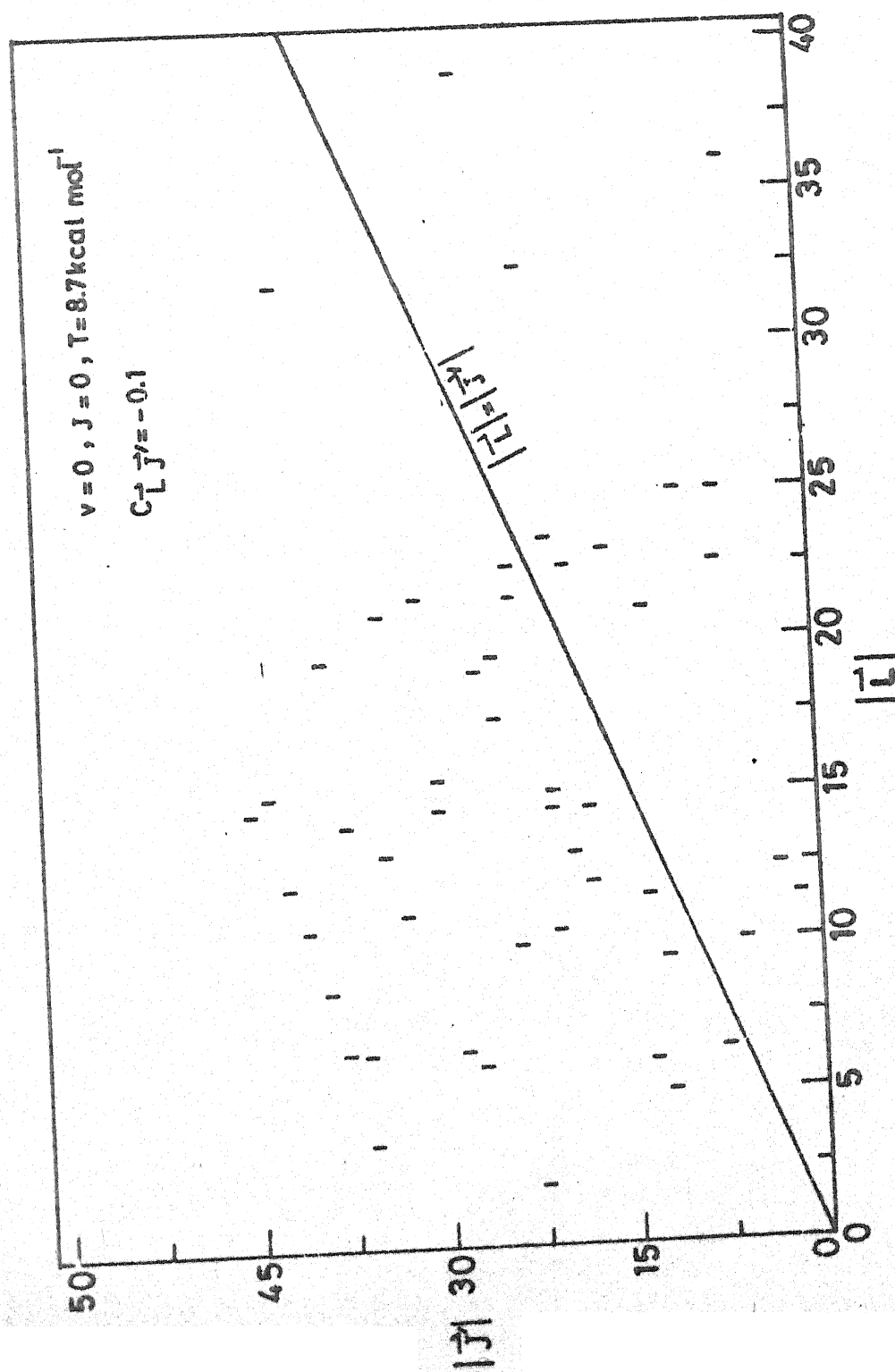
Fig. 29. Lack of correlation between $|\vec{L}|$ and $|\vec{J}|$ for $v=0$, $J=0$ at $T=8.7$ kcal mol^{-1}
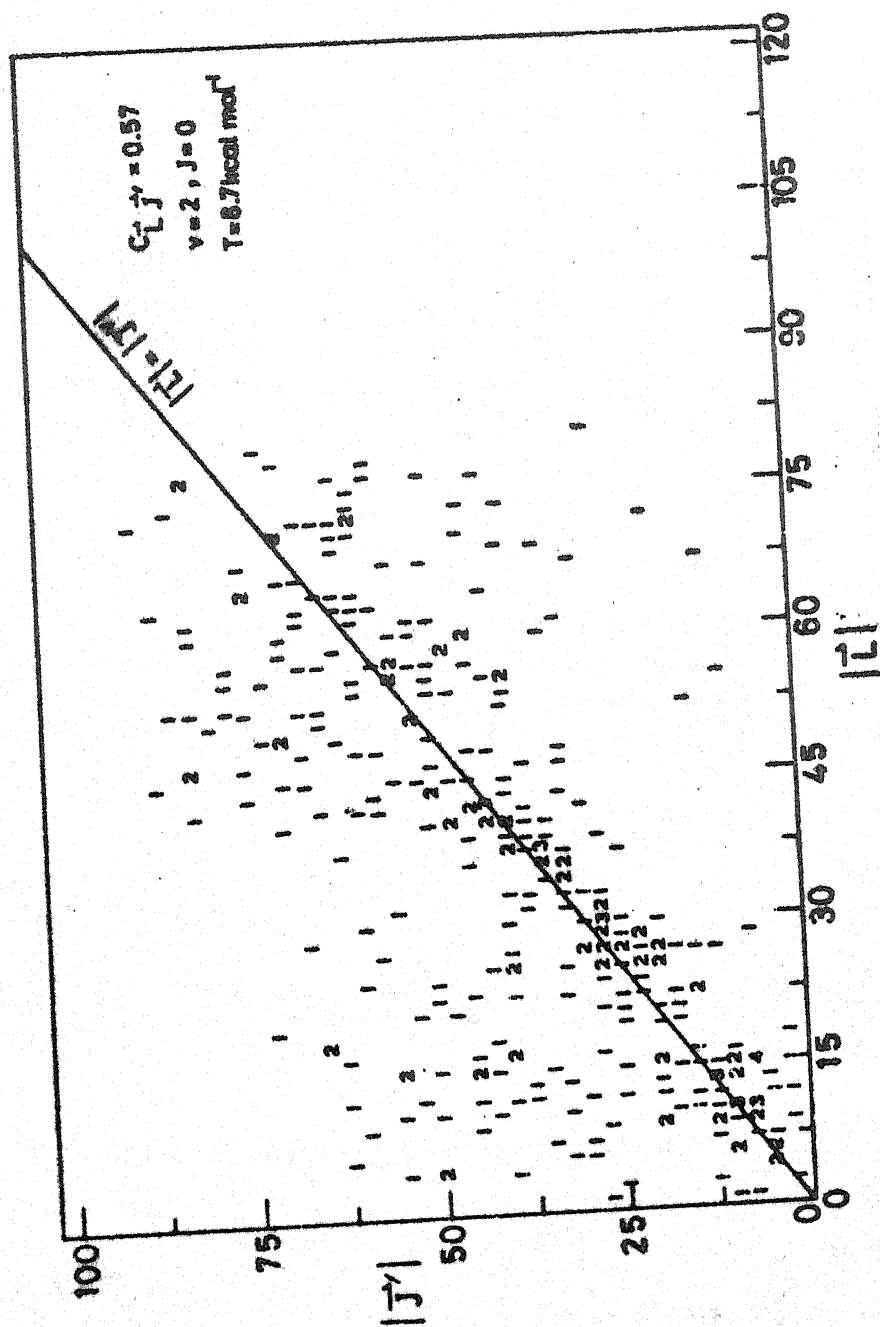
Fig. 30. Correlation between $|\vec{L}|$ and $|\vec{J'}|$ for $v=2$, $J=0$ at $T=8.7$ kcal mol^{-1}. The numbers 1, 2, 3, 4 indicate the number of points in that position

$C_{LJ'} = 0.57$
$v=2, J=0$
$T=8.7$ kcal mol^{-1}
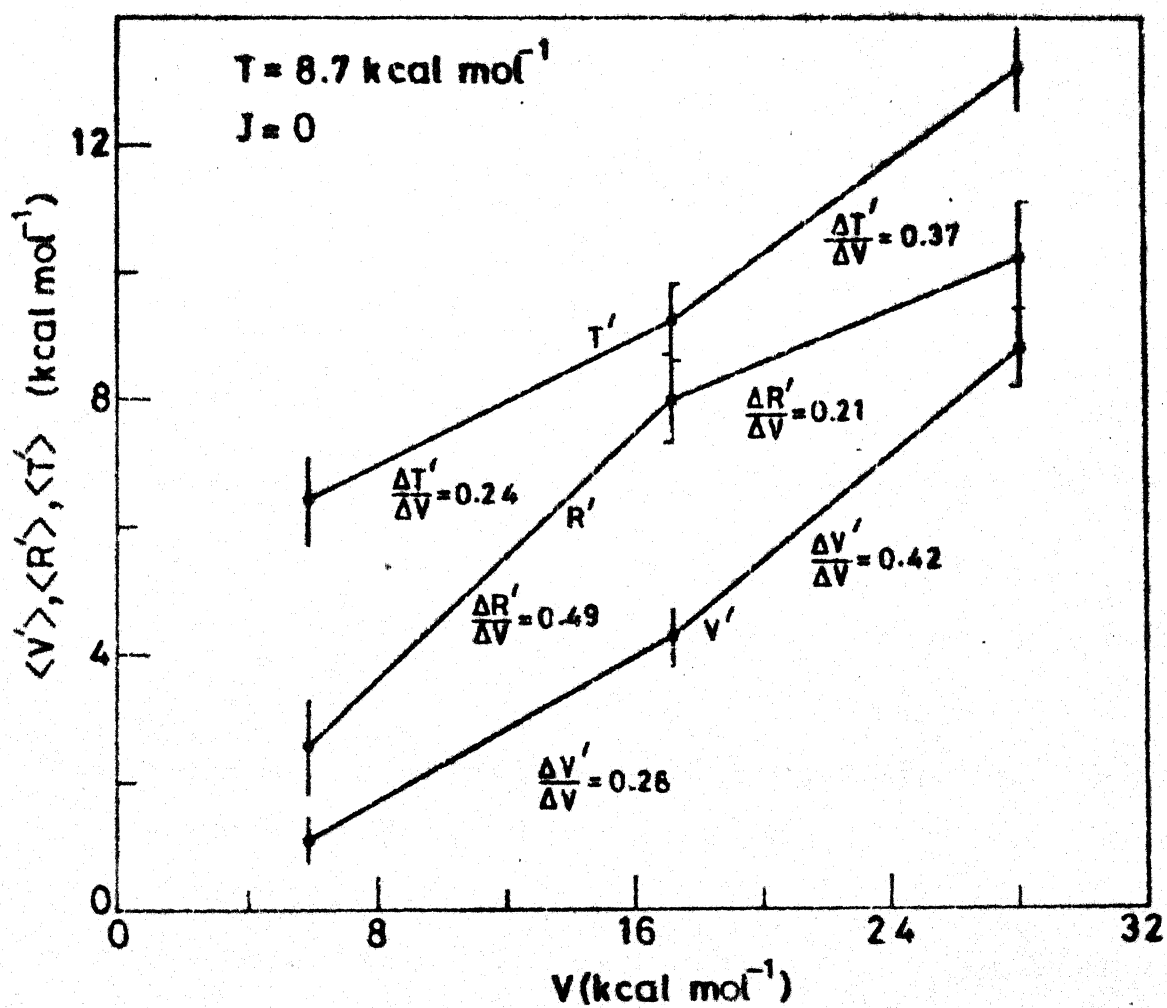
Fig. 31. Variation of $\langle V \rangle$, $\langle R \rangle$ and $\langle T \rangle$ with V at
T = 8.7 kcal mol^{-1} for J = 0

$\Delta V \rightarrow \Delta V'$ conversion to be less efficient on a _sudden_ surface than on a _gradual_ surface and ΔT to become mostly $\Delta T' + \Delta R'$ on the former. We observe the same trend in our system when T is increased from 8.7 to 20.46 kcal mol^{-1}: $\Delta V'/\Delta T = 0.35$, $\Delta R'/\Delta T = 0.26$ and $\Delta T'/\Delta T = 0.38$. The variation of $\langle V' \rangle$, $\langle R' \rangle$ and $\langle T' \rangle$ with R is erratic and no clear cut picture of the R dependence could emerge. However, for the particular case of J changing from 5 to 7 ($R = 1.81$ kcal $mol^{-1} \rightarrow 3.38$ kcal mol^{-1}) $\langle R' \rangle$ changes from 10.21 to 13.81 kcal mol^{-1} implying that $\Delta R \rightarrow \Delta R'$; in addition, part of V and T have been converted to R'.

3.3.3 Product angular distribution

The product angular distribution (PAD) in Fig. 32 shows peaks at an atomic scattering angle (θ_{at}) of 0° and 180° for $v = 0$, $J = 0$, $T = 8.7$ kcal mol^{-1}. For reaction proceeding via a long-lived complex, the PAD is determined solely by the conservation of the total angular momentum. This conservation implies for cases in which $\vec{L} \gg \vec{J}$ a _symmetric_ distribution proportional to $1/\sin \theta$ will occur.[89] The distribution we have reported is not completely symmetrical. The product molecule is preferentially forward scattered. The dynamics is not completely statistical because T is larger than the well depth (~ 6 kcal mol^{-1}, for $\widehat{LiFH}$ = 114°) in the PES. At a still higher T of 20.46 kcal mol^{-1}, the peak at $\theta_{at} = 0^{\circ}$ becomes prominent implying that the product
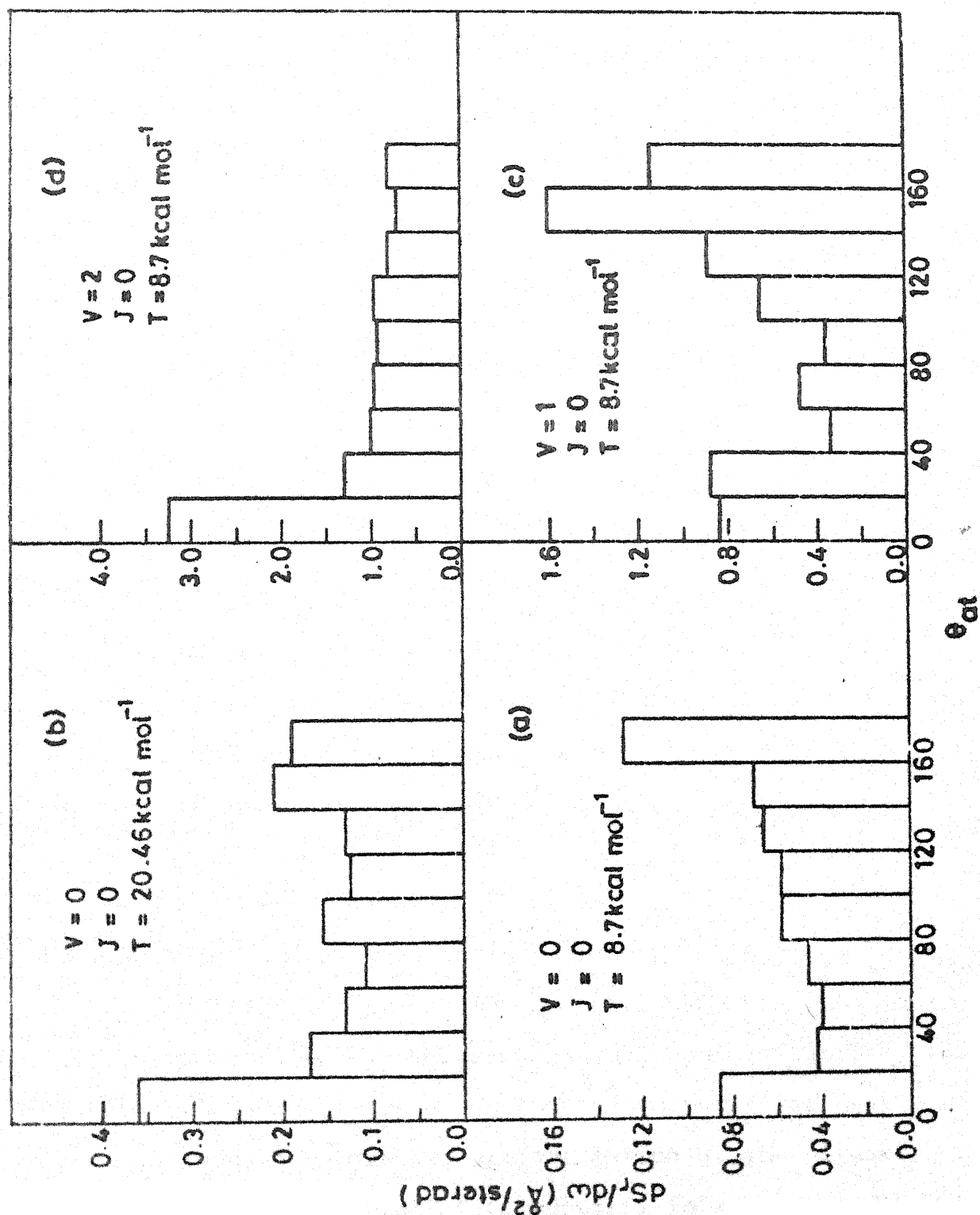
Fig. 32. Product angular distribution for different v and
T for J = 0

molecule is more backward scattered. For $v = 2$, the peak at $\langle \theta_{at} \rangle = 180^o$ essentially disappears. That is, the product molecule is predominantly backward scattered. This is surprising as the vibrational enhancement arises partly from an increased b_{max} and under these conditions one expects more forward scattering. For $v = 2$, at $T = 9.7$ kcal mol^{-1}, changes in $\langle \theta_{at} \rangle$ are within the statistical error estimates for $J = 0 - 9$, but a further increase in J from 9 to 15 results in a change in $\langle \theta_{at} \rangle$ from 92 ± 4.6^o to 107 ± 7.2^o. That is, a large rotational excitation results in a larger forward scattering of LiF. We have no explanation for this observation at this stage.

3.3.4 Planarity of the collision

When the rotation of the reactant molecule and the orbital motion of the incoming atom with respect to the rotor are coplanar, there is no component of motion to move the three atoms out of the initial plane and the reaction remains coplanar. An observable of planarity[90] is the polarization angle γ, that is the angle between the initial relative velocity vector and $\vec{J}'$. Results in Fig. 33 show the distribution of γ to be mostly around 90° which corresponds to planar collisions. This is because the centre-of-mass of the rotating HF is nearly at the F-end and therefore the orbital motion of the attacking Li atom is nearly the motion of Li about F, in a plane defined by the relative velocity vecotr and the centre of mass of FH.
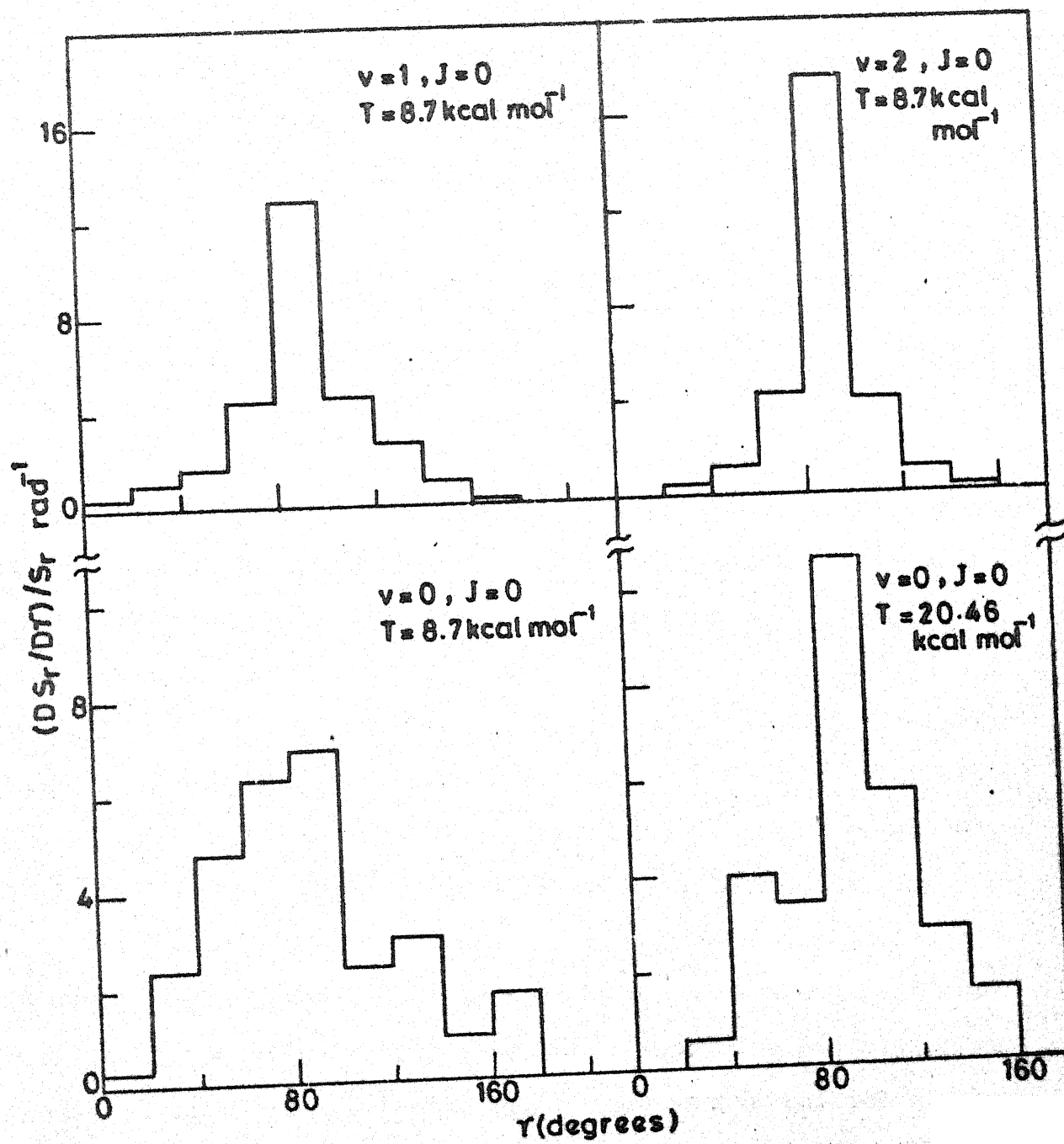
Fig. 33. Distribution of γ for different v and T for J=0

Since the H atom departs with negligible momentum, Li and F continue to rotate in the same plane after formation of the new bond. The shape of the distribution in γ can be seen to be correlated with the $\vec{L} - \vec{J}'$ correlation or lack thereof.

3.3.5 Effect of initial orientation

In recent years it has become possible[2,91,92] to select the relative orientation of reactants and study its effect on various reaction attributes. Although no experimental results are available for the reaction (R4), Zare and coworkers[2] have reported recently on the effect of initial reagent orintation on PVD for the strontium analog. We have computed S_r at three different orientations α (defined in Fig. 34) = $0°$, $90°$ and $180°$ for $v = 2$, $J = 0$ at $T = 8.7$ kcal mol^{-1}. In these calculations, α was chosen at a fixed value while all other variables were selected randomly from appropriate distribution functions, as usual. The results are reported in Table 3 and they show that S_r is the largest for $\alpha = 0°$, less for $90°$ and the least for $180°$, indicating that the approach of Li towards the F end of HF is much more preferred over the H end. The product energy disposal also shows a definite dependence on the initial orientation of the reagents. As α increases, the average fraction of vibrational energy, $\langle f_v \rangle$ increases at the expense of $\langle f_R' \rangle$. Effect of changing α on PVD is shown in Fig. 35. As α changes from $0°$ to $90°$, more of higher v' levels become populated and
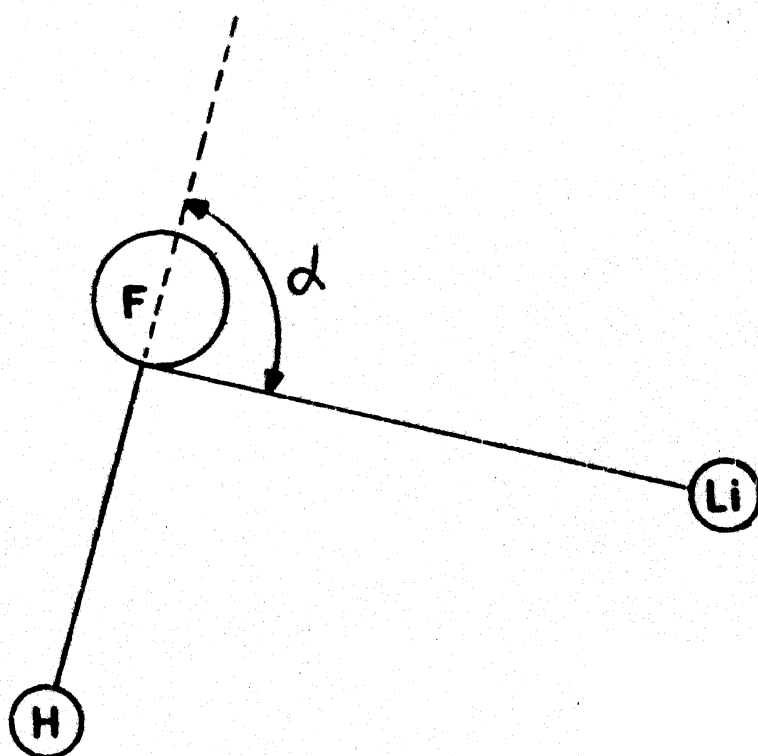
Fig. 34. Definition of α

Table 3. Effect of orientation on various reaction attributes, for $v=2$, $J=0$ at $T = 8.7$ kcal mol^{-1}

		α	
	0°	90°	180°
$S_r'(\mathring{A}^2)$	19.60 ± 1.55	12.55 ± 0.70	1.93 ± 0.29
$\langle f_V' \rangle$	0.19	0.24	0.37
$\langle f_R' \rangle$	0.32	0.28	0.09
$\langle f_T' \rangle$	0.44	0.44	0.50
Total No. of traj.	331	243	220
No. of reactive traj.	233	197	32
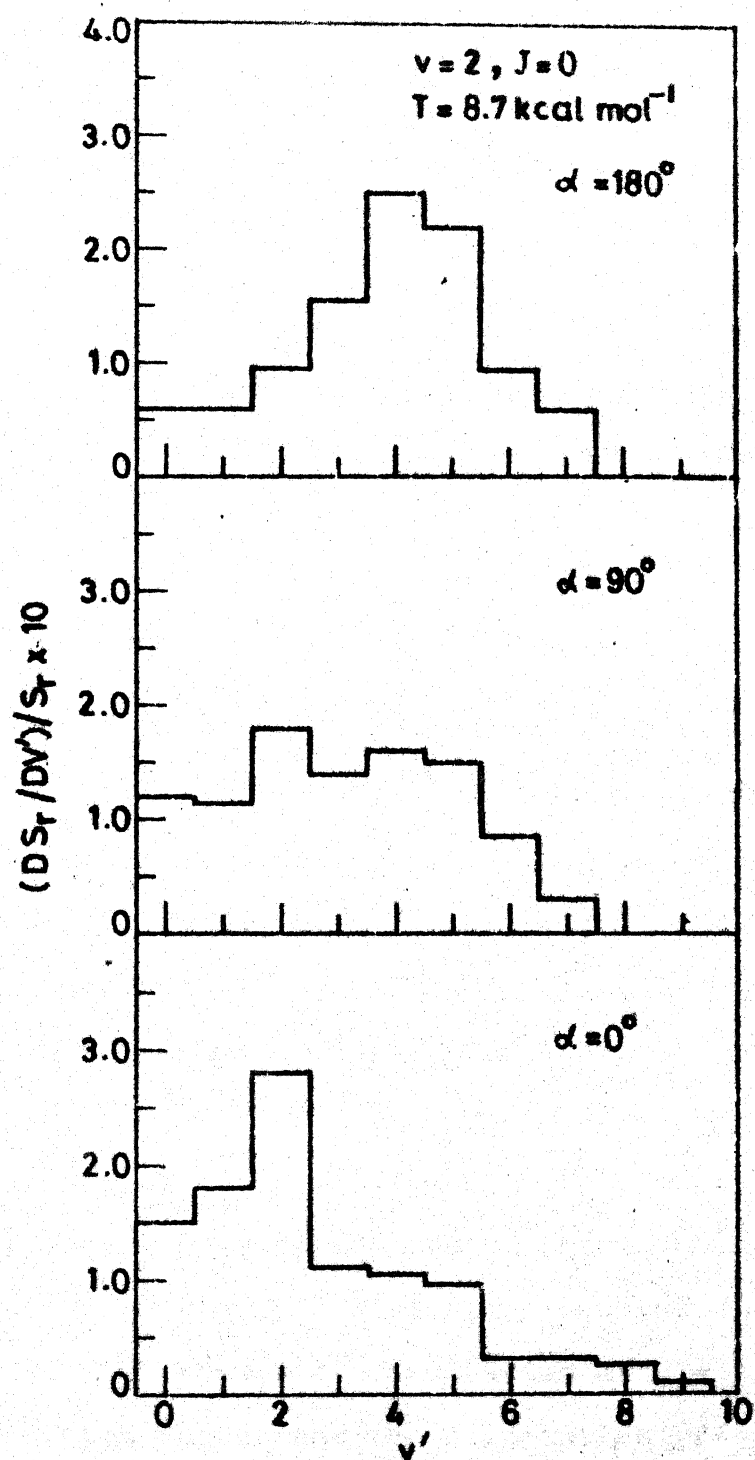
Fig. 35. Product vibrational state distribution for different α.

the PVD becomes broader. At $\alpha = 180^{\circ}$, the PVD becomes narrower, with the $v' = 4$ level being preferentially populated.

It is clear from Fig. 36 that the PRD becomes more specific for the broadside attack. Though the maximum of PRD for $\alpha = 0^{\circ}$ and 90° remains unchanged at $J' \simeq 50$, for $\alpha = 180^{\circ}$, PRD becomes narrower and the histogram peak shifts back to $J' \simeq 25$. As α changes from 0° to 90°, the peak of the PAD histogram shifts from $\theta_{at} \simeq 0^{\circ}$ to $\theta_{at} \simeq 180^{\circ}$ as shown in Fig. 37. For $\alpha = 180^{\circ}$, the PAD becomes broader and the product is scattered in all the directions.

We have also investigated the effect of orientation at different J values, by calculating 50 trajectories in the range $b = 1 - 1.5$ Å, at which J is found to have a large effect and the results are given in Table 4. The orientation that is reactive at $J = 0$ becomes nonreactive at $J = 5$ and vice versa. At $J = 9$, the reagent rotation is found to have very little effect. This is because, half of the rotational period for FH at $J = 5$ is about the same as that of the time taken by Li to approach FH. Thus, even though Li was at the H end initially ($\alpha = 180^{\circ}$), as it approaches FH, it encounters the F end and the reaction takes place readily. A similar argument holds for the non-reactivity of the $\alpha = 0^{\circ}$ orientation at $J = 5$. At $J = 9$, the molecule rotates faster and the orientation effect becomes minimal.
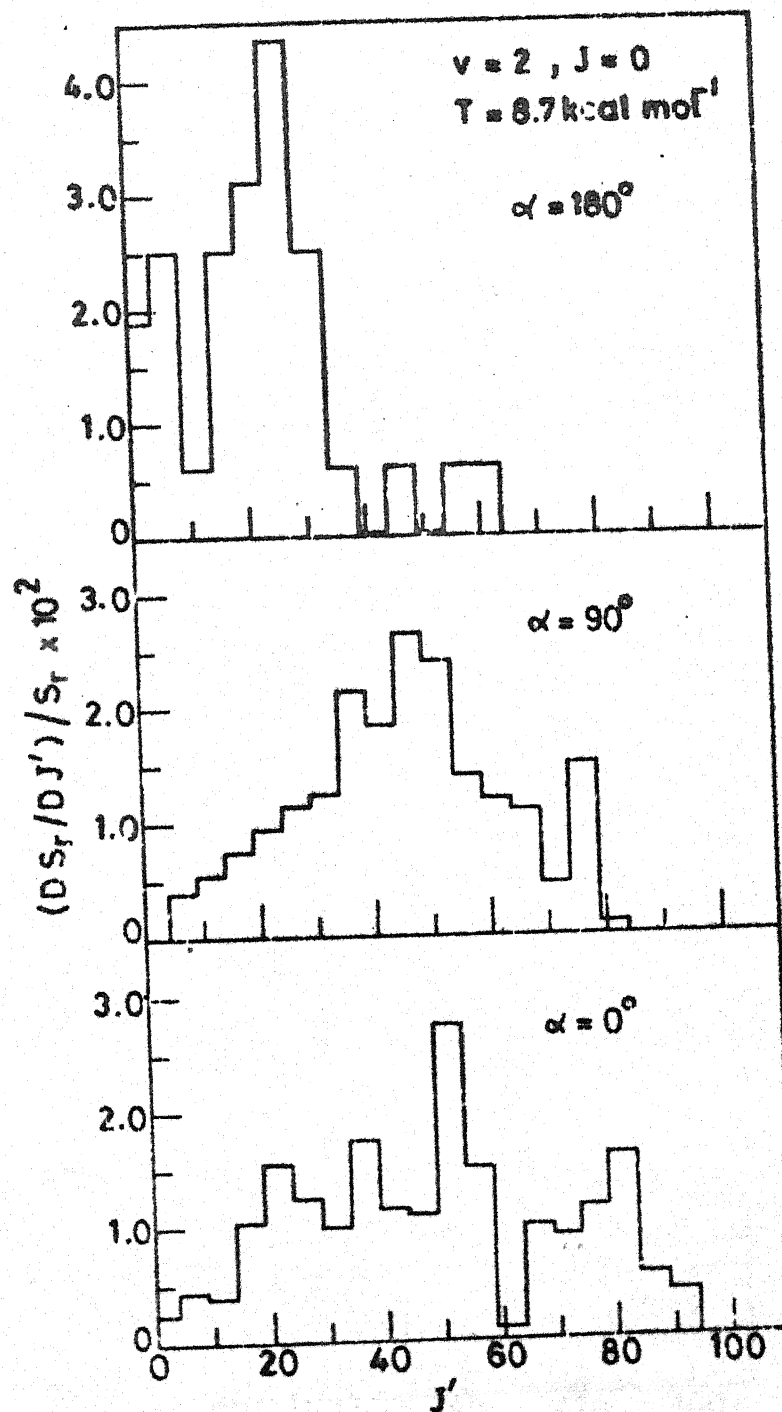
Fig. 36. Product rotational state distribution for different α.
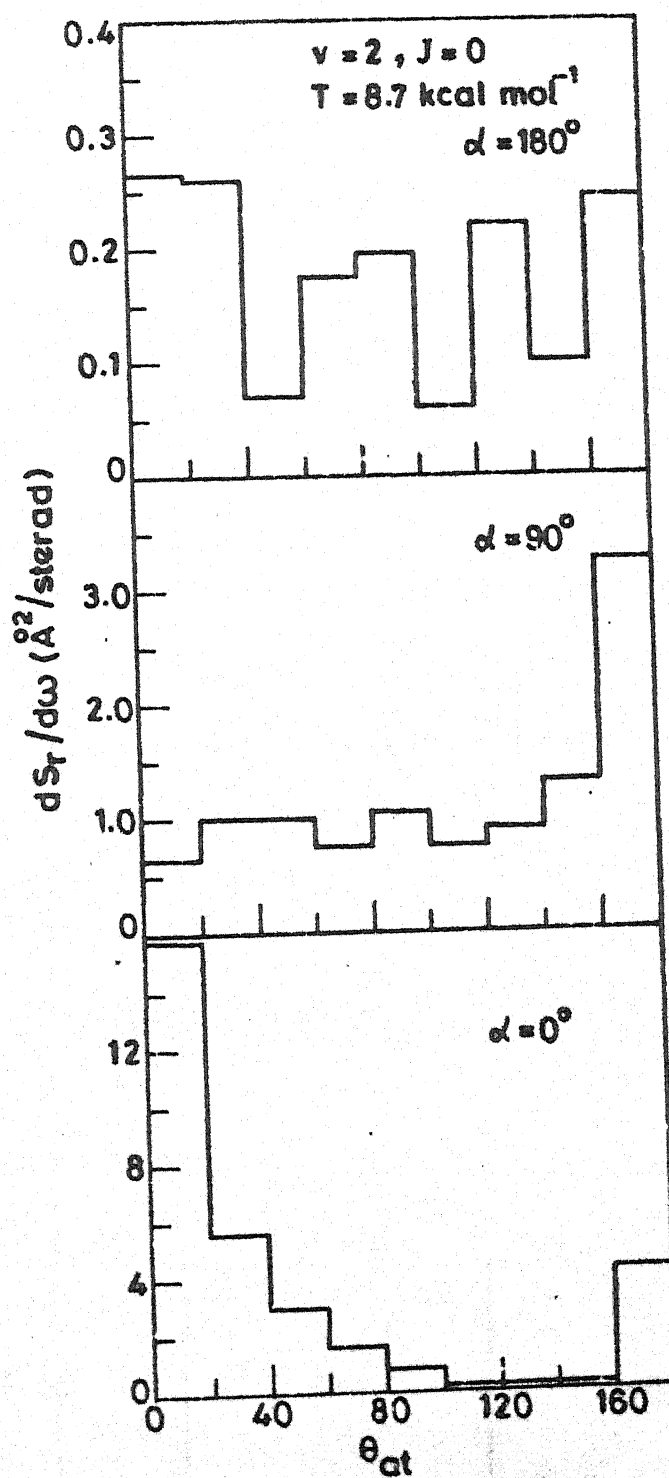
Fig. 37. Product angular distribution for different α.

Table 4. Reaction probability as a function of the approach angle α, for different J values for (R1) at $v=2$ and $T=8.7$ kcal mol^{-1} in the impact parameter range $1-1.5$ Å, $\alpha=0^o$ corresponds to the Li-F-H collinear configuration.

J	α			
	0°	90°	180°	Random in 0°-180°
0	0.92	0.94	0.00	0.81
5	0.00	0.28	0.96	0.19
9	0.90	0.72	0.98	0.84

3.3.6 Comparison with other theoretical studies

A general feature of the alkali-hydrogen halide reactions is that they involve the dissociation of a covalent bond and the formation of an ionic bond. Historically, such reactions were explained on the basis of a 'harpoon model'.[23] That is, the alkali atom pulls the halogen atom by inducing a strong coulombic attractive force between the reactants by transferring its valence electron to the hydrogen halide molecule. The metal atom in effect uses its valence electron as a 'harpoon' to pull the halogen atom. The critical separation r_c, at which this transfer can take place is given by

$$\frac{e^2}{r_c} \simeq IP(M) - EA(HX)$$

where $IP(M)$ is the ionization potential of the alkali atom, $EA(HX)$ is the electron affinity of the hydrogen halide and e is the electronic charge. Then S_r is related to r_c by

$$S_r = \pi\, r_c^{\,2}$$

The ionization potential of Li is known (124.3 kcal mol^{-1}). The EA of HF at each v is calculated following the procedure used by Polanyi et al.[17] The value of r_c is found to be 1.87, 2.00 and 2.16 Å for $v = 0$, 1 and 2, respectively. The corresponding S_r values are 11.0, 12.6 and 14.7 Å^2 compared

to our QCT results of 0.75, 8.69 and 12.41 $Å^2$, respectively. Considering the simplicity of the harpoon model, the discrepancy is not surprising. The reasonable agreement between the two sets of results at $v = 2$ suggests that the harpoon mechanism may be realistic at the higher v values for (R4).

The only other QCT result available for the reaction (R4) is due to Zeiri et al.[33] on their semi-empirical ZS surface. They have computed an S_r of 2.46 $Å^2$ at $T = 23.3$ kcal mol^{-1}. This is larger than what one would expect from the experimental value of $S_r = 0.94$ $Å^2$ at $T = 8.7$ kcal mol^{-1} and using the experimentally determined $\Delta S_r/\Delta T = 0.025$ $Å^2$/(kcal mol^{-1}) in the T range 3 - 8.7 kcal mol^{-1}. It is also larger than what we would predict based on our QCT result at $T = 20.46$ kcal mol^{-1} and our computed $\Delta S_r/\Delta T$ in this T range (see above). This discrepancy can not be due to the difference in E_b for the two different PES. The ZS surface has an E_b which is ~4 kcal mol^{-1} higher than that of the CSCM surface and therefore one would expect a lower value of S_r on the former than on the latter. The pronounced backward molecular scattering predicted by Zeiri et al.[33] is contrary to the experimental result. Therefore, there must be some other topological difference between the two surfaces. Visual examination of the PE contours shows that the ZS surface is not as sudden as the CSCM. Collinear QM and QCT calculations[31,33] do not reveal any vibrational threshold reiterating our view that their ZS surface is lacking in its

sudden character. This would explain the larger value of S_r at a higher T on the ZS surface.[33]

3.3.7 Comparison with experimental results

In this section we compare our 3D QCT results with the experimental results available for the LiFH and related systems. Our calculated value of S_r = 0.75 $\pm$ 0.24 Å^2 compares well with the only molecular beam[22] result of 0.94 Å^2 at T = 8.7 kcal mol^{-1}. The experimental PAD shows a prominent forward molecular (LiF) scattering in agreement with the QCT predictions in Fig. 32. Our calculated $\langle T' \rangle$ is $\simeq$ 60% of the total energy, in excellent accord with the experimental value[22] of $\langle T' \rangle \simeq$ 55%. The calculated distribution of θ_{JL} shows prominent peaks at θ_{JL} = 0° or 180° with a minimum around 90°. This type of distribution is characteristic of reactions proceeding via coplanar configurations,[86] and the experimental results also suggest that the reaction (R4) is mainly coplanar.

The excellent agreement between the QCT and the experimental results noted above implies that the CSCM surface is of reasonable validity. Although no other experimental result is available on this particular system, we can compare our predictions with results on similar systems. The marked vibrational enhancement predicted by us is in keeping with the vibrational enhancement observed experimentally[15,16,18] for reactions (R8), (R21) and (R22):

$$Ba + FH \longrightarrow BaF + H \tag{R21}$$

$$Sr + FH \longrightarrow SrF + H \tag{R22}$$

In particular, V has been shown to be an order of magnitude more efficient than T in causing the reactions (R7) and (R8). The marked vibrational enhancement observed for (R9) by Bartoszek et al.[17] suggests the PES of these systems to be of the sudden category lending further credence to the quality of the ab initio surface for (R4).

The decline in $S_r(J)$ followed by an increase and a possible levelling off of S_r with increase in J has been found experimentally for a variety of systems.[19] In particular, Blackwell et al.[20] have found such a behaviour for (R9). Dispert et al.[21] and Heismann and Loesch[16] have observed a steep decline in $S_r(J)$ for (R7) and Man and Estler[93] for (R22). The effect of J on S_r for (R4) remains to be verified. Here, we wish to stress the contrasting J-dependence predicted for $v = 0$ and $v = 2$.

The effect of relative orientation of the reactants on PVD has been studied by Karny et al.[2] for the reaction (R22) and their results are in qualitative accord with ours for (R4). That is, a broad side attack populates the higher vibrational states of the products more.

On the whole, one could see that based on the satisfactory agreement between the QCT results on the CSCM surface and the only available molecular beam results we have ventured to predict

a variety of observables for the prototype alkali-hydrogen halide exchange reaction and we do hope that this stimulates further experimental study of this reaction in the near future.

3.4 Nonreactive Collisions

We have investigated the effect of v, J and T on the vibrational energy transfer (VET) processes occurring in this potentially reactive system. The purpose is two-fold: one is that experimental studies like chemiluminescence depletion[17] assume that the depletion is essentially due to reaction and this remains to be verified. Another is that there is a lot of interest[94] on the effect of v, J and T on the VET processes. The total vibrationally inelastic integral cross sections (S_v) computed by the QCT method for Li + FH collisions are listed in Table 5 for different v, J and T, along with S_r values under the same conditions. It is clear that S_v is an order of magnitude smaller than S_r implying that the error introduced in neglecting VET processes in the chemiluminescence depletion studies is small, particularly in comparison to the vibrational enhancement and the rotational inhibition. The S_v values for this system are unusually low - mainly due to the sudden nature of the surface, that is, V is weakly coupled to T. For the same reason, S_v is nearly independent of T in agreement with the results of elaborate QCT studies of Thompson[94] on HF-Ar. It is tempting to state that S_v varies with J in the same fashion as

Table 5. Vibrationally inelastic cross sections in Å^2. The error bars correspond to 95% confidence level

T kcal mol^{-1}	v	J	S_v	S_r
8.7	0	0	0.0	0.75 ± 0.24
20.46	0	0	0.16 ± 0.14	1.76 ± 0.40
8.7	1.0	0	1.08 ± 0.47	8.69 ± 0.94
8.7	2.0	0	0.63 ± 0.36	12.41 ± 1.04
8.7	2.0	3	0.41 ± 0.32	9.98 ± 1.06
8.7	2.0	5	0.39 ± 0.33	4.92 ± 0.94
8.7	2.0	7	0.62 ± 0.42	17.29 ± 1.41
8.7	2.0	9	0.68 ± 0.43	14.54 ± 1.14
8.7	2.0	15	0.25 ± 0.36	11.92 ± 1.33

S_r. But the statistical error estimates are of the same magnitude as S_v and therefore we are not able to make any definite statement on the effect of J on VET processes. This is surprising as Thompson[94] has observed dramatic changes in S_v with changing J for Ar + FH collisions.

We have also investigated the rotational energy transfer (RET) processes in Li + FH (v = 2, J = 0) collisions at T = 8.7 kcal mol^{-1}. The purpose of this study is to examine the effect of Li as a collision partner when compared to the potentially nonreactive Ar, for example and also to test the validity of the power gap law for RET processes as it has been shown to fail for rigid rotor CO_2-H_2 collisions (Appendix III).[95] Unfortunately, the Li-FH collision is rotationally inelastic upto R_{Li-FH} = 10 Å and therefore our studies, on this topic are not complete. We report, however, $\langle J'(J'+1) \rangle$ as a function of b in Fig. 38. We hope to complete the calculation of $S_{J_i \longrightarrow J_f}$ for RET processes for Li-HF (v = 2, J = 0) and also for Li-rigid HF and compare them with experimental[96] and theoretical[94] results on HF -Ar and related systems in the near future.
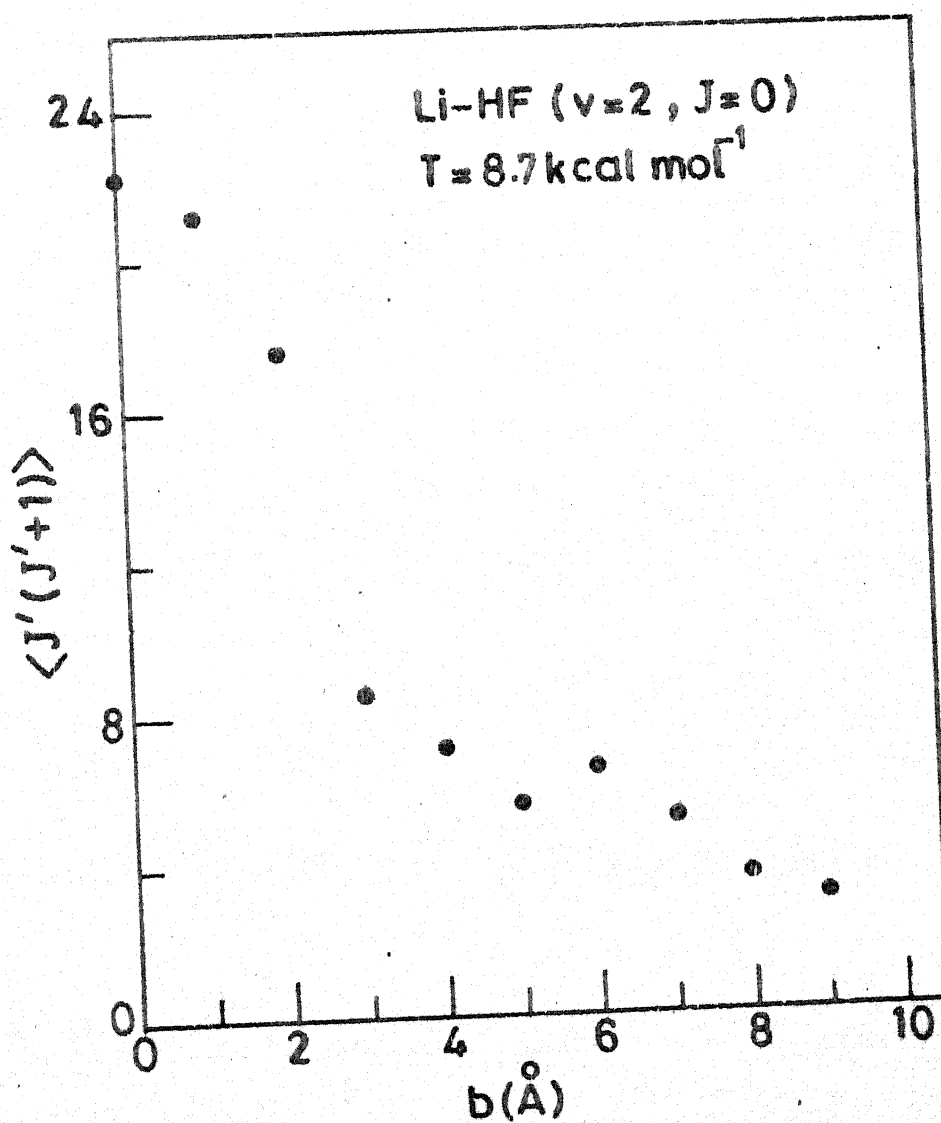
Fig. 38. Average final rotational energy as a function
of impact parameter

CHAPTER FOUR

DYNAMICS OF A MODEL SIX-CENTER EXCHANGE REACTION

We model a six-center exchange reaction as occurring between a van der Waals (VDW) molecule, A_2---B_2 and a diatomic molecule C_2 as shown,

$$\begin{array}{c} \overset{A}{\underset{|}{}} \\ A \\ \vdots \\ B \\ \searrow B \end{array} \quad + \quad \overset{C}{\underset{C}{|}} \quad \longrightarrow \quad AB + AC + BC \qquad (R23)$$
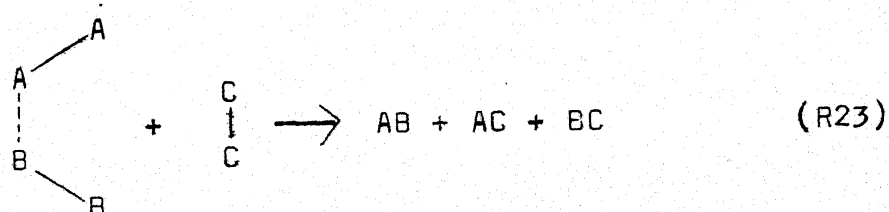
Since this is the first time a QCT study of this type of reaction is being reported, we describe here the method of our calculation in detail.

We assume that the motion of the atoms can be described by Hamilton's equations,[97]

$$\dot{q}_i = \frac{\partial H}{\partial P_i}$$

$$\dot{P}_i = -\frac{\partial H}{\partial q_i} \quad (i = 1, 2 \dots 3N) \tag{1}$$

where q_i's are the Cartesian coordinates and p_i's the conjugate mementa of an N-particle system. The dot on the variables represents the derivative with respect to time. H is the classical Hamiltonian of the system which for a conservative system is defined by

$$H = T + V = constant \tag{2}$$

where T is the kinetic energy and V is the PE of the system. Now the QCT technique involves setting up of the Hamiltonian and following the time evolution of the system by solving the Hamilton's equations numerically till it reaches a final state as specified by the final conditions.

It has been found that Cartesian coordinates are the most suitable for defining the Hamiltonian for the systems with more than three atoms.[98] The coordinates used in this study are:

(i) molecule-fixed coordinates xyz for A_2, x'y'z'for B_2 and x"y"z"for C_2, with the C.M. of the respective molecules as the origin,

(ii) space-fixed coordinates X'Y'Z', with the C.M. of the tetra-atomic species (VDW molecule), as the origin,

(iii) space-fixed coordinates XYZ with C.M. of the whole system (hexa-atomic) as the origin.

Using the Cartesian coordinates described in Fig. 39.

$$T = \frac{1}{2} \sum_{i=1}^{18} \frac{P_i^2}{m_i}$$

$$V = V(q_1, q_2, \text{---} q_{18}) \tag{3}$$

The equations of motion are:

$$\dot{q}_i = \frac{P_i}{m_i}$$

$$\dot{P}_i = \frac{-\partial V}{\partial q_i}, \quad i = 1,2,\text{---}18 \tag{4}$$

where $m_1 = m_2 = \ldots = m_6 = m_A,$

$m_7 = m_8 = \ldots = m_{12} = m_B$ and

$m_{13} = m_{14} = \ldots = m_{18} = m_C$.

m_A, m_B and m_C are the masses of the atoms A, B and C respectively. In order to solve these equations we need to know the derivatives of the PE with respect to the coordinates, in addition to the initial conditions (coordinates and momenta).
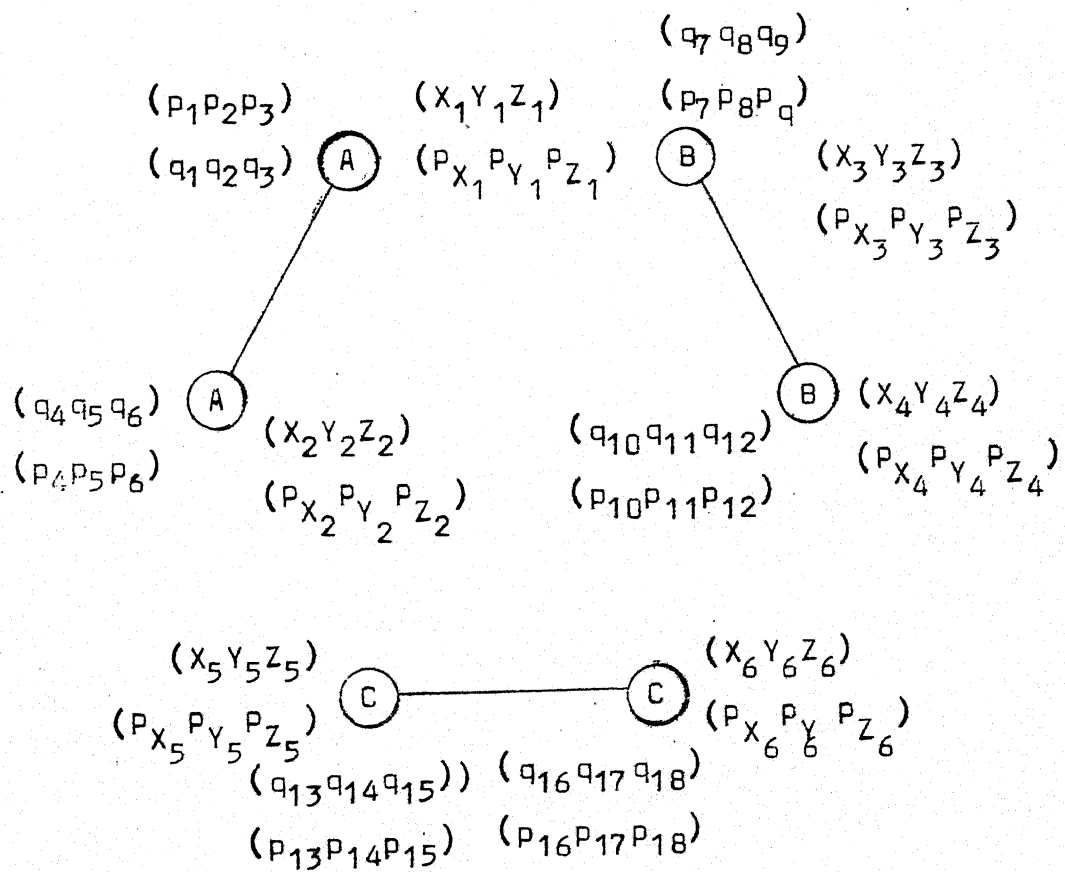
Fig. 39. Coordinates and their conjugate momenta in the space-fixed frame XYZ.

4.1 Potential Energy and its Derivatives

Following the treatment of London, Eyring and coworkers[99] derived the secular equation for the six-electron problem. Thompson and Suzukawa[57] as well as Dixon and Herschbach[100] have used this approach to study the 6-C reactions. Their calculated E_b (~ 88) was higher than the ab initio value[58] of ~ 69 kcal mol^{-1}. In our present study we will use the same formalism, but with the inclusion of a sato parameter S, to scale down the E_b, to that of the ab initio value.

The fifth order secular determinant given by Eyring and coworkers[99] is of the form

$$\left| H_{ij} - ES_{ij} \right| = 0 \qquad\qquad (5)$$

where H_{ij} are the integrals

$$H_{ij} = \left\langle \chi_i \left| H \right| \chi_j \right\rangle$$

and S_{ij} are the overlap terms

$$S_{ij} = \left\langle \chi_i \left| \chi_j \right.\right\rangle$$

The individual terms of the determinant have been given in ref. 99. These consist of Coulombic integrals Q_{ij} and exchange integrals J_{ij} , which are functions of the corresponding (one of the 15) internuclear distances. Instead of solving these integrals

we have made use of the LEPS formulation to evaluate these integrals. Thus

$$^{1}E_{ij} = \frac{Q_{ij} + J_{ij}}{1 + S} \tag{6}$$

and
$$^{3}E_{ij} = \frac{Q_{ij} - J_{ij}}{1 - S}, \tag{7}$$

where $^{1}E_{ij}$ and $^{3}E_{ij}$ are the singlet and triplet energies for the diatomic molecule given by,

$$^{1}E_{ij} = {}^{1}D_{ij} \left\{ \exp\left[-2\alpha_{ij} \left(r_{ij} - r_{ij}^{e} \right) \right] \right.$$
$$\left. -2 \exp\left[-\alpha_{ij}(r_{ij} - r_{ij}^{e}) \right] \right\} \tag{8}$$

$^{1}D_{ij}$ is the dissociation energy (including zero-point energy), r_{ij}^{e} is the equilibrium internuclear distance and α_{ij} is the Morse parameter. The triplet state curve for the atom pair ij is represented by the Pedersen-Porter[101] functions:

$$^{3}E_{ij} = {}^{3}D_{ij} \left\{ \exp\left[-2\beta_{ij}(r_{ij} - r_{ij}^{e}) \right] + 2 \exp\left[-\beta_{ij}(r_{ij} - r_{ij}^{e}) \right] \right\} \tag{9}$$

for $r_{ij} \leq R_{c}$ and

$$^{3}E_{ij} = C_{ij}(r_{ij} + A_{ij}) \exp(-\sigma_{ij} r_{ij}) \tag{10}$$

for $r_{ij} > R_{c}$.

We make use of the parameters computed by Raff et al.[37] for H_2, as these values had been used in a number of trajectory calculations for three- and four-atom systems, for which the agreement with the experimental results was satisfactory. The sato parameter S, was varied till the E_b for the regular hexagonal geometry calculated using this method agreed with that of the *ab initio* value. These parameters are given in Table 6.

Once the matrix elements are evaluated, the secular determinant is solved for the lowest eigenvalue using the NICER subroutine package[102] which makes use of the Householder method for diagonalization. The PE for the regular hexagonal H_6, obtained from these calculations are shown in Fig. 40. The E_b for the hexagonal configuration is found to be 69 kcal mol^{-1}. It should be noted that this calculation predicts that

$$2 H_2 + H_2' \longrightarrow H_2 + 2 HH' \qquad (R24)$$

is a possible mechanism for the H_2 exchange reactions, since this energy is less than that of the dissociation energy of H_2.

An important and the most time consuming process in the QCT technique is the calculation of the PE derivatives with respect to the various coordinates. This is a straightforward process when the PES is known in the form of an analytical function. In the present case, however, PE is calculated by solving the fifth order secular determinant for each nuclear
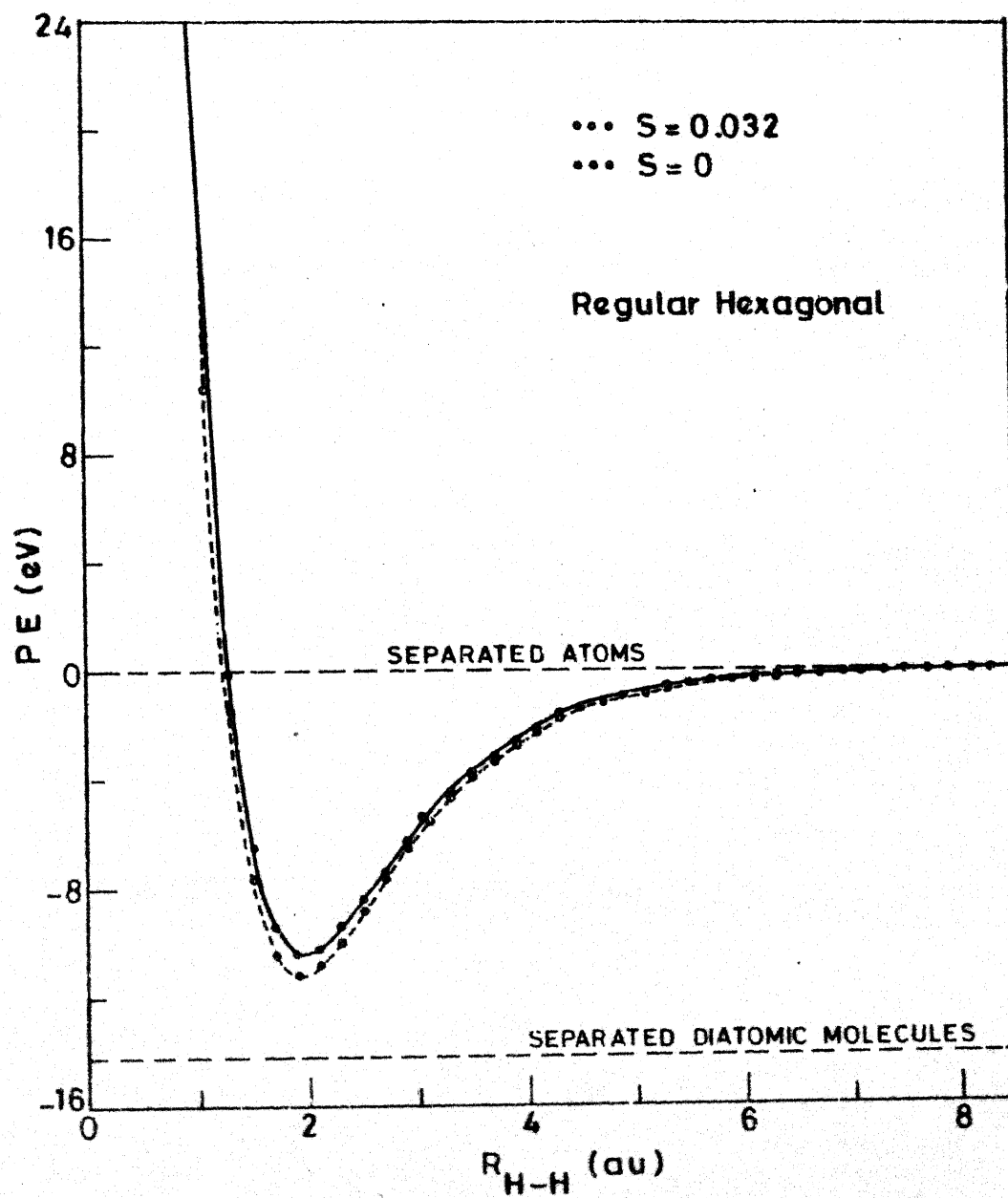
Fig. 40. PE for the regular hexagonal H_6 as a function of R_{HH}.

Table 6. Potential-Energy parameters

$^1D(\text{kcal mol}^{-1})$	109.46086
$r^e(\text{Å})$	0.74127
$\alpha(\text{Å}^{-1})$	1.97357
$^3D(\text{kcal mol}^{-1})$	45.35618
$\beta(\text{Å}^{-1})$	1.88999
$C(\text{kcal mol}^{-1}.\text{Å}^{-1})$	1113.59090
$A(\text{Å})$	0.529167
$\sigma(\text{Å}^{-1})$	3.166560
$R_c(\text{Å})$	0.84667

configuration as (see above) the lowest of the five eigenvalues. This exercise has to be repeated for all the nuclear configurations during the course of a collision. We calculate the PE derivatives by making use of Hellmann-Feynman theorem (HFT).[103]

According to HFT the force acting on a particle is given by

$$\frac{\partial E}{\partial X} = \left\langle \psi \left| \frac{\partial H}{\partial X} \right| \psi \right\rangle \tag{11}$$

where ψ is the wave function of the system and depends on the space and spin coordinates of the electrons, denoted by $\vec{r}$, and on the N parameters $\{C_n\}$ which in turn depend on the nuclear configuration. X is any parameter on which H is dependent. However, HFT assumes a knowledge of the exact wave function. Hurly[104] has given the conditions under which the theorem holds for an approximate wavefunction also. If $E(X_\alpha, Y_\alpha, Z_\alpha, \{C_n\})$ is the electronic energy for the particular nuclear configuration denoted by $(X_\alpha, Y_\alpha, Z_\alpha)$ for $\alpha = 1, --- m$ (m nuclei), the force (PE gradient) in the x direction on nucleus α is given as

$$F_{\alpha x} = -\frac{\partial E}{\partial X_\alpha} - \sum_{n=1}^{N} \frac{\partial E}{\partial C_n} \frac{\partial C_n}{\partial X_\alpha} \tag{12}$$

The term $\partial E/\partial X_\alpha$ takes into account the direct dependence of E on X_α, i.e., the occurrence of X_α in the Hamiltonian. The second term takes into account the dependence of ψ on X_α through the parameters $\{C_n\}$. Invoking HFT means calculating only the

first term. Thus HFT holds when the second term vanishes. This requires for each $\vec{r}$, either C_n be independent of X_α, or $\partial E / \partial C_n = 0$. The latter holds when $\{C_n\}$ is chosen variationally. In general, HFT holds for an approximate function in which all parameters which change with nuclear displacement have been chosen variationally.

A generalisation of the HFT is as follows:[105] the secular equation can be written in the matrix form as

$$\bar{H} \, \bar{C} = \bar{E} \, \bar{S} \, \bar{C} \tag{13}$$

If $\bar{M} = \bar{H} - \bar{E} \, \bar{S}$, then

$$\bar{M} \, \bar{C} = 0 \tag{14}$$

and also $\bar{C}^{+} \, \bar{M} = 0 \tag{15}$

Differentiating Eqn. (14) with respect to X, we have

$$\frac{\partial \bar{M}}{\partial X} \bar{C} + \bar{M} \, \frac{\partial \bar{C}}{\partial X} = 0 \tag{16}$$

Multiplying by $\bar{C}^{+}$ and using $\bar{C}^{+} \, \bar{M} = 0$, we have

$$\bar{C}^{+} \frac{\partial \bar{M}}{\partial X} \bar{C} = 0 \tag{17}$$

But

$$\frac{\partial \bar{M}}{\partial X} = \frac{\partial \bar{H}}{\partial X} - \bar{E} \frac{\partial \bar{S}}{\partial X} - \frac{\partial \bar{E}}{\partial X} \bar{S} \tag{18}$$

Hence Eqn. (17) becomes

$$\bar{c}^+ \frac{\partial \bar{M}}{\partial X} \bar{c} = \bar{c}^+ \frac{\partial \bar{H}}{\partial X} \bar{c} - \bar{E} \bar{c}^+ \frac{\partial \bar{S}}{\partial X} \bar{c} - \frac{\partial \bar{E}}{\partial X} \bar{c}^+ \bar{S} \bar{c} \qquad (19)$$

$$= 0$$

$$\text{or} \quad \frac{\partial \bar{E}}{\partial X} = \frac{\bar{c}^+ \frac{\partial \bar{H}}{\partial X} \bar{c} - \bar{E} \bar{c}^+ \frac{\partial \bar{S}}{\partial X} \bar{c}}{\bar{c}^+ \bar{S} \bar{c}} \qquad (20)$$

If X is taken to be r_i, the ith internuclear distance and zero differential overlap of atomic orbitals is assumed,

$$\frac{\partial \bar{E}}{\partial r_i} = \frac{\bar{c}^+ \frac{\partial \bar{H}}{\partial r_i} \bar{c}}{\bar{c}^+ \bar{S} \bar{c}}$$

$$\text{or} \quad \frac{\partial E_k}{\partial r_i} = \frac{\vec{c}_k^+ \left(\frac{\partial \bar{H}}{\partial r_i}\right) \vec{c}_k}{\vec{c}_k^+ \bar{S} \vec{c}_k} \qquad (21)$$

where $\vec{c}_k$ is the eigenvector corresponding to the eigenvalue E_k, which is the lowest eigenvalue in our case. Hence by knowing the eigenvector corresponding to an eigenvalue, it is possible to calculate the derivative of this particular eigenvalue. In our program the diagonalisation is carried out using NICER subroutine package,[102] which produces appropriately normalised eigenvectors, $\vec{d}_k = \bar{S}^{\frac{1}{2}} \vec{c}_k$, so that the denominator in Eqn. (21) becomes unity. Recently, we have learnt that Kroger and Muckerman had used the same HFT approach in calculating

the PE derivatives in their QCT study of hot atom reactions.[106]

4.2   Calculation of Initial Coordinates and Momenta

Initially the molecule A_2 is aligned along the z-axis with its C.M. as the origin. Hence in the molecule-fixed system the coordinates of A_2 are given by

$$x_1 = y_1 = x_2 = y_2 = 0$$

$$z_1 = r_1/2$$

$$z_2 = -r_1/2 \qquad\qquad (22)$$

where r_1 is the internuclear distance of A_2.

To calculate the initial angular momenta, the rotation of the molecule is assumed to be   in a plane perpendicular to the xy-plane and if this plane makes an angle η_i with the xz-plane, the components of the angular momentum are:

$$M_x (A_2) = [2I_A E_r(A_2)]^{1/2} \cos \eta_1$$

$$M_y (A_2) = [2I_A E_r(A_2)]^{1/2} \sin \eta_1$$

$$M_z (A_2) = 0 \qquad\qquad (23)$$

where $I_A = m_1(z_1^2 + z_2^2)$ and

$$E_r(A_2) = J_1(J_1+1)\hbar^2/2I_A .$$

$$(v + \tfrac{1}{2})h = 2(2\mu)^{1/2} \int_{r_<}^{r_>} [E(v,J) - U(r,J)]^{1/2} \, dr \qquad (27)$$

and $\quad U(r,J) = U_M(r) + \dfrac{J(J+1)\hbar^2}{2I}$

and $\quad U_M(r) = D_e[1 - \exp[-\beta(r-r_e)]]^2$.

$r_<$ and $r_>$ are the inner and outer turning points.

From Eqn.(25) and (26) we have

$$\overline{P}_v = \pm \left\{ 2\mu_{A_2}[E(v,J) - U(r,J)] \right\}^{1/2}$$

$\vec{P}_v$ will be negative in one half of the vibrational phase and positive in the other half. The initial x, y, z components of the total momentum conjugate to the molecule- fixed coordinates are,

$$P_{x_1} = m_1 z_1 \omega_y \quad (A_2)$$

$$P_{y_1} = -m_1 z_1 \omega_x \quad (A_2)$$

$$P_{z_1} = \vec{P}_v \qquad\qquad\qquad (28)$$

$$P_{x_2} = m_1 z_2 \omega_y \quad (A_2)$$

$$P_{y_2} = -m_1 z_2 \omega_x \quad (A_2)$$

$$P_{z_2} = -\vec{P}_v \qquad\qquad\qquad (29)$$

Having determined the coordinates and momenta for a molecule aligned with the z-axis, we can now calculate the initial coordinates and momenta of the molecule in any position in 3D-space by multiplying by the appropriate combination of rotation matrices. The two rotation matrices used for this purpose are

$$
R_z(\beta) = \begin{bmatrix} \cos\beta & \sin\beta & 0 \\ -\sin\beta & \cos\beta & 0 \\ 0 & 0 & 1 \end{bmatrix}
$$

$$
R_y(\beta) = \begin{bmatrix} \cos\beta & 0 & -\sin\beta \\ 0 & 1 & 0 \\ \sin\beta & 0 & \cos\beta \end{bmatrix} \tag{30}
$$

Similar relations hold for B_2 and C_2 also.

The molecule-fixed coordinates (x, y, z) of A_2 and (x', y', z') of B_2 are transformed into space-fixed coordinates (X', Y', Z') by the following transformations (see Fig. 41):

$$
\begin{bmatrix} X_i' \\ Y_i' \\ Z_i' \end{bmatrix} = \begin{bmatrix} \rho_1 \sin\theta_4 \cos\phi_4 \\ \rho_1 \sin\theta_4 \sin\phi_4 \\ \rho_1 \cos\theta_4 \end{bmatrix} + R_z(\phi_1) R_y(\theta_1) \begin{bmatrix} x_i \\ y_i \\ z_i \end{bmatrix}
$$

$$
(i = 1, 2) \tag{31a}
$$
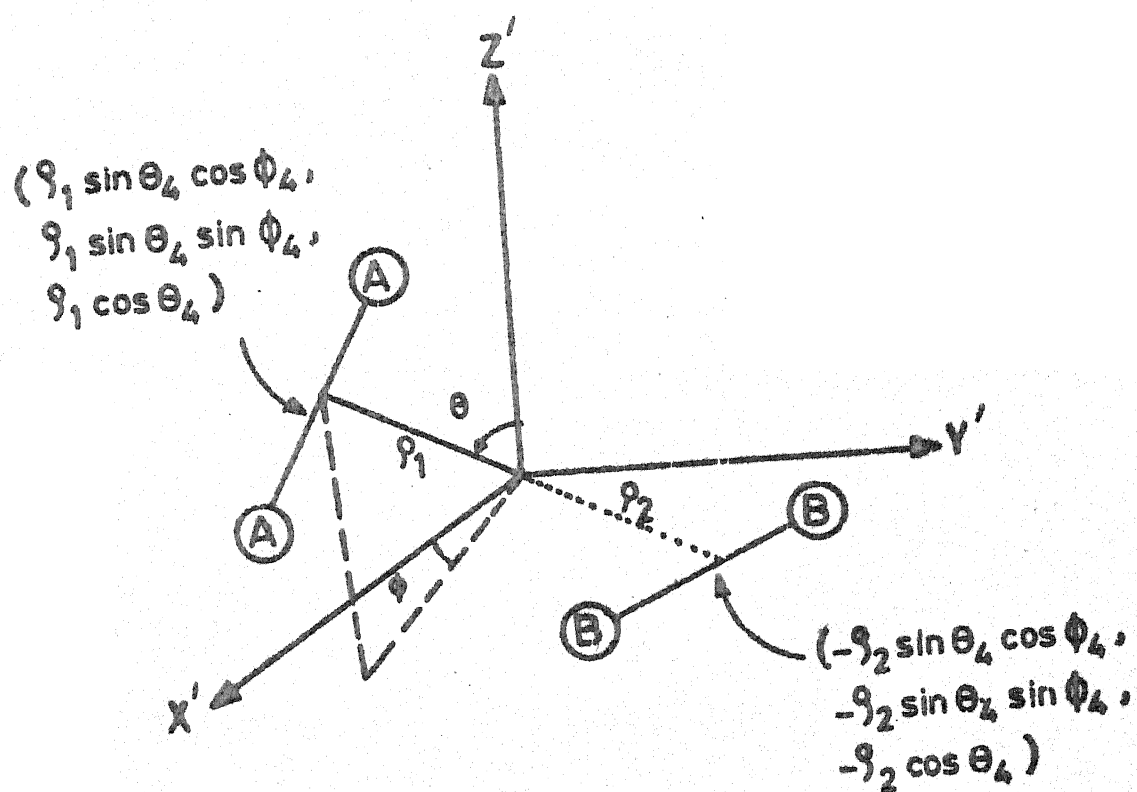
Fig. 41. Orientation of the VDW bond and the coordinates of the C.M. of A_2 and B_2 in the $(X'Y'Z')$ frame

$$
\begin{bmatrix} X_i' \\ Y_i' \\ Z_i' \end{bmatrix} = \begin{bmatrix} -\rho_2 \sin\theta_4 \cos\phi_4 \\ -\rho_2 \sin\theta_4 \sin\phi_4 \\ -\rho_2 \cos\theta_4 \end{bmatrix} + R_z(\phi_2)R_y(\theta_2) \begin{bmatrix} x_i' \\ y_i' \\ z_i' \end{bmatrix}
$$

$$(i = 3, 4) \tag{31b}$$

θ_1 and ϕ_1 are the orientation angles of A_2, θ_2 and ϕ_2 are the orientation angles of B_2 in the molecule-fixed frame $x'y'z'$. θ_4 and ϕ_4 are the orientation angles for the VDW bond, of distance ρ . ρ_1 is the distance between the C.M. of A_2B_2 with that of A_2 and ρ_2 is the distance between C.M. of A_2B_2 with that of B_2.

The corresponding momenta in the space-fixed frame will be given by

$$
\begin{bmatrix} P_{X_i}' \\ P_{Y_i}' \\ P_{Z_i}' \end{bmatrix} = R_z(\phi_1)\, R_y(\theta_1) \begin{bmatrix} P_{X_i} \\ P_{Y_i} \\ P_{Z_i} \end{bmatrix}
$$

$$(i = 1, 2)$$

$$
\begin{bmatrix} P_{X_i}' \\ P_{Y_i}' \\ P_{Z_i}' \end{bmatrix} = R_z(\phi_2)\, R_y(\theta_2) \begin{bmatrix} P_{X_i}' \\ P_{Y_i}' \\ P_{Z_i}' \end{bmatrix}
$$

$$(i = 3, 4) \tag{32}$$

To study the collision between (A_2B_2) and C_2 it is convenient to transform the coordinates X'Y'Z' to XYZ. For this, it is assumed that the relative velocity $\vec{V} = \vec{v} - \vec{C}$, where $\vec{v}$ is the C.M. velocity of C_2 and $\vec{C}$ is the C.M. velocity of (A_2B_2), lies along the Z-direction. If the C.M. of $(A_2B_2C_2)$ is taken as the origin of the XYZ frame, we have

$$2(m_1 + m_2)\,\vec{C} + 2\,m_3\,\vec{v} = 0 \qquad\qquad (33)$$

where m_2 and m_3 are the atomic masses of B and C respectively. Hence it follows that

$$(m_1 + m_2)\,\vec{C} + m_3\,(\vec{V} + \vec{C}) = 0$$

$$\vec{C} = \frac{-m_3\vec{V}}{m_1 + m_2 + m_3}$$

$$\text{and} \qquad \vec{v} = \frac{(m_1 + m_2)\vec{V}}{m_1 + m_2 + m_3}$$

The position and momenta of the C_2 molecule in the XYZ frame (Fig. 42) are:

$$\begin{bmatrix} X_i \\[2mm] Y_i \\[2mm] Z_i \end{bmatrix} = - \begin{bmatrix} 0 \\[2mm] \dfrac{(m_1+m_2)b}{(m_1+m_2+m_3)} \\[3mm] \dfrac{(m_1+m_2)(R_s{}^2 - b^2)^{1/2}}{(m_1+m_2+m_3)} \end{bmatrix} + R_{z''}(\phi_3) R_{y''}(\theta_3) \begin{bmatrix} x_i{}'' \\[2mm] y_i{}'' \\[2mm] z_i{}'' \end{bmatrix}$$
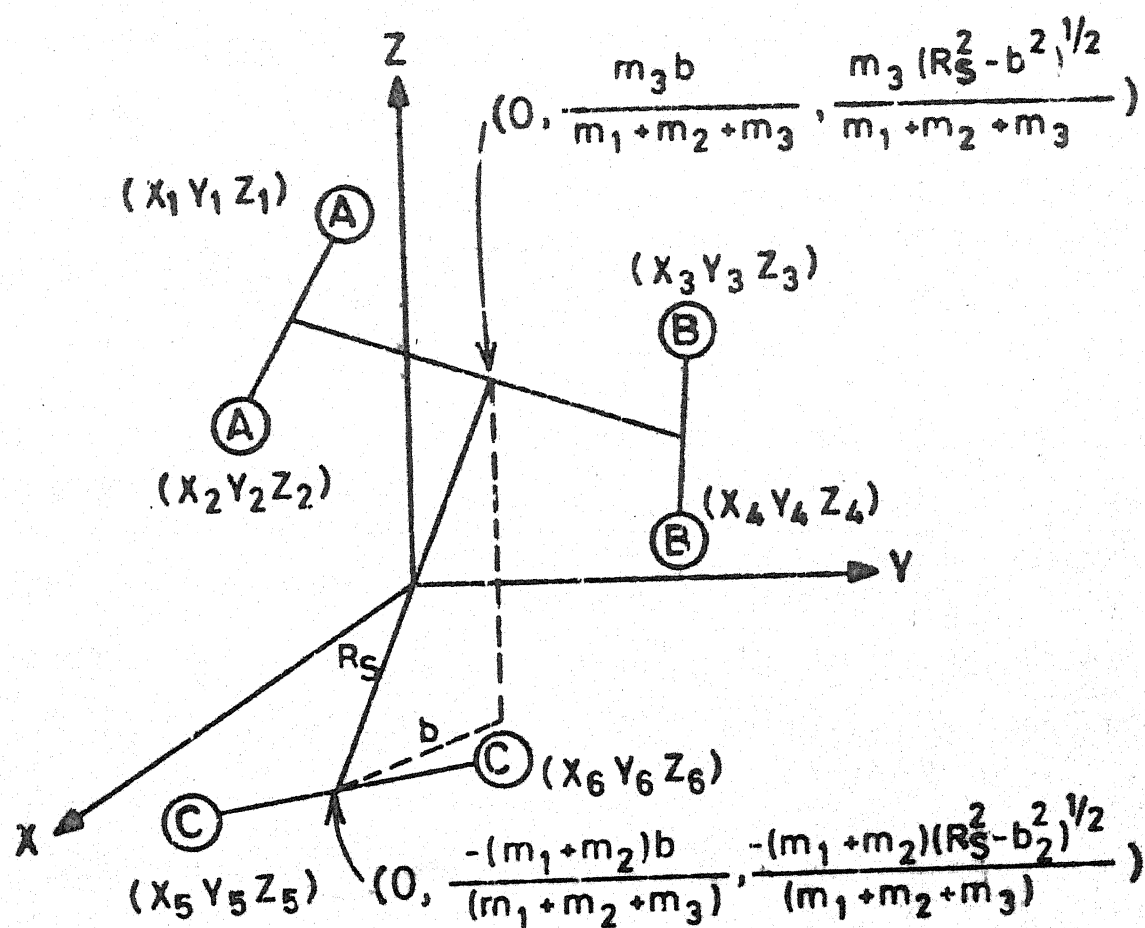
Fig. 42. Coordinates of the molecules A_2, B_2 and C_2 in the space-fixed-frame XYZ

$$
\begin{bmatrix} P_{X_i} \\ P_{Y_i} \\ P_{Z_i} \end{bmatrix} = \begin{bmatrix} 0 \\ 0 \\ \dfrac{m_3(m_1+m_2)V}{(m_1+m_2+m_3)} \end{bmatrix} + R_{z''}(\phi_3)R_{y''}(\theta_3) \begin{bmatrix} P_{x_i''} \\ P_{y_i''} \\ P_{z_i''} \end{bmatrix}
$$

$$(i = 5, 6) \qquad (35)$$

where R_s is the distance between the C.M. of (A_2B_2) and C.M. of C_2 and b is the impact parameter. The position and momenta of C_2 in molecule-fixed frame $(x''y''z'')$ are calculated as in the case of A_2. θ_3 and ϕ_3 are the orientation angles of C_2 in $x''y''z''$ coordinates. In the above transformation it is assumed that the molecule C_2 approaches (A_2B_2) system from the $-Z$ direction and the C.M. of (A_2B_2) and C_2 lie in the YZ plane. The initial coordinates and momenta in the XYZ coordinates are:

$$
\begin{bmatrix} X_i \\ Y_i \\ Z_i \end{bmatrix} = \begin{bmatrix} 0 \\ \dfrac{m_3 b}{(m_1+m_2+m_3)} \\ \dfrac{m_3(R_s^2-b^2)^{1/2}}{(m_1+m_2+m_3)} \end{bmatrix} + \begin{bmatrix} X_i' \\ Y_i' \\ Z_i' \end{bmatrix}
$$

$$
\begin{bmatrix} P_{X_i} \\ P_{Y_i} \\ P_{Z_i} \end{bmatrix} = \begin{bmatrix} 0 \\ 0 \\ -\dfrac{m_k m_3 V}{(m_1+m_2+m_3)} \end{bmatrix} + \begin{bmatrix} P_{X_i'} \\ P_{Y_i'} \\ P_{Z_i'} \end{bmatrix}
$$

$$(i = 1, 2, 3 \text{ and } 4) \qquad (36)$$

$m_k = m_1$ when $i = 1$ and 2, and

$m_k = m_2$ when $i = 3$ and 4.

Hence by specifying r_i, v_i, J_i, η_i, θ_i ($i = 1$ to 4), ϕ_i ($i = 1$ to 4), ρ, R_s, b and $\vec{V}$ the initial conditions for the system is completely defined.

4.3 Selection of Initial Conditions

In the present study we have restricted ourselves to the fixed values of $\left\{v_i, J_i\right\}$, b and $\vec{V}$, though provision for selecting these variables from appropriate distribution functions exists in the software package developed by us. The orientation angles have been selected randomly as:

$$\theta = \cos^{-1} (1 - 2\varepsilon)$$

$$\phi = 2\pi |\varepsilon|$$

$$\eta = 2\pi |\varepsilon| \tag{37}$$

where ε is the random number in the interval $[-1, 1]$ generated from the IMSL subroutine GGUB.[80] The vibrational phase was selected as for a rotating Morse oscillator and is described elsewhere.[81]

4.4 Solution of the Hamilton's Equations and the Product Analysis

Once the initial conditions are selected and the corresponding coordinates and momenta calculated, the equations of motion (4) are solved numerically using the same predictor-

corrector method used in the REACTS program mentioned in Chapter 3. We only mention that we have made use of a stepsize $= \Delta t = (0.5 - 1.0) \times 10^{-16}$ s. The accuracy of the integration was checked by the energy and angular momentum conservation, back integration and stepsize reduction criteria.

In this section we will discuss the criteria we have used to identify the products and analyse their characteristics.

In the collision between (A_2B_2) and C_2 the possible channels are:

$$\longrightarrow A_2 + B_2 + C_2 \qquad (R25)$$

$$\longrightarrow AB + AC + BC \qquad (R26)$$

$$\longrightarrow 2\,AB + C_2 \qquad (R27)$$

$$\longrightarrow 2\,AC + B_2 \qquad (R28)$$

$$\longrightarrow 2\,BC + A_2 \qquad (R29)$$
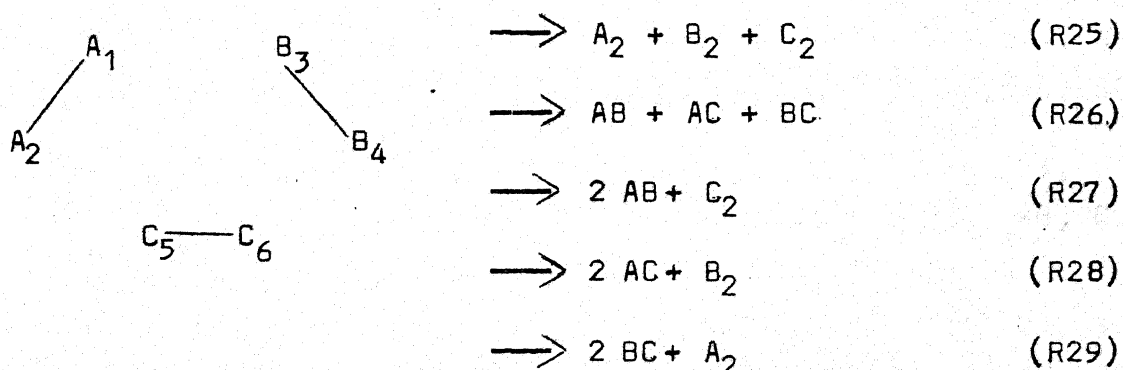
(R25) is a non-reactive process and (R26) is a genuine 6-C reaction. In (R27), (R28) and (R29), C_2, B_2 and A_2 acts as the energising partner in that order. That is, it transfers its energy to the other collision partner without undergoing any bond breakage. All the possible combinations of the atoms along with their identification labels are shown in Table 7. To identify which of the processes has occurred we make use of the distance criteria. We compare all the 15 internuclear distances

Table 7. Species labels for different reactive channels

Process	Combination of atoms in sets of three	
Non-reactive (R25)	12, 34, 56	
	AA, BB, CC	
Six-centered reaction (R26)	13, 25, 46	13, 26, 45
	AB, AC, BC	AB, AC, BC
	14, 25, 36	14, 26, 45
	AB, AC, BC	AB, AC, BC
	15, 23, 46	15, 24, 36
	AC, AB, BC	AC, AB, BC
	16, 23, 45	16, 24, 35
	AC, AB, BC	AC, AB, BC
C_2 acts as an energising partner (R27)	13, 24, 56	14, 23, 56
	AB, AB, CC	AB, AB, CC
B_2 acts as an energising partner (R28)	15, 34, 26	16, 25, 34
	AC, BB, AC	AC, AC, BB
A_2 acts as an energising partner (R29)	12, 35, 46	12, 36, 45
	AA, BC, BC	AA, BC, BC

and continue the integration until only three of those 15 distances are less than a specific distance R_s, after which the interaction between the species concerned is negligible. Then the molecules corresponding to the three shortest distances are identified and their energy analysed.

Once a product molecule is identified, its C.M. velocity in space-fixed frame is calculated as

$$(v'_{ij})_X = \frac{(P'_X)_i + (P'_X)_j}{m_i + m_j}$$

$$(v'_{ij})_Y = \frac{(P'_Y)_i + (P'_Y)_j}{m_i + m_j}$$

$$(v'_{ij})_Z = \frac{(P'_Z)_i + (P'_Z)_j}{m_i + m_j} \tag{38}$$

Then the components of the linear momentum in molecule fixed coordinates are

$$P'_{X_k} = P'_{X_k} - m_k (v'_{ij})_X$$

$$P'_{Y_k} = P'_{Y_k} - m_k (v'_{ij})_Y$$

$$P'_{Z_k} = P'_{Z_k} - m_k (v'_{ij})_Z ,$$

$$(k = i, j) \tag{39}$$

To calculate the internal angular momentum, the space-fixed coordinates are transformed into molecule-fixed coordinates as:

$$x_k = X_k - \frac{(m_i X_i + m_j X_j)}{(m_i + m_j)}$$

$$y_k = Y_k - \frac{(m_i Y_i + m_j Y_j)}{(m_i + m_j)}$$

$$z_k = Z_k - \frac{(m_i Z_i + m_j Z_j)}{(m_i + m_j)} \; ,$$

$$(k = i, \; j) \tag{40}$$

The final internal angular momentum of the species (ij) is,

$$(M'_{ij})_x = (y_i P'_{z_i} - z_i P'_{y_i}) + (y_j P'_{z_j} - z_j P'_{y_j})$$

$$(M'_{ij})_y = (z_i P'_{x_i} - x_i P'_{z_i}) + (z_j P'_{x_j} - x_j P'_{z_j})$$

$$(M'_{ij})_z = (x_i P'_{y_i} - y_i P'_{x_i}) + (x_i P'_{y_j} - y_j P'_{x_j})$$

The final rotational energy is given by

$$E'_{rot} (ij) = \frac{(M'_{ij})^2}{2I}$$

where $(M'_{ij})^2 = (M'_{ij})^2_x + (M'_{ij})^2_y + (M'_{ij})^2_z \; ,$

$$I = \mu r^2_{ij} \; ,$$

$$\mu = \frac{m_i m_j}{m_i + m_j} \; ,$$

and $r_{ij} = [(x_i - x_j)^2 + (y_i - y_j)^2 + (z_i - z_j)^2]^{1/2}$

The internal kinetic energy of the species (ij) is

$$E'_{int}(ij) = \frac{1}{2} (P'^2_{x_i} + P'^2_{y_i} + P'^2_{z_i})/m_i$$

$$+ (P'^2_{x_j} + P'^2_{y_j} + P'^2_{z_j})^2 /m_j]$$

and the vibrational energy is calculated from

$$E'_{vib}(ij) = E'_{int}(j) + V_{ij} - E'_{rot}(ij)$$

V_{ij} is the Morse potential for the diatomic species (ij). The final translational energy is calculated by substrating E'_{vib} and E'_{rot} from the initial total energy.

4.5 Preliminary Results

We report here the preliminary results of our investigation using the program developed by us for studying the 6-C processes. The value of VDW bond distance ($= P_1 + P_2$) has been taken[107] to be 3.0 Å and R_s as 6.0 Å. As our objective is to explore the conditions under which the 6-C pathway is dominant, we have restricted ourselves to follow the collision at fixed impact parameters. Further, because of the enormous amount of computer time taken for the completion of individual trajectories, we could compute only a few test trajectories. Also despite the integration over 10,000 steps (1 step size = 1 x 10^{-16} s) most of the trajectories at large impact parameters,

do not go to completion. These trajectories take~9 min. of cpu time each, in DEC-1090 computer.

To illustrate the accuracy of the integration and to demonstrate the utility of the developed computer program, we give the initial and final coordinates and momenta as well as the results of the back integration for a typical trajectory in Table 8. Several test runs were made for a wide range of initial conditions: $v_i = 0 - 4$, $J_i = 0 - 4$ ($i = 1-3$) and T = 10-100 kcal mol^{-1}.

In Table 9, we are presenting the results for 52 trajectories with all three molecules being in their ground vibrational and rotational states and with a relative translational energy of 80 kcal mol^{-1}. Under these conditions, all the trajectories lead to the decomposition of the VDW molecule as expected. As a result we could only examine the energy transfer processes occurring in these collisions. It can be seen that $T \longrightarrow R$ is the major energy transfer process occurring in this system. In all cases, the molecule-3, i.e. the molecule that collides with the VDW molecule, takes away the major portion of the energy that is transferred.

In spite of the fact that T is greater than E_b, no reaction has been observed. We should stress that, because of the small number of trajectories computed, no conclusion can be drawn at this stage. An understanding of the dynamics of the 6-C processes should await a detailed study, using our new program.

Table 8. Initial and final coordinates and momenta and back-integration results for a typical trajectory with $v_i = J_i = 0$, $i = 1-3$; $b = 0.5499$ Å; $\Delta t = 1 \times 10^{-16}$ s; $T = 80$ kcal mol^{-1}; $R_s = 6.0$ Å; Energy non-conservation = 0.0008142 kcal mol^{-1}

i	Initial	Final	After back-integration	Initial $\times 10^{-3}$	Final $\times 10^{-3}$	After back-integration $\times 10^{-3}$
	X			**P_X**		
1	0.66675	6.99138	0.66675	1.02527	10.82880	1.02527
2	0.87677	7.59427	0.87677	-1.02527	8.75035	-1.02527
3	-0.61108	-1.31634	-0.61108	1.26203	-1.33790	1.26203
4	-0.93244	-1.17650	-0.93244	-1.26203	-5.86484	-1.26203
5	-0.07941	-5.96634	-0.07941	0.501312	-8.19660	0.501311
6	0.07941	-6.12646	0.07941	-0.501312	-9.45813	0.501311
	Y			**P_Y**		
1	-0.65700	2.03237	-0.65700	3.06010	2.33634	3.06010
2	-0.03016	2.24150	-0.03016	-3.06010	4.07562	-3.06010
3	-0.33341	0.91982	-0.33410	-2.95930	-0.95608	-2.95930

...contd.

Table 8 (contd.)

		Z			P_Z	
4	1.08696	1.43921	1.08696	2.95930	3.25219	2.95930
5	0.04984	-3.59433	0.04984	-2.62902	-1.99691	-2.62902
6	-0.78305	-3.03857	-0.78305	2.62902	-6.71116	2.62902
1	4.55589	2.20357	4.55589	-5.07231	12.74790	-5.07230
2	5.04687	2.49699	5.04687	-9.86602	-4.81253	-9.86602
3	7.04643	-2.06699	7.04643	-8.26784	-3.92045	-8.26784
4	7.24980	-2.41874	7.24980	-6.67048	-6.22940	-6.67048
5	-12.01197	-0.01201	-12.01197	15.33280	2.57281	15.33270
6	-11.88702	-0.20281	-11.88702	14.54390	-0.35831	14.54390

Table 9. Average energy transferred (in kcal mol^{-1}) at different impact parameters

$v_1 = 0; \quad v_2 = 0; \quad v_3 = 0; \quad T = 80$ kcal mol^{-1};

$J_1 = 0; \quad J_2 = 0; \quad J_3 = 0$

b (Å)	$\langle \Delta T \rangle$	$\langle \Delta R_1 \rangle$	$\langle \Delta R_2 \rangle$	$\langle \Delta R_3 \rangle$	$\langle \Delta V_1 \rangle$	$\langle \Delta V_2 \rangle$	$\langle \Delta V_3 \rangle$	No. of traj.
0.0	19.07	3.02	5.81	7.81	1.31	0.89	0.24	26
1.0	16.75	4.37	3.31	3.51	0.95	0.53	4.43	10
2.0	6.95	2.27	1.18	3.62	-	-	-	6

CHAPTER FIVE

SUMMARY AND CONCLUSION

Our investigation of the dynamics of collinear reaction (R4) on an _ab_ _initio_ surface reveals a sharp vibrational threshold equal to E_b and this we attribute to the _sudden_ nature of the PES. Our 3D calculations do not show such a threshold, as the surface is less _sudden_ for noncollinear geometries and the sideways approach is the (energetically) most favoured configuration for this reaction. Nevertheless, there is a substantial vibrational enhancement in qualitative agreement with the experimental results for other alkali-hydrogen halide exchange reactions and with other theoretical results on PES with the barrier crest in the exit channel.

Our collinear QCT results on the CSCM surface agree well with the corresponding QM results except for the oscillations in the p^R _versus_ E curves of the latter. Our attempts to construct an LEPS surface with the characteristics of the

ab initio surface have not been successful in that our best LEPS surface is not sudden enough and does not show any vibrational threshold.

Product angular distribution predicted by our 3 D QCT study for $v = 0$, $J = 0$, $T = 8.7$ kcal mol^{-1} is in qualitative agreement with the molecular beam results lending credence to the validity of the ab initio surface. Based on this success, we have ventured to predict other observables for this reaction. We have paid special attention to the effect of J for this reaction.

An increase in J (from 0 through 9) for $v = 0$ at $T = 8.7$ kcal mol^{-1} results in an increase in S_r in qualitative accord with the PST prediction. That is, the rotational enhancement results partly from an increase in the number of product channels becoming available with increase in the total energy. Some amount of statistical behaviour for this reaction is reflected in some trajectories being long lived and product vibrational energy distribution being nearly statistical.

The effect of R on S_r is definitely dynamical in origin for $v = 2$ at $T = 8.7$ kcal mol^{-1}. There is a marked decline in $S_r(J)$ (for $J = 0 - 5$) followed by a dramatic increase (for $J = 5 - 7$) and a possible levelling off of S_r with further increase in J (from 9 to 15). These results are similar to the effect of J on S_r observed experimentally for a few other alkali (and alkaline earth)-hydrogen halide exchange reactions. The decline is attributed to the disruption of the preferred orientation for

the reaction. Just as the molecule rotates away from the preferred 'alignment', it can bring the molecule back into alignment and this would explain the subsequent increase. Further increase in J resulting in increased rotational velocity would only make the molecule appear as a blur and this would explain the levelling off of $S_r(J)$. We must stress that in the J range 5-7 for $v = 2$, the rotational enhancement is nearly four times larger than the vibrational enhancement which in turn is an order of magnitude larger than the effect of T on S_r.

Our ideas on the effect of rotation being linked to the relative orientation of the reactants are corroborated by detailed QCT investigations of the reaction at $\alpha = 0^0$, 90^0 and 180^0 and the effect of increasing J at these angles on the reaction probability at a fixed impact parameter. The initial orientation has a noticeable effect on the product energy disposal also. We find that for the reaction (R4), a sideways approach of Li to FH results in an increase in the population of the product LiF molecules in their higher vibrational states. This result is in accord with the only such experimental result available till this date, for its strontium analog. This orientation effect deserves further attention.

In spite of the reaction (R4) being the prototype of the alkali-hydrogen halide exchange reactions, Li is not heavy enough for this reaction to exhibit the $|\vec{L}| \rightarrow |\vec{J'}|$ behaviour that can be expected of other members of this family of

reactions, from kinematic considerations. This is reflected in the lack of a 100% correlation between $|\vec{L}|$ and $|\vec{J}'|$ for this reaction.

An interesting result of our QCT study is that the distribution of the polarization angle γ is centered around 90° indicating the reaction to be coplanar, in agreement with the molecular beam results.

Therefore we see that the available _ab initio_ surface for the reaction (R4), despite its shortcomings, leads to results in reasonable accord with the available experimental results and has made us go a step further to predict the effect of T, V and R on various attributes for this reaction. We hope that this study would stimulate further experimental study of this reaction.

We have compared some of our results with the available experimental results for some of the alkaline earth analogs. An important difference between the two families of reactions is that configurations such as F-M-H are possible in the case of the alkaline earths and they must lead to certain interesting dynamical results. The prototype of this family, Be + FH has been receiving attention[108] lately and experimental and theoretical studies of this reaction can be expected in the near future.

In Chapter 4 we described the methodology, adopted in building up our software package to study the six-center (6-C)

processes. A special feature of our study is the use of Hellmann-Feynman theorem in extracting the derivative of the potential energy. Although we have not observed any reactive trajectories for the model 6-C exchange process that we had taken up for our studies, the preliminary results reveal a dominant $T \rightarrow R$ process in the collision between a diatom and a tetra-atomic van der Waals molecule. Apart from opening up the venue for a study of several 6-C exchange reactions on model and realistic surfaces, our software package makes it possible to study the collision-induced-dissociation of van der Waals molecules among other things as this topic has been in the forefront in the last couple of years.[109,110] We hope to get definitive results on some of these problems in the near future.

REFERENCES

1. (a) P.R. Brooks and E.F. Hayes, State-to-State Chemistry, American Chemical Society Symp. Ser. 56 (1977);

   (b) Physics Today, Nov. 1980 - a Special issue.

2. Z. Karny, R.C. Estler and R.N. Zare, J. Chem. Phys., 69, 5199 (1978).

3. M.G. Prisant, C.T. Rettner, and R.N. Zare, J. Chem. Phys., 75, 2222 (1981).

4. R.B. Bernstein, Atom-Molecule Collision Theory: A guide to Experimentalist, Plenum, New York (1979).

5. G.C. Schatz and A. Kuppermann, J. Chem. Phys., 65, 4668 (1976).

6. M. Redmon and R.E. Wyatt, Chem. Phys. Lett., 63, 209 (1979).

7. R.N. Porter and L.M. Raff in: Dynamics of Molecular Collisions, Part B, ed. W.H. Miller (Plenum, New York, 1976), Ch. 1.

8. D.G. Truhlar and J.T. Muckerman in: Atom-Molecule Collision Theory, ed. R.B. Bernstein (Plenum, New York, 1979), Ch. 16.

9. (a) J.C. Polanyi, Accounts Chem. Res., 5, 161 (1972);

   (b) P.J. Kuntz, in: Dynamics of Molecular Collisions, Part B, ed. W.H. Miller (Plenum, New York, 1976), Ch. 1.

10. D.S.Perry, J.C. Polanyi and C.W. Wilson, Jr., Chem. Phys., 3, 317 (1974).

11. M. Kneba and J. Wolfrum, Ann. Rev. Phys. Chem., 31, 47 (1980).

12. C.B. Moore and I.W.M. Smith, Faraday Disc. Chem. Soc., 67, 146 (1979).

13. J.C. Polanyi and N. Sathyamurthy, Chem. Phys., 33, 287 (1978).

14. E.H. Taylor and S. Datz, J. Chem. Phys., 23, 1711 (1955).

15. (a) T.J. Odiorne, P.R. Brooks and J.V.V. Kasper, J. Chem. Phys., 55, 1980 (1971);

    (b) J.G. Pruett, F.R. Grabiner and P.R. Brooks, J. Chem. Phys., 60, 3335 (1974); ibid., 63, 1173 (1975).

16. (a) F. Heismann and H.J. Loesch, Chem. Phys., 64, 43 (1982).

    (b) M. Hoffmeister, L. Potthast and H.J. Loesch, Abstracts of the XII International Conference on the Physics of Electronic and Atomic Collisions, Gatlinburg, 1981.

17. F.E. Bartoszek, B.A. Blackwell, J.C. Polanyi and J.J. Sloan, J. Chem. Phys., 74, 3400 (1981).

18. (a) Z. Karny and R.N. Zare, J. Chem. Phys., 68, 3360 (1978).

    (b) A. Gupta, D.S. Perry and R.N. Zare, J. Chem. Phys., 72, 6237 (1980); 72, 6250 (1980).

19. N. Sathyamurthy, Chem. Rev. - submitted for publication.

20. B.A. Blackwell, J.C. Polanyi and J.J. Sloan, Chem. Phys., 30, 299 (1978).

21. H.H. Dispert, M.W. Geis and P.R. Brooks, J. Chem. Phys., 70, 5317 (1979).

22. C.H. Becker, P. Casavecchia, P.W. Tiedemann, J.J. Valentini and Y.T. Lee, J. Chem. Phys., 73, 2833 (1980).

23. R.D. Levine and R.B. Bernstein, Molecular Reaction Dynamics, Oxford, New York, 1974, p. 86.

24. P.J. Kuntz, M.H. Mok and J.C. Polanyi, J. Chem. Phys., 50, 4623 (1969).

25. (a) W.A. Lester, Jr. and M. Krauss, J. Chem. Phys., 52, 4775 (1970);

(b) W.A. Lester, Jr., J. Chem. Phys., 53, 1611 (1970).

26. M. Trenary and H.F. Schaefer III, J. Chem. Phys., 68, 4047 (1978).

27. G.G. Balint-Kurti and R.N. Yardley, Faraday Disc. Chem. Soc., 62, 77 (1977).

28. (a) Y. Zeiri and M. Shapiro, Chem. Phys., 31, 217 (1978).

    (b) M. Shapiro and Y. Zeiri, J. Chem. Phys., 70, 5264 (1979).

29. M.M.L. Chen and H.F. Schaefer III, J. Chem. Phys., 72, 4376 (1980).

30. S. Carter and J.N. Murrell, Mol. Phys., 41, 567 (1980).

31. R.B. Walker, Y. Zeiri and M. Shapiro, J. Chem. Phys., 74, 763 (1981).

32. J.M. Alvarino, O. Gervasi and A. Lagana, Chem. Phys. Lett., 87, 254 (1982).

33. Y. Zeiri, M. Shapiro and E. Pollak, Chem. Phys., 60, 239 (1981).

34. J.H. Sullivan, J. Chem. Phys., 46, 73 (1967).

35. L.D. Spicer and B.S. Rabinowitch, Ann. Rev. Phys. Chem., 21, 376 (1970).

36. L.M. Raff, D.L. Thompson, L.B. Sims and R.N. Porter, J. Chem. Phys., 56, 5998 (1972); erratum, J. Chem. Phys., 65, 4338 (1976).

37. L.M. Raff, L. Stivers, R.N. Porter, D.L. Thompson and L.B. Sims, J. Chem. Phys., 52, 3449 (1970).

38. R.L. Jaffe, J.M. Henry and J.B. Anderson, J. Am. Chem. Soc., 98, 1140 (1976).

39. S.B. Jaffe and J.B. Anderson, J. Chem. Phys., 49, 2859 (1968); 51, 1059 (1969).

40. H. Horiguchi and S. Tsuchiya, Int. J. Chem. Kin., 13, 1085 (1981).

41. D.L. Thompson and D.R.McLaughlin, J. Chem. Phys., 62, 4284 (1975).

42. J.C. Brown, H.E. Bass and D.L. Thompson, J. Chem. Phys., 70, 2326 (1979).

43. S.H. Bauer, Ann. Rev. Phys. Chem., 30, 271 (1979).

44. S.H. Bauer and E. Ossa, J. Chem. Phys., 45, 434 (1966).

45. A. Burcat and A. Lifshitz, J. Chem. Phys., 47, 3079 (1967).

46. R.D. Kern and G.G. Nika, J. Phys. Chem., 75, 1615 (1971); 75, 2541 (1961).

47. S.H. Bauer, D.M. Lederman, E.L. Resler, Jr. and E.R. Fisher, Int. J. Chem. Kin., 5, 93 (1973).

48. G. Pratt and D. Rogers, J. Chem. Soc. Faraday Trans. I, 72, 1589 (1976).

49. C. Marteau, F. Gaillard-Cusin and H. James, J. Chem. Phys., 75, 491, 498 (1978).

50. I.P. Herman, J. Chem. Phys., 72, 5777 (1980).

51. J.M. Silver and R.M. Stevens, J. Chem. Phys., 59, 3378 (1973).

52. N.J. Brown and D.M. Silver, J. Chem. Phys., 65, 311 (1976).

53. N.J. Brown and D.M. Silver, J. Chem. Phys., 68, 3607 (1978).

54. (a) R.B. Woodward and R. Hoffmann, The Conservation of Orbital Symmetry, Verlag Chemie, Gmbh, Weinheim, 1970. (b) R. Hoffmann, J. Chem. Phys., 49, 3739 (1968).

55. J.S. Wright, Can. J. Chem., 53, 549 (1975).

56. J.S. Wright, Chem. Phys. Lett., 6, 476 (1970).

57. D.L. Thompson and H.H. Suzukawa, J. Am. Chem. Soc., 99, 3614 (1977).

58. D.A. Dixon, R.M. Stevens and D.R. Herschbach, Faraday Disc. Chem. Soc., 62, 110 (1977).

59. D.A. Dixon and D.R. Herschbach, J. Am. Chem. Soc., 97, 6268 (1975),

60. D.A. Dixon and D.R. Herschbach, Ber. Bunsenges. Phys. Chem., 81, 145 (1977).

61. J.F. Durana, J.D. McDonald, J. Am. Chem. Soc., 98, 1289 (1976).

62. R.N. Yardley and G.G. Balint-Kurti, Mol. Phys., 31, 921 (1976).

63. D.R. McLaughlin and D.L. Thompson, J. Chem. Phys., 59, 4393 (1973).

64. N. Sathyamurthy and L.M. Raff, J. Chem. Phys., 63, 464 (1975).

65. S. Glasstone, K.J. Laidler and H. Eyring, The Theory of Rate Processes, McGraw Hill, New York, 1945.

66. S. Sato, Bull. Chem. Soc. (Japan), 28, 450 (1955), J. Chem. Phys., 23, 592 (1955).

67. J.C. Polanyi, J. Quant. Spectrosc. Radiat. Transf., 3, 471 (1963)

68. N. Sathyamurthy, R. Rangarajan and L.M. Raff, J. Chem.Phys., 64, 4606 (1976).

69. For example,J.C. Polanyi and J.L. Schreiber, Faraday Disc. Chem. Soc., 62, 267 (1977).

70. H. Schor, S. Chapman, S. Green and R.N. Zare, J. Chem. Phys., 69, 3790 (1978).

71. N. Sathyamurthy, J.W. Duff, C.L.Stroud and L.M. Raff, J. Chem. Phys., 67, 3563 (1977).

72. For example, A. Hunding and G.D. Billing, Nonlinear Constrained Optimization Procedure MINEQ, Medicinsk-Kemisk Institut,Copenhagen,1975.

73. N. Sathyamurthy, The Challenge of Fitting ab initio Potential-Energy Surfaces - in preparation.

74. Tomi Joseph and N. Sathyamurthy - to be published.

75. A. Lagana, Computers and Chem., 4, 137 (1980).

76. A. Kuppermann, in: Theoretical Chemistry, Theory of Scattering: Papers in Honor of Henry Eyring, Vol. 6, Part A, ed. D. Henderson (Academic Press, New York, 1981).

77. J.C. Polanyi and J.L. Schreiber in: Physical Chemistry-An Advanced Treatise, Vol. VIA, Kinetics of Gas Reactions, ed. H. Eyring, W. Jost and D. Henderson (Academic Press, New York, 1974), Ch. 6.

78. J.L. Schreiber, University of Toronto, Canada, 1975.

79. International Mathematical and Statistical Libraries, Inc., Houston, Texas, U.S.A.

80. L. Holmlid and K. Rynefors, Chem. Phys., 14, 403 (1976).

81. J.L. Schreiber, Ph.D. Thesis, University of Toronto, Canada, 1973.

82. (a) C.W. Gear, Numerical Initial Value Problems in Ordinary Differential Equations, Prentice-Hall, New York, 1971.
    (b) C.A. Parr, Ph.D. Thesis, California Institute of Technology, U.S.A., 1968.

83. I. NoorBatch and N. Sathyamurthy, J. Am. Chem. Soc., 104, 1766 (1982).

84. (a) P. Pechukas, J.C. Light and C. Rankin, J. Chem. Phys., 44, 794 (1966).
    (b) J. Lin and J.C. Light, J. Chem. Phys., 45, 2545 (1966)

(c) J.C. Light, in Atom-Molecule Collision Theory, ed. R.B. Bernstein (Plenum, New York, 1979), Ch. 19.

85. C.P. Shukla and N. Sathyamurthy - to be published.

86. N.H. Hijazi and J.C. Polanyi, J. Chem. Phys., 63, 2249 (1975); Chem. Phys., 11, 1 (1975).

87. D.R. Herschbach, Faraday Disc. Chem. Soc., 33, 281 (1962).

88. J.C. Polanyi and N. Sathyamurthy, Chem. Phys., 37, 259 (1979) and references cited therein.

89. W.B. Miller, S.A. Safron and D.R. Herschbach, Discuss. Faraday Soc., 44, 108 (1967).

90. (a) C. Maltz, N.D. Weinstein and D.R. Herschbach, Mol. Phys., 24, 133 (1972).

(b) D.S.Y. Hsu and D.R. Herschbach, Faraday Disc. Chem. Soc., 55, 116 (1973).

(c) D.S.Y. Hsu, G.M. McClelland and D.R. Herschbach, J. Chem. Phys., 61, 4927 (1974).

(d) D.S.Y. Hsu, N.D. Weinstein and D.R. Herschbach, Mol. Phys., 29, 257 (1975).

91. P.R. Brooks, Science, 193, 11 (1976) and references cited therein.

92. R.C. Estler and R.N. Zare, J. Am. Chem. Soc., 100, 1323 (1978).

93. C.-K. Man and R.C. Estler, J. Chem. Phys., 75, 2779 (1981).

94. D.L. Thompson, Chem. Phys. Lett., 84, 397 (1981); J. Chem. Phys. - in press.

95. I. NoorBatcha and N. Sathyamurthy, Chem. Phys. Lett., 79, 264 (1981).

96. J.A. Barnes, M. Keil, R.E. Kutina, and J.C. Polanyi, J. Chem. Phys., 76, 913 (1982).

97.   H. Goldstein, Classical Mechanics, Addison-Wesley, Reading, Mass. (1950).

98.   L.M. Raff, J. Chem. Phys., 60, 2220 (1974).

99.   A. Shermann and H. Eyring, J. Am. Chem. Soc., 54, 2661 (1932); H.S. Taylor, H. Eyring and A. Shermann, J. Chem. Phys., 1, 68 (1933).

100. Ref. 33, of ref. 57.

101. L. Pedersen and R.N. Porter, J. Chem. Phys., 47, 4751 (1967).

102. Y. Beppu and I. Ninomiya, Comput. Phys. Commun., 23, 123 (1981); QCPE No. 409 (1981).

103. R.P. Feynman, Phys. Rev., 56, 340 (1939).

104. A.C. Hurly, Proc. Roy. Soc. Ser. A 226, 179, 193 (1954).

105. P.O. Lowdin, J. Mol. Spectrosc., 3, 2232 (1962).

106. P.M. Kroger and J.T. Muckerman, Radiochimica Acta, 28, 215 (1981).

107. J. Schafer and W. Meyer, J. Chem. Phys., 70, 344 (1979).

108. (a) P.J. Kuntz and A.C. Roach, J. Chem. Phys., 74, 3420 (1981).

      (b) A.C. Roach and P.J. Kuntz, J. Chem. Phys., 74, 3435 (1981).

109. J.C. Tully, Adv. Chem. Phys., 42, 63 (1980).

110. (a) J.W. Brady, J.D. Doll and D.L.Thompson, J. Chem. Phys., 73, 292 (1980).

      (b) D.L. Thompson and L.M. Raff, J. Chem. Phys., 76, 301 (1982).

      (c) D.L. Thompson, J. Chem. Phys., 76, 1806 (1982).

APPENDIX - I

The London-Eyring-Polanyi-Sato (LEPS) function[13] is defined as:

$$V(r_1, r_2, r_3) = \sum_{i=1}^{3} Q_i - \left[\frac{1}{2} \sum_{i}^{3} \sum_{j=1}^{3} (J_i - J_j)^2\right]^{1/2}$$

where

$$Q_i = \frac{1}{2}\left[{}^1E_i(r_i) + {}^3E_i(r_i)\right],$$

$$J_i = \frac{1}{2}\left[{}^1E_i(r_i) - {}^3E(r_i)\right],$$

$${}^1E_i = D_i X_i(X_i - 2),$$

$${}^3E_i = \left[(1-S_i)/(1+S_i)\right](D_i/2)X_i(X_i+2),$$

and

$$X_i = \exp\left[-\beta_i(r_i - r_i^0)\right].$$

The spectroscopic constants D_i, β_i, r_i^0, where $i = 1$-3 are dissociation energies, Morse parameters and equilibrium bond lengths respectively; S_i are the Sato parameters. These constants are listed below:

|	LiF	HF	LiH
D (eV)	6.0030	6.1150	2.5170
r^0 (Å)	2.9554	1.7330	3.0147
β (Å^{-1})	0.6366	1.1992	0.6076
S	0.5	0.0	-0.2

APPENDIX - II

reaction cross section (S_r) decreases initially and then increases with an increase in J. The former effect is attributed to the disruption of the favored orientation for the reaction. The latter effect is explained on the basis of the F H bond stretching due to centrifugal distortion at large (J, r). Under the conditions employed in this study, at large J, *reagent rotation is nearly 4 times more efficient than reagent vibration,* which in turn is more effective than reagent translation in causing the reaction.

Although the last 20 years have witnessed an increase in understanding of the effect of reagent translation and vibration[5] on the rates of chemical reactions, the study of the effect of reagent rotation has been limited, and as a result, the understanding of the role of reagent rotation in chemical reactions has remained poor.

The QCT studies[6] of the effect of J on S_r have mostly focused their attention on the reaction

$$F + H_2 \rightarrow FH + H \tag{2}$$

and its isotopic analogues. Depending on the PES employed, the effect of increasing J on S_r was varied: (1) a dramatic drop in S_r followed by a leveling off of the same; (2) a slight increase in S_r from $J = 0$ to 1 followed by a decrease in S_r; (3) a substantial initial decrease followed by an increase in S_r. Experimentally, Klein and Persky[7] showed that the rate of reaction 2 was nearly insensitive to J in the range $J = 0-2$. Bernstein[8] and co-workers showed that a small increase in the reagent rotational energy (R) resulted in a small increase in the reactivity for the reaction

$$K + FCs \rightarrow [KFCs] \rightarrow KF + Cs \tag{3}$$
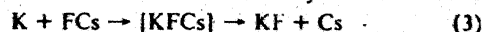
and a small decrease for the reaction

$$K + FRb \rightarrow [KFRb] \rightarrow KF + Rb \tag{4}$$
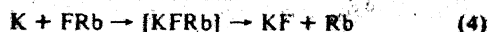
In both cases, the effect of reagent rotation on S_r was analogous to that of relative translation.

In recent years, there have been some experimental results available for some alkali atom–hydrogen halide reactions. Blackwell et al.[9] concluded from chemiluminescence depletion experiments on the reactions

$$Na + XH \ (X = F, Cl) \rightarrow NaX + H \tag{5}$$
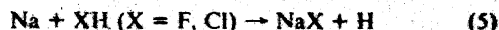
that there was an initial decrease followed by an increase in the reaction rate with increase in J. The initial decline was also observed by Dispert et al.[10] for the related reaction

$$K + ClH \rightarrow KCl + H \tag{6}$$
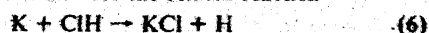
None of these reactions has been studied so far theoretically to understand why there is a decreasing/increasing effect of J on the reaction rate. Recently, however, for the simplest alkali atom–hydrogen halide reaction (1), a fairly accurate ab initio PES has become available[3,11] and has also been fitted to an analytic function.[4] Therefore we found this to be an ideal system for which the effect of reagent rotation on reaction cross section could be studied theoretically.

We have carried out QCT calculations for this reaction on an ab initio surface. We have chosen $v = 2$ since the chemiluminescence depletion experiments[9] on Na + FH had v in the range 1–6. The value of $T = 8.7$ kcal mol^{-1} employed in this study is the same as that employed in the only molecular-beam study[12] of this reaction (1). The details of the QCT method are described elsewhere.[2] We mention only that the impact parameter was sampled in a stratified manner and other variables of orientation angles and vibrational phase were selected randomly.

Effect of Reagent Rotation on Cross Section for the Reaction Li + FH → LiF + H

I. NoorBatcha[1a,b] and N. Sathyamurthy[1c,d]

Department of Chemistry
Indian Institute of Technology
Kanpur 208016, India

Received September 9, 1981

In this communication, we report on the effect of reagent rotation on the cross section for the reaction

$$Li + FH \rightarrow LiF + H \tag{1}$$

for HF in its $v = 2$ vibrational state in the range of rotational state $0 \le J \le 9$, at a relative translational energy of $T = 8.7$ kcal mol^{-1}, based on three-dimensional quasi-classical trajectory[2] (QCT) studies on an ab initio potential-energy surface (PES).[3,4] The

(1) (a) In partial fulfillment of the requirements for the degree of Doctor of Philosophy. (b) On leave from the American College. Madurai 625010, India, under the FIP scheme. (c) This research was supported in part by a grant from the Department of Science and Technology, India. (d) The calculations reported in this paper were carried out on a DEC-1090 computer at the Indian Institute of Technology, Kanpur.
(2) Porter, R. N.; Raff, L. M. In "Dynamics of Molecular Collisions"; part B; Miller, W. H., Ed.; Plenum Press: New York, 1976; Chapter 1.
(3) Chen, M. M. L.; Schaefer, H. F., III J. Chem. Phys. 1980, 72, 4376.
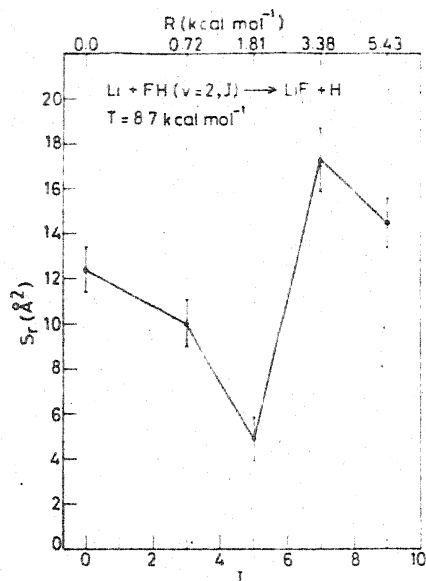(4) Carter, S.; Murrell, J. N. Mol. Phys. 1980, 41, 567.

(5) Kneba, M.; Wolfrum, J. Annu. Rev. Phys. Chem. 1980, 31, 47.
(6) Polanyi, J. C.; Schreiber, J. L. Faraday Discuss. Chem. Soc. 1977, 62, 267 and references therein.
(7) Klein, F. S.; Persky, A. J. Chem. Phys. 1974, 61, 2472.
(8) Stolte, S.; Proctor, A. E.; Pope, W. M.; Bernstein, R. B. J. Chem. Phys. 1977, 66, 3468. Zandee, L.; Bernstein, R. B. J. Chem. Phys. 1978, 68, 3760.
(9) Blackwell, B. A.; Polanyi, J. C.; Sloan, J. J. Chem. Phys. 1978, 30, 299.
(10) Dispert, H. H.; Geis, M. W.; Brooks, P. R. J. Chem. Phys. 1979, 70, 5317.
(11) Balint-Kurti, G. G.; Yardley, R. N. Faraday Discuss. Chem. Soc. 1977, 62, 77.
(12) Becker, C. H.; Casavecchia, P.; Tiedemann, P. W.; Valentini, J. J.; Lee, Y. T. J. Chem. Phys. 1980, 73, 2833.

Figure 1. Reaction cross section S_r as a function of the rotational state J (lower scale) for HF ($v = 2$) at $T = 8.7$ kcal mol^{-1}. The corresponding rotational energies (in kcal mol^{-1}) are shown in the upper scale. The error bars correspond to a 95% confidence level.

The results of the QCT study are plotted in the form of S_r as a function of J in Figure 1. With increase in J from 0 to 5, there is a monotonic decrease in S_r; further increase in J to 7 and 9 results in a dramatic increase in S_r.

For reaction 1, ab initio studies[3] show that an angular approach of Li to FH at an LiFH angle of 74° has the lowest barrier, ~10 kcal mol^{-1}, for the reaction. Also, detailed analysis of the initial conditions of the reactive trajectories shows that there is a preferred cone of reaction at the F end of the HF molecule. Therefore it is understandable that an increase in J from 0 to 3–5 disrupts the preferred orientation of the reaction, resulting in a drop in the magnitude of S_r. In the absence of any additional effect, we would have expected a leveling off of S_r. However, in this particular case, because of the large vibrational energy present in the molecule, increase in J results in substantial centrifugal distortion. This means a stretching of the FH bond under attack, and the result would be similar to increasing the vibrational energy. For example, when v is changed from 0 to 1 to 2, S_r increases from 0.8 ± 0.2 to 8.7 ± 0.9 to 12.4 ± 1.0 Å^2 at $T = 8.7$ kcal mol^{-1} for $J = 0$. This is explained on the basis of the *sudden* character of the PES.[3,11,13] It must be added that such an explanation for the observed dependence of S_r on J was suggested earlier by Blackwell et al.[9] although no dynamical results were available at that time.

At large J, even though the effect of reagent rotation on S_r is qualitatively similar to that of reagent vibration, there is a quantitative difference between the two. In the energy range we have studied, $\Delta S_r / \Delta V = 0.5$ Å^2/(kcal mol^{-1}) and $\Delta S_r / \Delta R = 2.7$ Å^2/(kcal mol^{-1}); that is, rotation is nearly 4 times more efficient than vibration in enhancing the reaction cross section. Reagent translation is the least effective in this case with a $\Delta S_r / \Delta T$ value of 0.086 Å^2/(kcal mol^{-1}).

In summary our findings are significant for these reasons: (1) Ours is the first dynamical study of the effect of reagent rotation for a prototype alkali atom–hydrogen halide reaction, on an ab initio PES. (2) Increase in J results in a substantial decrease followed by a rapid increase in S_r, with a minimum occurring around $J = 5$. The results are in qualitative accord with the experimental results on the related alkali atom–hydrogen halide exchange reactions. (3) For the first time we have shown that reagent rotation can be more effective than reagent vibration in enhancing a reaction.

Registry No. Li, 7439-93-2; FH, 7664-39-3.

(13) Polanyi, J. C.; Sathyamurthy, N. *Chem. Phys.* 1978, *33*, 287. NoorBatcha, I.; Sathyamurthy, N. *J. Chem. Phys.*, in press.

APPENDIX - III

ON THE VALIDITY OF THE POWER GAP LAW FOR ROTATIONAL ENERGY TRANSFER IN CO$_2$–H$_2$ COLLISIONS

I. NOOR BATCHA and N. SATHYAMURTHY

Department of Chemistry, Indian Institute of Technology, Kanpur 208016, India

The validity of the power gap law for rotational energy transfer has been tested in the case of rigid-rotor CO$_2$–H$_2$ collisions. The power law with a single parameter γ is shown to be adequate only for small amounts of energy transferred. For larger amounts, use of a different γ seems to be warranted suggesting a deficiency of the power law *or* operation of two mechanisms for rotational energy transfer.

1. Introduction

Polanyi and Woodall [1] proposed that the probability of transition from an initial rotational state J_i to a final rotational state J_f decreases exponentially with increase in absolute energy gap $|\Delta E_{if}| = |E_{J_f} - E_{J_i}|$ between the two states:

$$P_{J_i \to J_f} \propto \exp(-C|\Delta E_{if}|), \tag{1}$$

where C is a constant for a given collision system. Fitting of state-to-state integral inelastic cross sections (IICS) and rate constant data to the exponential gap relationship [2] has been shown [3] to be equivalent to a linear surprisal analysis [4]. Heller [5] tried to provide a theoretical justification for such an exponential dependence. Some computed inelastic cross-section data have been fitted to the exponential gap relationship (see refs. [6–11]). Apart from the compaction of data, such an approach has rendered a comparison with the experimentally determined rate data easy [7]. A study of the role of the collision partner, the effect of change in initial collision energy T_i and rotational state J_i, the validity of classical mechanics to rotational energy transfer (RET) processes, etc. could be directed to a single parameter C rather than an array of IICS [10]. However, there are limitations to the exponential gap relationship. In many instances (for example, see refs. [9,11]) a plot of the surprisal $\ln(\sigma_{J_i \to J_f}/g_f T_i^{1/2})$ versus $|\Delta E_{if}|$, where $\sigma_{J_i \to J_f}$ is the

state-to-state IICS, g_f the degeneracy of the final state $= 2J_f + 1$ and T_f the final collision energy, has shown a prominent sigmoidal behavior rather than a straight line.

Brunner and co-workers [12–15] proposed that

$$\sigma_{J_i \to J_f}/NR = a|\Delta E_{if}|^{-\gamma}, \tag{2}$$

where $N = N_\Delta = 2J_f + 1$ or $N = N_0 = (2J_< + 1)/(2J_i + 1)$, $J_<$ being the smaller of J_i and J_f, $R = \rho(T_f)/\rho(T_i)$ with ρ the translational density of states and γ a constant. They emphasized [13] "the power law is superior to the exponential gap law for all of the RET data sets considered when $|\Delta E_{if}|$ is less than 20% of the initial kinetic energy". With more refined data becoming available over a wide range of J_i (= 4, 16, 38, 66, 74 and 100) for Na$_2^*(J_i)$–Xe collisions, they found recently [16] that although the power law provided a good representation of the variation of $\sigma_{J_i \to J_f}$ with $|\Delta E_{if}|$ for any given J_i, it was not adequate for fitting $\sigma_{J_i \to J_f}$ over the complete range of J_i probably because γ was not allowed to vary with J_i. The energy-corrected sudden (ECS) scaling law of DePristo and co-workers [17,18] proved to be much better.

In this paper we analyse the state-to-state IICS values reported earlier for CO$_2$–H$_2$ collisions [9] and show that sometimes the power law with a single exponent is valid only up to $|\Delta E_{if}|/T_i$ values as low as 0.08. The deviations from a single-parameter power law, however, are not random. The deviating data

points fall on a straight line with a distinctly different slope γ_{high}, indicating two different mechanisms for the rotational energy transfer *or* a deficiency of the power law. We have also investigated the dependence of γ on J_i and T_i.

2. Results and discussion

The qualitative way to check the goodness of fit of the power law to the state-to-state IICS is to plot $\ln(\sigma_{J_i \to J_f}/NT_f^{1/2})$ against $\ln|\Delta E_{if}|$ to see if a straight line with a negative slope γ results. Such a plot for $CO_2(J_i = 0) - H_2(J_i = 0)$ collisions at $T_i = 0.2$ eV is shown in fig. 1 for the two different choices of N. It
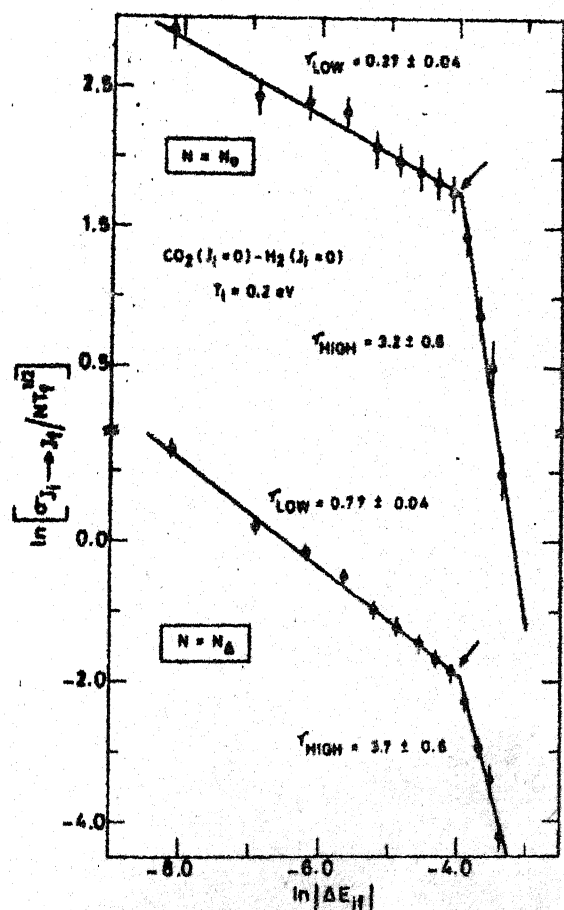

Fig. 1. Power law fits to state-to-state integral inelastic cross sections for $CO_2(J_i = 0) - H_2(J_i = 0)$ collisions at $T_i = 0.2$ eV using $N = N_\Delta$ and $N = N_0$. The arrow indicates approximately the point at which the switch from one power law to another begins to occur. The error bars represent 1σ values.

is clear that the results at small ΔE_{if} are fitted well by a straight line with a slope of γ_{low} up to $\Delta E_{if}/T_i = 0.08$, beyond which there are large deviations from the straight line. Such deviations were noticed by Pritchard et al. [13] for the N_2–Ar system, but only above $|\Delta E_{if}|$ values which were 20% of T_i. They ignored such deviations. We find them to be too large to be neglected in the case of CO_2–H_2. As a matter of fact, the deviations are large enough and over a wide enough ΔE_{if} to justify a separate straight-line fit with a slope of γ_{high}. When all the available $\sigma_{J_i \to J_f}$, $2 \leq J_f \leq 26$ are fitted by a *single* power law, χ^2/ν as defined in ref. [13] is equal to 17.1; when only the first nine values of $\sigma_{J_i \to J_f}$, $2 \leq J_f \leq 18$, are used, χ^2/ν drops to 0.38. Jendrek and Alexander [19] also noticed in the case of LiH–He collisions that the use of a single-parameter power law is justified for small $|\Delta E_{if}|$ only. Although they have not said so, it is clear that their values of $\ln(\sigma_{J_i \to J_f}/g_f T_f^{1/2})$ at large $|\Delta E_{if}|$ do warrant the use of a different γ in that region. Thus it is evident that a *single power law is not adequate*. It is also possible that this arises because of two different mechanisms for RET processes. For example, in the case of CO_2–H_2 it was shown in fig. 7 of ref. [9] that "small ΔJ transitions occur predominantly at large impact parameters (b) while large ΔJ transitions tend to occur at small to moderate values of b".

It may be argued that the deviations of the type noticed by us may be accounted for by using the ECS relationship to fit the data. The difficulty is that the ECS scaling applies to de-excitation ($J_f < J_i$) processes [17]:

$$\sigma_{J_i \to J_f}^{(T_i)} = (2J_f + 1) \sum_{L=J_i-J_f}^{J_i+J_f} (2L+1)$$

$$\times \begin{pmatrix} J_i & J_f & L \\ 0 & 0 & 0 \end{pmatrix}^2 |A_L^{J_i}|^2 \sigma_{L \to 0}^{(T_i)}, \qquad (3)$$

where $(:\,:\,:)$ is a 3-j symbol and $A_L^{J_i}$ an adiabaticity factor. In principle, one could relate the above equation to excitation cross sections by invoking the principle of microscopic reversibility [20]:

$$\sigma_{J_i \to J_f}^{(T_i)} = [(2J_f + 1)/(2J_i + 1)](T_i/T_i)\sigma_{J_f \to J_i}^{(T_i)}. \qquad (4)$$

Unfortunately, this involves values of σ at different collision energies. Also, the IICS calculated by the quasiclassical trajectory method [21] do not satisfy
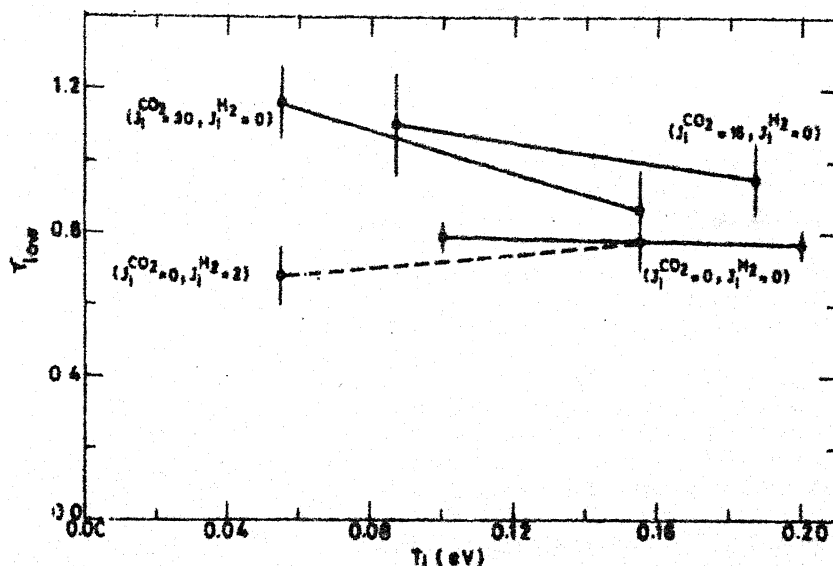
Fig. 3. Dependence of γ_{low} on T_i for different choices of initial rotational states of CO_2 and H_2. The error estimates represent 2σ values.

nearly the same $|\Delta E_{if}|$ for both. However, in some cases, the de-excitation cross sections do deviate from the straight line(s) much more than their excitation analogs. The γ values reported in this paper were obtained mostly by fitting the excitation cross sections only. In the particular case of $J_i = 30$, eq. (3) could have been directly tested in predicting $\sigma_{30 \to J_f}$ for $J_f < 30$ provided $\sigma_{L \to 0}(T_i)$ were known. But these values are not known. Substituting for the latter by a power law expression as was done in ref. [16] would not have been of much use as that will only test the power law.

Values of γ_{low} and γ_{high} for the different $J_i^{CO_2}$ and $J_i^{H_2}$ at different T_i are listed in table 1. The γ_{low} values are much more dependable than the γ_{high} values as the former were obtained from a larger number of σ values. Therefore we focused our attention on γ_{low} in studying the effect of the initial rotational state and the collision energy. Dependence of γ_{low} on T_i is displayed in fig. 3 for different $J_i^{CO_2}$ and $J_i^{H_2}$. It is seen that γ_{low} remains virtually unchanged with change in $J_i^{H_2}$ from 0 to 2. On the other hand, there is a noticeable change in γ_{low} with $J_i^{CO_2}$ (= 0, 16, 30) although not in any systematic manner. The value of γ_{low} is relatively independent of T_i, a conclusion previously arrived at by Pritchard et al. [13] for N_2–Ar. In con-

trast, the exponential gap parameter C had been shown to decrease monotonically with increase in T_i [9, 10, 22]. It must be added that, at least for CO_2–He, γ_{low} does seem to depend on T_i [23].

3. Conclusions

The power gap law for rotational energy transfer processes proposed by Brunner et al. [12] fits the state-to-state IICS values for rigid-rotor CO_2–H_2 collisions better than the exponential gap law. The slope of the straight line for a plot of $\ln(\sigma_{J_i \to J_f}/NT_i^{1/2})$ versus $|\Delta E_{if}|$ however, changes sharply from γ_{low} to γ_{high}, sometimes at $|\Delta E_{if}|$ as low as 8% of the initial collision energy, showing the inadequacy of the single-parameter power law. Alternatively, the change in γ is suggestive of two different mechanisms for RET processes in CO_2–H_2. We do not have sufficient information to distinguish between the two possibilities.

The available RET data for the CO_2–H_2 system suggest that γ_{low} may depend slightly on the initial rotational state (of the primary rotor) and remains unaltered with change in T_i. We also find $N = N_\Delta$ to be preferable to $N = N_0$ for the CO_2–H_2 system.

References

[1] J.C. Polanyi and K.B. Woodall, J. Chem. Phys. 56 (1972) 1563.

[2] A.M. Ding and J.C. Polanyi, Chem. Phys. 10 (1975) 39.

[3] R.B. Bernstein, J. Chem. Phys. 62 (1975) 4570.

[4] R.D. Levine, R.B. Bernstein, P. Kahana, I. Procaccia and E.T. Upchurch, J. Chem. Phys. 64 (1976) 2560.

[5] D.F. Heller, Chem. Phys. Letters 45 (1977) 64.

[6] M.D. Pattengill and R.B. Bernstein, J. Chem. Phys. 65 (1976) 4007.

[7] J.C. Polanyi and N. Sathyamurthy, Chem. Phys. 29 (1978) 9.

[8] J.C. Polanyi and N. Sathyamurthy, J. Phys. Chem. 83 (1979) 978.

[9] N. Sathyamurthy and L.M. Raff, J. Chem. Phys. 72 (1980) 3163.

[10] C. Gayatri and N. Sathyamurthy, Chem. Phys. 48 (1980) 227.

[11] R. Goldflam, D.J. Kouri, R.K. Preston and R.T Pack, J. Chem. Phys. 66 (1977) 2574.

[12] T.A. Brunner, R.D. Driver, N. Smith and D.E. Pritchard, Phys. Rev. Letters 41 (1978) 856.

[13] D.E. Pritchard, N. Smith, R.D. Driver and T.A. Brunner, J. Chem. Phys. 70 (1979) 2115.

[14] T.A. Brunner, R.D. Driver, N. Smith and D.E. Pritchard, J. Chem. Phys. 70 (1979) 4155.

[15] M. Wainger, I. Al-Agil, T.A. Brunner, A.W. Karp, N. Smith and D.E. Pritchard, J. Chem. Phys. 71 (1979) 1977.

[16] T.A. Brunner, N. Smith and D.E. Pritchard, Chem. Phys. Letters 71 (1980) 358.

[17] A.E. DePristo, S.D. Augustin, R. Ramaswamy and H. Rabitz, J. Chem. Phys. 71 (1979) 850.

[18] R. Ramaswamy, A.E. DePristo and H. Rabitz, Chem. Phys. Letters 61 (1979) 495.

[19] E.F. Jendrek and M. Alexander, J. Chem. Phys. 72 (1980) 6452.

[20] J.C. Polanyi and J.L. Schreiber, in: Physical chemistry, an advanced treatise, Vol. 6A. Kinetics of gas reactions, eds. H. Eyring, W. Jost and D. Henderson (Academic Press, New York, 1974) ch. 6.

[21] R.N. Porter and L.M. Raff, in: Dynamics of molecular collisions, part B, ed. W.H. Miller (Plenum Press, New York, 1976) ch. 1.

[22] I. Procaccia and R.D. Levine, J. Chem. Phys. 64 (1976) 808.

[23] I. Noor Batcha and N. Sathyamurthy, unpublished.